



Space mission trajectory optimization via competitive differential evolution with independent success history adaptation

Rui Zhong ^a, Abdelazim G. Hussien ^{b,c}, Shilong Zhang ^d, Yuefeng Xu ^d, Jun Yu ^e, ^{*}

^a Information Initiative Center, Hokkaido University, Sapporo, Japan

^b Department of Computer and Information Science, Linköping University, Linköping, Sweden

^c Faculty of Science, Fayoum University, Fayoum, Egypt

^d Graduate School of Science and Technology, Niigata University, Niigata, Japan

^e Institute of Science and Technology, Niigata University, Niigata, Japan

ARTICLE INFO

Dataset link: <https://github.com/RuiZhong961230/ISHACDE>

Keywords:

Space mission trajectory optimization (SMTO)
Differential evolution (DE)
Competitive mechanism
Independent success history adaptation

ABSTRACT

This paper proposes a novel Independent Success History Adaptation Competitive Differential Evolution (ISHACDE) algorithm to address the functional optimization problems and the Space Mission Trajectory Optimization (SMTO). ISHACDE is developed based on the efficient optimizer Competitive Differential Evolution (CDE) and integrates an independent success history adaptation scheme. This scheme inherits the hypothesis from Success History Adaptive Differential Evolution (SHADE) that the scaling factor F and crossover rate C_r from success evolution may contribute to accelerating the evolution of the whole population, and we further hypothesize that the independent evolution of F in CDE may perform better. We conduct comprehensive numerical experiments on median-scale CEC2017, large-scale CEC2020, small-scale CEC2022, and the single-objective GTOPX benchmark to evaluate the performance of ISHACDE. Ten state-of-the-art optimizers and ten recently proposed optimizers are employed as competitor algorithms. The experimental results and statistical analysis confirm the competitiveness of the proposed ISHACDE against twenty optimizers, and the ablation experiments practically prove the effectiveness of the independent success history adaptation scheme. The source code of this research can be found in <https://github.com/RuiZhong961230/ISHACDE>.

1. Introduction

Space mission trajectory optimization (SMTO) is critically important yet highly challenging in the aerospace and optimization fields [1,2]. A demonstration is presented in Fig. 1.¹ These problems aim to minimize the fuel consumption of trajectories while adhering to mission constraints [3]. The highly non-linear, black-box, and high-dimensional characteristics of these problems render traditional optimization techniques, including gradient-based methods and classical evolutionary algorithms (EAs), often insufficient for achieving satisfactory performance within a limited computational budget [4,5]. Consequently, researchers and scholars have to explore advanced optimization techniques to address these challenges efficiently [1,6].

Evolutionary computation (EC), renowned for its efficiency, user-friendliness, and flexibility, has attracted widespread attention from researchers and has experienced rapid development in recent years [7, 8]. Building on foundational approaches such as genetic algorithms (GA), differential evolution (DE), particle swarm optimization (PSO),

evolutionary strategies (ES), evolutionary programming (EP), and other swarm intelligence (SI) algorithms, innovative optimizers have sprung up like mushrooms. These advancements present promising avenues for tackling various optimization challenges [9,10].

This research aims to solve SMTO problems using advanced EC techniques. DE [11], a well-studied population-based stochastic optimization algorithm, has demonstrated superior performance in various tasks, including IEEE-CEC competitions [12–15] and real-world applications [16–19]. Consequently, developing an advanced optimization algorithm based on DE is promising for addressing SMTO tasks.

In this paper, we focus on the single-objective continuous SMTO benchmark provided by GTOPX [20], an extension of the original global trajectory optimization problems (GTOP) database collected by the European Space Agency (ESA). To address these problems, we propose a novel competitive differential evolution algorithm with independent success history adaptation (ISHACDE). ISHACDE inherits the main architecture of competitive DE (CDE) and incorporates the success

* Corresponding author.

E-mail addresses: rui.zhong.u5@elms.hokudai.ac.jp (R. Zhong), abdelazim.hussien@liu.se (A.G. Hussien), f24c130g@mail.cc.niigata-u.ac.jp (S. Zhang), f24c024f@mail.cc.niigata-u.ac.jp (Y. Xu), yujun@ie.niigata-u.ac.jp (J. Yu).

¹ This picture is generated by ChatGPT-4o.

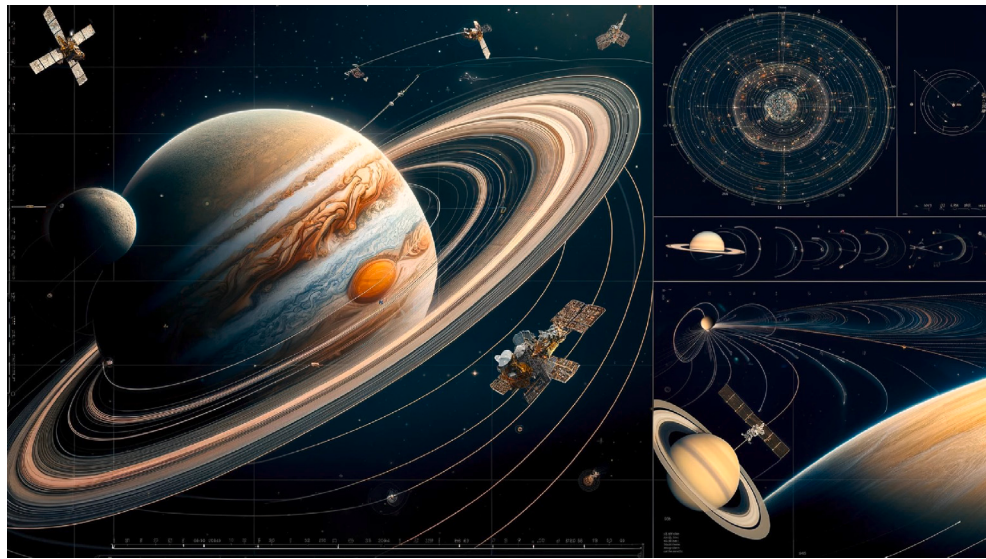


Fig. 1. A demonstration of the space mission trajectory optimization.

history adaptation scheme from JADE [21]. Furthermore, based on the hypothesis in JADE that the scaling factor F and crossover rate Cr from successful evolution may contribute to guiding the direction of optimization, we further notice that F in mutation strategies control distinctive differential vectors. Therefore, we reasonably hypothesize that the appropriate scaling factors F in the mutation operator are distinct and should evolve independently. To confirm the efficiency of our proposal, we conduct comprehensive numerical experiments on IEEE-CEC2017, CEC2020, CEC2022, and the GTOPX benchmark to evaluate the performance of ISHACDE. Ten state-of-the-art optimizers, including DE, PSO, their advanced variants, and covariance matrix adaptation evolution strategy (CMA-ES), and ten recently proposed optimization techniques such as marine predators algorithm (MPA), Fick's law algorithm (FLA), and the original CDE are employed as competitor algorithms. The experimental results and statistical analysis from comparison experiments confirm the efficiency and effectiveness of ISHACDE. Additionally, the ablation experiments are conducted to investigate the performance of the proposed independent success history adaptation scheme.

The remainder of this paper is organized as follows: Section 2 introduces the related works including CDE, success history adaptation scheme, and GTOPX benchmark. Section 3 demonstrates the proposed ISHACDE in detail. Section 4 presents numerical experiments and statistical analysis, and the performance of ISHACDE is discussed in Section 5. Finally, Section 6 concludes this paper.

2. Related works

2.1. Competitive differential evolution (CDE)

CDE [22] is an advanced variant of DE that shares a similar architecture with conventional DE, comprising four main components: population initialization, mutation, crossover, and selection. The following contexts will provide detailed descriptions of these components.

Population initialization: As a population-based optimization technique, CDE first initializes the population using Eq. (1).

$$P = \begin{bmatrix} X_1 \\ X_2 \\ X_3 \\ \vdots \\ X_N \end{bmatrix} = \begin{bmatrix} x_{11} & x_{12} & \cdots & x_{1D} \\ x_{21} & x_{22} & \cdots & x_{2D} \\ x_{31} & x_{32} & \cdots & x_{3D} \\ \vdots & \vdots & \ddots & \vdots \\ x_{N1} & x_{N2} & \cdots & x_{ND} \end{bmatrix}, \quad x_{ij} = r \cdot (ub_j - lb_j) + lb_j \quad (1)$$

where P denotes the whole population, X_i indicates the i th individual, and x_{ij} is the value of the i th individual in the j th dimension. r

represents a uniformly random value in $(0, 1)$, ub_j and lb_j are the lower and upper bound of the j th dimension, respectively.

Mutation operator: CDE integrates a novel mutation operator termed DE/winner-to-best/1 to construct mutant vector, as formulated in Eq. (2).

$$V_i^t = \begin{cases} X_{r1}^t + F_1 \cdot (X_{best}^t - X_{r1}^t) + F_2 \cdot (X_{r2}^t - X_{r3}^t), & \text{if } X_{r1}^t \text{ has a better fitness} \\ X_i^t + F_3 \cdot (X_{best}^t - X_i^t) + F_4 \cdot (X_{r2}^t - X_{r3}^t), & \text{otherwise} \end{cases} \quad (2)$$

where $r1$, $r2$, and $r3$ are three random integer in $[1, N]$ and mutually different. $r1$ is also being different from i . F_1 , F_2 , F_3 , and F_4 are four scaling factors sampled from a normal distribution $N(0.5, 0.3)$. Initially, the DE/winner-to-best/1 mutation scheme selects a random individual X_{r1}^t as the competitor individual to the current individual X_i^t . If X_{r1}^t has a better fitness value, it replaces X_i^t and acts as the base vector and implements the DE/rand-to-best/1 mutation scheme; otherwise, X_i^t survives and the DE/current-to-best/1 mutation scheme is activated. Essentially, the DE/winner-to-best/1 mutation scheme is an intelligent and automatic integration between DE/rand-to-best/1 and DE/current-to-best/1 mutation schemes, and the efficiency and effectiveness of this mutation scheme have been practically confirmed.

Crossover operator: The common binomial crossover operator is employed in CDE, as presented in Eq. (3).

$$U_{i,j}^t = \begin{cases} V_{i,j}^t, & \text{if } r \leq Cr \text{ or } j = j_{rand} \\ X_{i,j}^t, & \text{otherwise} \end{cases} \quad (3)$$

where Cr is the crossover rate sampled from $N(0.5, 0.3)$ to control the proportion between the mutant vector V_i^t and the parent individual X_i^t in the offspring individual U_i^t , and j_{rand} is a random integer in $\{1, 2, \dots, D\}$.

Selection mechanism: Inspired by the survival of the fittest, Eq. (4) describes the selection mechanism employed in CDE.

$$X_i^{t+1} = \begin{cases} U_i^t, & \text{if } U_i^t \text{ has a better fitness} \\ X_i^t, & \text{otherwise} \end{cases} \quad (4)$$

This one-to-one greedy selection can ensure the survival of elite individuals while maintaining population diversity.

2.2. Literature review of success history adaptation scheme

The success history adaptation scheme was first introduced in JADE by Zhang et al. [21], which is a significant milestone in the adaptive

Index	1	2	3	...	$H - 1$	H
F memory	$\mu_{F,1}$	$\mu_{F,2}$	$\mu_{F,3}$...	$\mu_{F,H-1}$	$\mu_{F,H}$
Cr memory	$\mu_{Cr,1}$	$\mu_{Cr,2}$	$\mu_{Cr,3}$...	$\mu_{Cr,H-1}$	$\mu_{Cr,H}$

Fig. 2. Memory of F and Cr .

control of parameters within DE. This scheme implicitly hypothesizes that the scaling factor F and crossover rate Cr from success evolution can accelerate the optimization for other individuals, and the success history adaptation scheme in JADE drives F and Cr to close to the success history. Eq. (5) formulates the DE/cur-topbest/1 mutation scheme in JADE.

$$\mathbf{V}_i^t = \mathbf{X}_i^t + F_i \cdot (\mathbf{X}_{pbest}^t - \mathbf{X}_i^t) + F_i \cdot (\mathbf{X}_{r1}^t - \mathbf{X}_{r2}^t) \quad (5)$$

where \mathbf{X}_{pbest}^t is an individual that randomly selected from the top 100p% elite individuals. Similarly, the conventional binomial crossover scheme in Eq. (3) is employed in JADE. Here, the specific F_i and Cr_i are sampled using Eq. (6).

$$\begin{aligned} F_i &= \text{randn}(\mu_F, \sigma_F^2) \\ Cr_i &= \text{randc}(\mu_{Cr}, \sigma_{Cr}^2) \end{aligned} \quad (6)$$

where $\text{randn}(\mu, \sigma^2)$ and $\text{randc}(\mu, \sigma^2)$ are sampling values from Gaussian and Cauchy distributions with expectation μ and standard deviation σ . μ_F and μ_{Cr} are recommended as 0.5, while σ_F^2 and σ_{Cr}^2 are fixed at 0.1. These parameter settings are inherited in the most advanced success history adaptation schemes. Additionally, F_i is strictly limited in (0, 1] as is Cr_i . When F_i samples a value smaller than 0, it will be resampled using Eq. (6). Once the constructed offspring individual using the specific F_i and Cr_i has a better fitness value than its parent, F_i and Cr_i will be saved in the success history memory S_F and S_{Cr} . At the end of this iteration, μ_F and μ_{Cr} are updated using Eqs. (7) and (8), respectively.

$$\begin{aligned} \mu_F &= (1 - c) \cdot \mu_F + c \cdot \text{mean}_L(S_F) \\ \text{mean}_L(S_F) &= \frac{\sum_{k=1}^{|S_F|} S_{F,k}}{\sum_{k=1}^{|S_F|} 1} \end{aligned} \quad (7)$$

$$\begin{aligned} \mu_{Cr} &= (1 - c) \cdot \mu_{Cr} + c \cdot \text{mean}(S_{Cr}) \\ \text{mean}(S_{Cr}) &= \frac{\sum_{k=1}^{|S_{Cr}|} S_{Cr,k}}{|S_{Cr}|} \end{aligned} \quad (8)$$

where c is a weight factor recommended in [0.05, 0.2] [21], $\text{mean}_L(S_F)$ denotes the Lehmer mean of S_F and $\text{mean}(S_{Cr})$ is the usual arithmetic mean of S_{Cr} , respectively. The success history adaptation scheme hypothesizes that the scaling factor F_i and crossover rate Cr_i from the successfully evolved i th individual may potentially benefit other individuals in constructing superior offspring. Therefore, this scheme can guide the evolution of hyper-parameters to fit the specific problem and accelerate optimization convergence.

Building on the foundation of the adaptation scheme in JADE, this adaptation scheme was further refined in Success History Adaptive DE (SHADE) [23]. SHADE introduced a memory vector with the length of H to save the updated μ_F and μ_{Cr} , which is presented in Fig. 2.

In each iteration, SHADE randomly samples $\mu_{F,i}$ and $\mu_{Cr,j}$ from the memory, and F_i and Cr_j from success evolution and stored in S_F and S_{Cr} update $\mu_{F,i}$ and $\mu_{Cr,j}$ using Eqs. (9) and (10).

$$\begin{aligned} \mu_{F,i} &= (1 - c) \cdot \mu_{F,i} + c \cdot \text{mean}_{WL}(S_F) \\ \text{mean}_{WL}(S_F) &= \frac{\sum_{k=1}^{|S_F|} w_k \cdot S_{F,k}^2}{\sum_{k=1}^{|S_F|} w_k \cdot S_{F,k}} \\ w_k &= \frac{\Delta f_k}{\sum_{j=1}^{|Cr|} \Delta f_j} \end{aligned} \quad (9)$$

$$\mu_{Cr,j} = (1 - c) \cdot \mu_{Cr,j} + c \cdot \text{mean}_{WA}(S_{Cr}) \quad (10)$$

$$\text{mean}_{WA}(S_{Cr}) = \sum_{k=1}^{|Cr|} w_k \cdot S_{Cr,k}$$

where $\Delta f_k = |f(\mathbf{U}_i^t) - f(\mathbf{U}_j^t)|$ is the absolute fitness difference between the i th parent and offspring individual.

Subsequently, SHADE was later advanced in SHADE with Linear Population Reduction (L-SHADE) [24], an advanced SHADE algorithm that modifies the success history adaptation mechanism from SHADE and aims to enhance optimization performance through dynamically adjusting the population size. In the early optimization stage, L-SHADE initializes with a large population, which enables a broader search of the solution space and facilitates extensive exploration. As optimization progresses, the population size is gradually reduced in a controlled linear reduction strategy, which intensifies exploitation by refining search efforts around promising regions.

iL-SHADE, an Improved L-SHADE [12], further controls the F_i and Cr_i based on the iteration information using Eqs. (11) and (12).

$$F_i = \begin{cases} \min(F_i, 0.7), & \text{if } t < 0.25T \\ \min(F_i, 0.8), & \text{else if } t < 0.5T \\ \min(F_i, 0.9), & \text{else if } t < 0.75T \\ F_i, & \text{else} \end{cases} \quad (11)$$

$$Cr_i = \begin{cases} \min(Cr_i, 0.5), & \text{if } t < 0.25T \\ \min(Cr_i, 0.25), & \text{else if } t < 0.5T \\ Cr_i, & \text{else} \end{cases} \quad (12)$$

where t and T are current and maximum iterations, respectively. Furthermore, iL-SHADE ignores the weights between memory and success history experience and adopts Eq. (13) to update $\mu_{F,i}$ and $\mu_{Cr,j}$.

$$\begin{aligned} \mu_{F,i} &= \frac{\mu_{F,i} + \text{mean}_{WL}(S_F)}{2} \\ \mu_{Cr,j} &= \frac{\mu_{Cr,j} + \text{mean}_{WA}(S_{Cr})}{2} \end{aligned} \quad (13)$$

The success history adaptation mechanism has been widely applied in various SHADE-based algorithms, including L-SHADE-E [25], AL-SHADE [26], L-SHADED [27], and other recent variants [28–30]. These adaptations largely focus on enhancing the efficiency of the success history scheme by combining multi-strategy frameworks or diverse parameter adaptation techniques to improve convergence performance and solution quality. However, most of these approaches ignore the foundational hypothesis behind the success history adaptation scheme. In particular, while this scheme dynamically adjusts parameters to improve individual performance, it generally samples different F_i from a distribution. This design ignores the fact that different scaling factors F_i in differential components of the mutation scheme influence distinct differential vectors, where each differential component contributes unique evolutionary information. Building on this insight, we hypothesize that the appropriate scaling factors F for the mutation operators should evolve independently, which is the motivation of this research.

2.3. GTOPX benchmark

GTOPX introduces seven constrained or unconstrained single-objective continuous minimization problems in space mission

Table 1
The basic information of GTOPX benchmark.

No.	Problem	Number of variables	Number of constraints	Best known optimum
1	Cassini1	6	4	4.9307
2	Cassini2	22	0	8.3830
3	Messenger (reduced)	18	0	8.6299
4	Messenger (full)	26	0	1.9579
5	GTOC1	8	6	-1 581 950.0
6	Rosetta	22	0	1.3434
7	Sagas	12	2	18.1877

trajectory scheduling. Without loss of generality, the problem in the GTOPX benchmark can be defined as follows [31].

$$\text{minimize } f(X), \text{ s.t. : } X \in \mathbb{R}^D$$

$$\begin{aligned} g_i(X) &\geq 0, \quad i = \{1, 2, \dots, j\} \\ h_i(X) &= 0, \quad i = \{1, 2, \dots, k\} \end{aligned} \quad (14)$$

where $f(X)$ is the objective function, $X = \{x_1, x_2, \dots, x_D\}$ is a trial solution. $g_i(X)$ and $h_i(X)$ denote the inequality and equality constraints, with the number of j and k , respectively. Different from the common definition of minimization problems, the inequality constraints are satisfied when the value is larger than 0. Table 1 summarizes the basic information of the GTOPX benchmark.

Cassini1 simulates a complex interplanetary mission trajectory to Saturn which consists of six decision variables representing trajectory parameters of velocity changes and the timing of this mission. The primary objective of this mission is for the spacecraft to be captured by Saturn's gravitational field and enter an elliptical orbit characterized by a pericenter radius of 108,950 km and a high eccentricity of 0.98. The mission trajectory requires a careful sequence of planetary flybys with the order Earth–Venus–Venus–Earth–Jupiter–Saturn. Each flyby contributes a gravitational boost, propelling the spacecraft toward Saturn while minimizing fuel consumption. Therefore, the objective function of this mission is to minimize the total velocity change accumulated across all phases of the mission.

Cassini2 simulates an advanced interplanetary mission to Saturn based on Cassini1, which contains 22 decision variables representing deep space maneuver (DSM) timings, flyby conditions, and approach velocities and is challenging for optimizers. The mission follows the trajectory of Earth–Venus–Venus–Earth–Jupiter–Saturn. Unlike the orbit insertion objective in Cassini1, Cassini2 requires a rendezvous with Saturn, where the spacecraft will match Saturn's velocity upon arrival. The primary objective of the Cassini2 benchmark is to minimize the total accumulated velocity change across all mission phases, which includes the launch from Earth, intermediate DSMs, and the final rendezvous maneuver, where the spacecraft must achieve a precise match with Saturn's orbital velocity. The mission sequence and DSMs allow for trajectory corrections in the vast interplanetary space between planetary encounters and provide the necessary fine-tuning required for a rendezvous mission.

Messenger (reduced) contains 18 decision variables involving timing and velocity changes for each flyby, and trajectory corrections en route to Mercury. This mission simulates a challenging interplanetary mission trajectory to Mercury similar to the real-world Messenger (full) mission but without the resonant flybys of Mercury. This simplification presents a streamlined trajectory that still captures the inherent complexities of this mission, which focuses on minimizing fuel consumption and efficient navigation through gravity assists. The specified sequence of planetary flybys is Earth–Earth–Venus–Venus–Mercury. Each flyby provides a critical gravitational boost, helping the spacecraft adjust its velocity and trajectory toward the inner solar system.

Messenger (full) involving 26 decision variables models a complex interplanetary mission to Mercury, structured to incorporate multiple

resonant flybys at Mercury itself, which serve as critical maneuvers to gradually reduce the spacecraft's velocity and achieve a controlled approach. The planetary sequence for this mission is defined as Earth–Venus–Venus–Mercury–Mercury–Mercury–Mercury. These consecutive flybys at Mercury are designed to use the planet's gravitational pull multiple times, allowing for incremental adjustments to the spacecraft's speed and trajectory without excessive fuel consumption, which is essential for missions to inner planets where deceleration is a significant challenge.

GTOC1 contains eight decision variables representing mission-critical parameters that govern the spacecraft's flyby maneuvers. This mission simulates a multi-gravity assist mission designed to reach and influence the orbit of asteroid TW229. The primary objective of this mission is to maximize the cumulative change in the asteroid's semi-major axis. To achieve this, the mission utilizes gravitational support from a carefully orchestrated sequence of planetary flybys with Earth–Venus–Earth–Venus–Earth–Jupiter–Saturn–TW229 to gain momentum efficiently while conserving fuel.

Rosetta simulates a complex multi-gravity assist mission to reach comet 67P/Churyumov-Gerasimenko. The objective of this mission is to minimize the cumulative velocity change required throughout the sequence of planetary flybys with Earth–Earth–Mars–Earth–Earth–67P, where 22 decision variables represent parameters critical to the mission's trajectory and maneuvers. The optimization of this sequence is essential in missions for deep-space bodies, where efficient fuel utilization is critical due to the extended distances and gravitational forces.

Sagas has 12 decision variables representing launch window timing, flyby encounter timing, and the direction of any required course adjustments. This mission simulates a maneuver aimed at enabling a spacecraft to perform a flyby of Jupiter and ultimately reach a target distance of 50 Astronomical Units (AU) from the Sun. The mission is designed to utilize the gravitational pull of Earth and Jupiter to accelerate the spacecraft and to achieve the high velocity needed to escape the inner solar system efficiently. The specific sequence is Earth–Earth–Jupiter, which capitalizes on the Earth's gravitational influence for an initial energy gain, then harnesses Jupiter's powerful gravitational field to impart a significant trajectory change and speed increase.

More details and problem definitions can refer to [20].

2.4. Literature review of space mission trajectory optimization

Space mission trajectory optimization is an important challenge in aerospace. The standard space mission trajectory optimization suite is provided by the European Space Agency's (ESA) Global Trajectory Optimization Competition (GTOC) named GTOPX. Each benchmark problem in GTOPX represents a specific space mission scenario, such as interplanetary trajectory design, flybys, rendezvous missions, or multi-objective optimizations involving fuel consumption, flight time, and mission costs. These problems are not only mathematically challenging but also reflect real-world constraints faced in space exploration, such as limited fuel, gravitational assists, orbital mechanics, and mission feasibility under strict constraints. In the meantime, many researchers and scholars attempt to develop efficient metaheuristic algorithms (MAs) to address these challenges.

Martin et al. [32] introduced MIDACO, a powerful optimization software designed to tackle the complex GTOPX benchmark. MIDACO is developed based on the Ant Colony Optimization (ACO) framework and integrated with the Oracle Penalty Method (OPM). By leveraging advanced heuristics and intelligent search strategies, MIDACO significantly accelerates the optimization convergence and reduces the required computational budget to reach near-optimal solutions from several years, as previously necessary with traditional methods, to just a few days.

Zuo et al. [33] introduced a Case Learning-based Differential Evolution (CLDE) to address space mission trajectory optimization challenges. The proposed CLDE features storing successful control parameters during the optimization process and retrieving reference information based on geographic similarity in each generation to facilitate parameter adaptation. Furthermore, two variants were developed to enhance the performance: Global CLDE (G-CLDE) and Local CLDE (L-CLDE), which aim to address different aspects of the optimization landscape. G-CLDE focuses on global exploration, which encourages the optimization direction to the unknown search domain, while L-CLDE emphasizes local exploitation and refines solutions in promising regions. By integrating G-CLDE and L-CLDE, the proposal achieves a balanced optimization and produces highly competitive results on the GTOP benchmark within a reasonable computational budget.

Zuo et al. [34] identified that the optimal value of fuel consumption configuration in the GTOP benchmark is challenging. To address this task, a Guided Differential Evolution (G-DE) was proposed, which incorporates a two-stage evolutionary process designed to enhance both global and local search capabilities. In the initial stage, G-DE focuses on learning the global structure of the problem landscape, while in the later stage, G-DE transitions to a self-adaptive approach to refine solutions by exploiting promising areas more intensively. Through these two phases, G-DE employs four distinct guidance strategies based on insights from the population distribution, which allows it to adjust its search behavior according to the optimization landscape dynamically. The experimental results on both the CEC2017 and GTOP benchmark suites demonstrate the competitiveness of G-DE against recently proposed DE variants.

Choi et al. [35] introduced a Self-Adaptive/Self-Learning Differential Evolution (SASLDE) to address the limitations of dependency on predetermined mutation strategies and fixed control parameters. Unlike conventional DE approaches, SASLDE dynamically adjusts both the mutation strategy and control parameters during the optimization process. To further enhance its robustness, SASLDE incorporates a re-initialization technique to mitigate premature convergence to local optima, a common challenge when solving complex problems. By reintroducing diversity into the population, this technique significantly improves the ability of SASLDE to explore the solution space effectively. Extensive comparative analyses with state-of-the-art EAs demonstrate that SASLDE achieves remarkable performance, which successfully converges better than five advanced EAs. Additionally, SASLDE exhibits strong potential as a local or auxiliary search algorithm to effectively enhance the performance of other EAs through integration.

Tang et al. [36] addressed the extreme nonlinearity and the abundance of locally optimal solutions in the GTOP benchmark by proposing a Hybrid L-SHADE (HL-SHADE) algorithm. Recognizing the difficulty of navigating in complex search spaces, HL-SHADE combines the strengths of L-SHADE with an enhanced exploitation mechanism to improve local search efficiency. Once the global search identifies a promising solution, a novel two-step local search process is activated. This local search equipped with an adaptive control parameter strategy dynamically adjusts search parameters based on the problem landscape. The effectiveness of HL-SHADE is thoroughly validated through rigorous numerical experiments on the CEC benchmark and the GTOP benchmark against ten L-SHADE variants, six well-known optimizers, and eleven optimizers from the PyGMO library. The results consistently demonstrated the superior performance of HL-SHADE with significant improvements in optimization accuracy and convergence speed.

Peng et al. [37] identified significant challenges in tackling the GTOP benchmark, including the presence of multiple constraints, extreme non-linearity, and high sensitivity to initial conditions. To address these challenges, they proposed an innovative Reinforcement Learning-based Hybrid DE termed RL-HDE, which introduces a novel

multi-mutation L-SHADE-based strategy to enhance global exploration capability. To further refine the balance between global exploration and local exploitation within RL-HDE, a parameter adaptive strategy based on Q-Learning is developed to dynamically adjust two critical parameters. The efficacy of RL-HDE is rigorously validated using the GTOP benchmarks. Comprehensive experimental comparisons are conducted against ten state-of-the-art hybrid evolutionary algorithms, four interplanetary trajectory design algorithms, and seven reinforcement learning-based approaches. The results demonstrate that RL-HDE consistently outperforms its competitors in terms of both convergence efficiency and solution accuracy.

Song et al. [38] observed that SMT0 presents significant challenges due to its inherent characteristics, such as long flight durations, high fuel consumption, complex gravity-assist sequences, and stringent constraints. These factors contribute to an exceptionally large number of decision variables and an expansive search space for transfer trajectory design, which limit the convergence quality and global searchability of traditional MAs. To tackle these issues, an improved gravity-assist space pruning algorithm was proposed to effectively reduce the search space and enhance trajectory optimization. The algorithm introduces a unique pruning procedure that systematically eliminates less promising regions of the search space. To better represent the feasible solution domain, the algorithm employs a hybrid solution space box bounds approach. Additionally, an automatic determination method for solution space box bounds is incorporated into dynamic adjustments based on the characteristics of problems. The effectiveness of the improved algorithm is verified through a sensitivity analysis of the pruning effect to key parameters, as well as a performance comparison of three representative MAs: DE, Bat Algorithm (BA), and Firefly Algorithm (FA). Simulation results demonstrated that the improved pruning algorithm significantly enhanced the performance of the DE algorithm, which outperformed both the BA and FA in terms of convergence speed and optimization accuracy.

Yuan et al. [39] built upon the success of the Improved Multi-Operator DE (IMODE), the winner of CEC2020, to propose an enhanced variant called IMODE-TMS, which integrates a novel Two-Phase Migration Strategy (TMS) into IMODE to improve its efficiency in handling the inefficiency of the random information-sharing mechanism of IMODE. In the first phase of TMS, the elite individuals within each sub-population are preserved to focus on exploitation. Simultaneously, all lower-ranked individuals are reassigned to three sub-populations to maintain sufficient population diversity and prevent premature convergence. The second phase is designed to counteract stagnation. When a sub-population is identified as stagnant through a stagnation indicator, the optimal individual from another sub-population migrates into the stagnant one with a uni-directional ring structure. The performance of IMODE-TMS is investigated in CEC2020, CEC2021, CEC2022, and the GTOP benchmark. The experimental results demonstrate that IMODE-TMS significantly outperforms IMODE and several state-of-the-art optimizers in solution quality and convergence speed.

Although numerous advanced MAs have been developed to address the challenges of SMT0, much of the existing research has primarily concentrated on the GTOP benchmark - a seminal and widely utilized SMT0 benchmark introduced in 2005. While GTOP has played a pivotal role in advancing optimization methods for trajectory design, its scope is now considered limited in capturing the broader complexities of modern space exploration missions. Therefore, this paper shifts focus to a more demanding and comprehensive benchmark: GTOPX, an extended version of GTOP that introduces additional tasks and greater diversity in problem scenarios. GTOPX inherits the multi-constraint, non-linear, and high-dimensional nature of the GTOP benchmark and incorporates new challenges. We propose an advanced ISHACDE to handle these tasks, which aims to address the gaps in current research and evaluate the adaptability of advanced MAs in more intricate SMT0 problems.

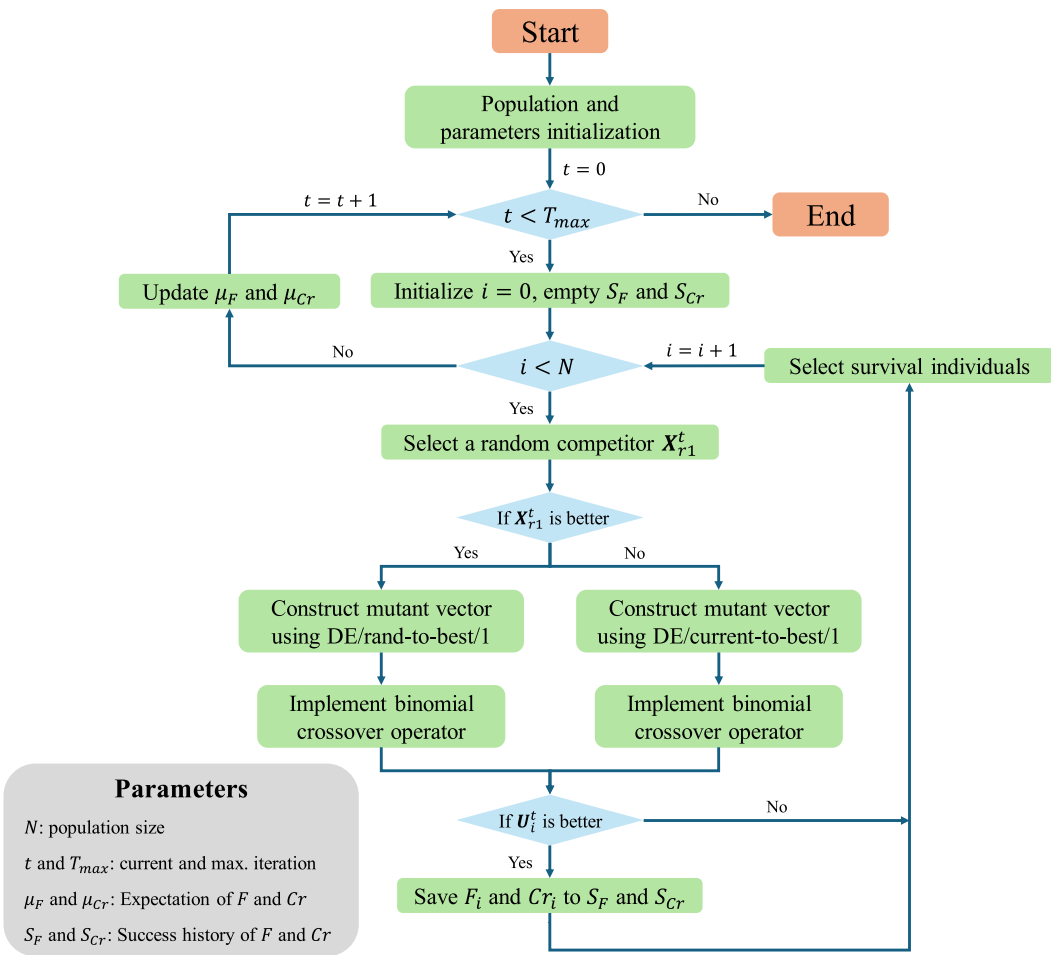


Fig. 3. The flowchart of ISHACDE.

3. Our proposal: ISHACDE

This section begins by presenting the flowchart of ISHACDE in Fig. 3. We first introduce the parameters used in ISHACDE: N represents the population size, t and T_{max} denote the current and maximum iteration, μ_F and μ_{Cr} are the sampling expectations of the scaling factor F and crossover rate Cr , and S_F and S_{Cr} are arrays that store F and Cr values from the success history.

Initially, ISHACDE begins by initializing the population and setting the required parameters to ensure a set of candidate solutions to explore the search space. Subsequently, ISHACDE enters the main optimization loop, where it iteratively refines the population to converge toward optimal solutions. For each individual in the population, ISHACDE inherits its main search operators from CDE that selects a competitor individual X_{r1}^t from the population. If the competitor X_{r1}^t has a better fitness than the current individual X_i^t , ISHACDE constructs an offspring using the DE/rand-to-best/1 mutation operator coupled with the binomial crossover operator. This combination introduces diversity while guiding the search toward the global optimum by utilizing the current best individual in the population, and the DE/rand-to-best/1 strategy ensures that ISHACDE effectively explores promising regions of the search space and allows a probability to escape local optima.

On the other hand, if the competitor X_{r1}^t has a worse fitness value, ISHACDE activates the DE/current-to-best/1 mutation operator with the binomial crossover. This approach emphasizes local exploitation, as it refines the current individual by perturbation constructed using the current best individual with a degree of randomness. This adaptive switching mechanism between the two efficient mutation

operators introduces flexibility into the search process and enhances the population diversity. By automatically and intelligently switching between global exploration (i.e., DE/rand-to-best/1) and local exploitation (i.e., DE/current-to-best/1), ISHACDE ensures a dynamic balance during optimization, which promotes rapid optimization while maintaining robustness against stagnation.

In the selection process, if the constructed offspring individual U_i^t is better, U_i^t will survive, and the corresponding F_i and Cr_i are stored in S_F and S_{Cr} , respectively; otherwise, X_i^t will survive. This mutation-crossover-selection process continues for each individual until the current population is updated. Then, μ_F and μ_{Cr} are adjusted using the independent success history adaptation scheme. In the following sections, we will introduce the independent success history adaptation scheme in detail.

The mutation operator DE/winner-to-best/1, as defined in Eq. (2), utilizes four key scaling factors - F_1 , F_2 , F_3 , and F_4 - each sampled from related distributions. These scaling factors provide nuanced control over different elements of the mutation scheme. However, studies such as those by Tanabe et al. [23,24], Brest et al. [40], Biswas et al. [41], Kitamura [42], and Ghosh [43] have often ignored the independent significance of each scaling factor. Instead, F is frequently sampled from identical distributions multiple times or even reused directly across mutation steps, which neglects the distinct amplification roles. However, each scaling factor uniquely influences mutation by amplifying or moderating specific vector components, which can be critical in guiding convergence and exploration. For instance, in DE/current-to-best/1 formulated in Eq. (15), the scaling factor F_1 and F_2 enable differential weight adjustments for different components as shown in

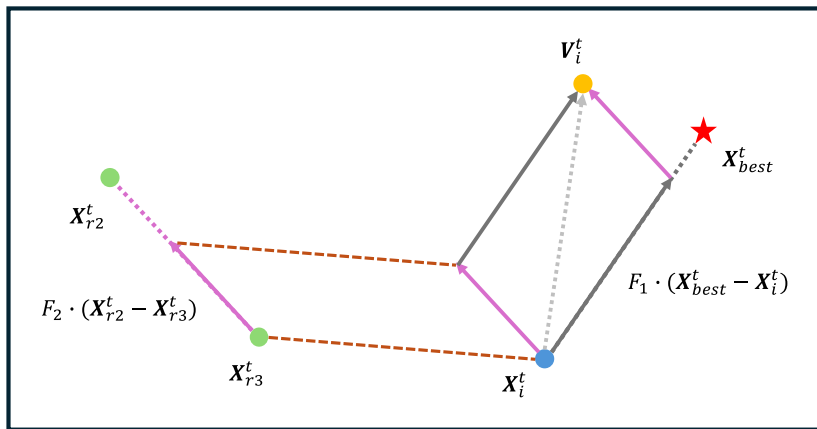


Fig. 4. A demonstration of the DE/current-to-best/1 mutation scheme.

Fig. 4.

$$V_i^t = X_i^t + F_1 \cdot (X_{best}^t - X_i^t) + F_2 \cdot (X_{r2}^t - X_{r3}^t) \quad (15)$$

In this visualization, the blue circle represents the current individual X_i^t , while the green circles indicate the randomly selected individuals X_{r2}^t and X_{r3}^t . The yellow circle denotes the mutant individual V_i^t generated using DE/current-to-best/1 mutation strategy, and the red star is the current best individual X_{best}^t in the population. Two critical components of this scheme are the differential vectors represented by $F_1 \cdot (X_{best}^t - X_i^t)$ and $F_2 \cdot (X_{r2}^t - X_{r3}^t)$, denoted by gray and purple arrow lines, respectively. Clearly, the differential vectors $(X_{best}^t - X_i^t)$ and $(X_{r2}^t - X_{r3}^t)$ in different directions reflect the capacity of ISHACDE to balance exploration (i.e., using differential vector constructed by X_{r2}^t and X_{r3}^t) and exploitation (i.e., using differential vector constructed by X_i^t and X_{best}^t). These vectors are controlled by the scaling factors F_1 and F_2 , which determine the magnitude of the movement in each direction. These scaling factors are crucial since they dictate the extent to which ISHACDE moves toward either the global best or other diverse areas in the search space.

Based on the distinct impact of these differential vectors, we reasonably hypothesize that the optimal distribution of F_1 and F_2 may vary depending on the specific characteristics of the optimization problem. A fixed or simultaneous evolution of F_1 and F_2 may not fully capture the nuances of the search dynamics needed for efficient convergence. Therefore, we propose an independent success history adaptation scheme for F_1 and F_2 , which allows ISHACDE to adaptively adjust these scaling factors based on historical experiences. This approach is designed to promote successful evolution by tailoring the search behavior to the fitness landscape of the problem, thereby enhancing both convergence speed and solution quality.

Since four scaling factors from F_1 to F_4 exist in the DE/winner-to-best/1 mutation operator, we reasonably believe that the equipment of four hyper-parameters with the independent success history adaptation scheme can accelerate optimization rather than sampling them from an identical distribution. In summary, the pseudocode of the proposed ISHACDE is presented in Algorithm 1.

4. Numerical experiments

This section provides numerical experiments to validate the competitiveness of our proposed ISHACDE with state-of-the-art optimization algorithms. Section 4.1 summarizes the experimental settings including experimental environments and parameters of competitor algorithms. Section 4.2 presents the experimental results and performance analysis.

Algorithm 1: ISHACDE

```

Input: Population size:  $N$ , Dimension:  $D$ , Max. iteration:  $T$ 
Output: Optimum:  $X_{best}^t$ 
1 Function ISHACDE( $N, D, T$ ):
2   Population initialization and evaluation
3   Set  $\mu_{F_1} = 0.5$ ,  $\mu_{F_2} = 0.5$ ,  $\mu_{F_3} = 0.5$ , and  $\mu_{F_4} = 0.5$ 
4   Set  $\mu_{Cr_1} = 0.5$  and  $\mu_{Cr_2} = 0.5$ 
5    $t = 0$ 
6   while  $t < T$  do
7     Initialize empty arrays  $S_{F_1}$ ,  $S_{F_2}$ ,  $S_{F_3}$ , and  $S_{F_4}$ 
8     Initialize empty arrays  $S_{Cr_1}$  and  $S_{Cr_2}$ 
9     for  $i = 0$  to  $N$  do
10       Select a random competitor  $X_{r1}^t$ 
11       if  $X_{r1}^t$  has a better fitness than  $X_i^t$  then
12         Sampling  $F_1$ ,  $F_2$ , and  $Cr_1$  using Eq. (5)
13         Construct mutant vector using
14           DE/rand-to-best/1 mutation scheme
15         Construct offspring individual  $U_i^t$  using binomial
16           crossover
17         if  $U_i^t$  has a better fitness than  $X_i^t$  then
18             Survive the individual  $U_i^t$ 
19             Save  $F_1$  and  $F_2$  to  $S_{F_1}$  and  $S_{F_2}$  respectively
20             Save  $Cr_1$  to  $S_{Cr_1}$ 
21         end
22     end
23     else
24       Sampling  $F_3$ ,  $F_4$ , and  $Cr_2$  using Eq. (5)
25       Construct mutant vector using
26         DE/current-to-best/1 mutation scheme
27       Construct offspring individual  $U_i^t$  using binomial
28         crossover
29       if  $U_i^t$  has a better fitness than  $X_i^t$  then
30         Survive the individual  $U_i^t$ 
31         Save  $F_3$  and  $F_4$  to  $S_{F_3}$  and  $S_{F_4}$  respectively
32         Save  $Cr_2$  to  $S_{Cr_2}$ 
33       end
34     end
35   Update  $\mu_{F_1}$ ,  $\mu_{F_2}$ ,  $\mu_{F_3}$ , and  $\mu_{F_4}$  using Eq. (6)
36   Update  $\mu_{Cr_1}$  and  $\mu_{Cr_2}$  using Eq. (7)
37   Optimum  $X_{best}^t$  update
38    $t = t + 1$ 
39 end
40 return  $X_{best}^t$ 

```

4.1. Experimental settings

4.1.1. Experimental environments and implementation

We conduct numerical experiments using Python 3.11, executed on a Lenovo Legion R9000P running Windows 11. The configuration of system hardware includes an AMD Ryzen 7 5800H processor with Radeon Graphics, clocked at 3.20 GHz, and 16 GB of RAM.

4.1.2. Benchmark functions

We conduct numerical experiments on diverse benchmark functions to comprehensively evaluate the performance of ISHACDE. The details of benchmarks are listed as follows:

- CEC2017:** CEC2017 contains 29 benchmark functions ranging from multimodal to composite functions. It is worth noticing that f_2 is disabled and f_{30} serves as compensation. We employ 30- and 50-D functions to investigate the performance of ISHACDE in solving median-scale optimization problems. This benchmark is provided by Opfunu library [44].
- CEC2020:** CEC2020 contains 10 various benchmark functions. We employ 50- and 100-D functions to investigate the performance of ISHACDE in solving large-scale optimization problems. This benchmark is provided by Opfunu library [44].
- CEC2022:** CEC2022 contains 12 benchmark functions. We employ 10- and 20-D functions to investigate the performance of ISHACDE in solving small-scale optimization problems. This benchmark is provided by Opfunu library [44].
- GTOPX:** We employ single-objective SMTO problems from GTOPX to investigate the performance of ISHACDE in real-world scenarios. The GTOPX benchmark can be downloaded from <http://www.midaco-solver.com/index.php/about/benchmarks/gtopx> and <https://github.com/RuiZhong961230/ISHACDE>.

For more details of CEC benchmark functions refer to [Appendix A](#).

4.1.3. Compared methods and parameters

To comprehensively and fairly evaluate the performance of our proposed ISHACDE on SMTO tasks, we employ a total of twenty optimization algorithms as competitors. This set includes ten state-of-the-art optimizers and ten recently proposed approaches, which are provided by the MEALPY [45] and summarized as follows.

- State-of-the-art optimizers and their variants:** PSO [46], DE [11], covariance matrix adaptation evolution strategy (CMA-ES) [47], self-adaptive DE (SaDE) [48], comprehensive learning PSO (CL-PSO) [49], chaotic PSO [50], JADE [21], SHADE [23], L-SHADE [24], and phasor PSO (PPSO) [51].
- Recently proposed approaches:** MPA [52], fox optimizer (FOX) [53], pelican optimization algorithm (POA) [54], osprey optimization algorithm (OOA) [55], energy valley optimizer (EVO) [56], coati optimization algorithm (COA) [57], FLA [58], RIME algorithm [59], DE architecture based adaptive hyper-heuristic (DEA^2H^2) [60], and CDE [22].

The parameters of these approaches are summarized in [Tables 2](#) and [3](#). The μ_F and μ_{Cr} in ISHACDE are fixed at 0.5, σ_F and σ_{Cr} are set to 0.1 as suggested in [23,24]. Except for L-SHADE, the population size of other optimizers is fixed at 100, and the maximum fitness evaluation (Max_{FE}) for CEC benchmarks and SMTO is set to $1000 \times$ dimension and 200,000, respectively. Each algorithm is independently repeated 30 times to alleviate the impact of randomness. Furthermore, Cassini1, GTOC1, and Sagas in the GTOPX benchmark contain constraints, while the original optimization approaches cannot address contained optimization problems. Therefore, we equip the static penalty function [61] to all algorithms, which is defined in Eq. (16).

$$F(X) = f(X) + w \cdot \sum_{i=1}^m (\max(0, -g_i(X))) \quad (16)$$

Table 2

The parameters of state-of-the-art optimizers.

Alg.	Parameters	Value
PSO	Inertia factor w	1
	Acceleration coefficients c_1 and c_2	2.05
	Max. and min. speed	2 and -2
DE	Scaling factor F	0.8
	Crossover rate Cr	0.9
	Mutation scheme	DE/cur-to-best/1/bin
CMA-ES	Hyperparameter-free	
SaDE	μ_F and σ_F	0.5 and 0.3
	μ_{Cr} and σ_{Cr}	0.5 and 0.1
	Mutation scheme	DE/rand/1 and DE/cur-to-best/1
CL-PSO	Local coefficient c_{local} Max. and min. weight	1.2 0.9 and 0.4
CPSO	σ , C , and ϵ	0.05, 100, and 0.5
	Mutation scheme	DE/cur-to-pbest/1
	μ_F and μ_{Cr} σ_F and σ_{Cr}	0.5 and 0.5 0.1 and 0.1
JADE	μ_F and μ_{Cr} σ_F and σ_{Cr}	0.5 and 0.5 0.1 and 0.1
	Population size	18 \times D
	μ_F and μ_{Cr} σ_F and σ_{Cr}	0.5 and 0.5 0.1 and 0.1
L-SHADE	Hyperparameter-free	

Table 3

The parameters of recently proposed approaches.

Alg.	Parameters	Value
MPA	$FAdS$	0.2
FOX	Jumping probabilities c_1 and c_2	0.18 and 0.82
POA	Parameter-free	
OOA	Parameter-free	
EVO	Parameter-free	
COA	Parameter-free	
FLA	C_1, C_2, C_3, C_4 , and C_5	0.5, 2.0, 0.1, 0.2, 2.0
	D	0.01
RIME	Parameter w	5
DEA 2 H 2	Search radius R	1
CDE	Distribution of F and Cr	$N(0.5, 0.3)$ and $N(0.5, 0.3)$

where $F(\cdot)$ is the fitness function, $f(\cdot)$ is the objective function, and $g_i(\cdot)$ is the constraint function. In this research, $g_i(\cdot) \geq 0$ indicates that the constraint is satisfied. w is a constant set to $10e7$ to control the level of penalty [62].

4.2. Experimental results and analysis

This section presents the experimental results and statistical analysis to confirm the competitiveness of our proposed ISHACDE. We first present the optimization results on CEC2017, CEC2020, and CEC2022 on Sections 4.2.1, 4.2.2, and 4.2.3, respectively. Finally, the experimental results and statistical analysis on GTOPX the benchmark are summarized in Section 4.2.5.

4.2.1. Experimental results on CEC2017

The detailed experimental results and statistical analysis of ISHACDE and competitor algorithms on CEC2017 are summarized in [Appendix B](#). To identify the statistical significance between our proposed ISHACDE and other optimizers, we initially employ the Mann-Whitney U test between every pair of optimizers, and the obtained p-values are corrected using the Holm multiple comparison test with the p-value rank. Markers +, \approx , and - indicate that our proposed ISHACDE is significantly better, without statistical significance, and significantly worse than the specific competitor optimizer.

Table 4

The summary of statistical analysis between ISHACDE and state-of-the-art optimizers on CEC2017.

	Dims	PSO	DE	CMA-ES	SaDE	CL-PSO	CPSO	JADE	SHADE	L-SHADE	PPSO
+/- summary	30-D	29/0/0	29/0/0	24/1/4	24/4/1	29/0/0	28/0/1	25/4/0	22/5/2	22/4/3	28/1/0
+/- summary	50-D	29/0/0	29/0/0	25/2/2	23/4/2	27/2/0	27/0/2	22/7/0	17/8/4	18/7/4	27/2/0

Table 5

The summary of statistical analysis between ISHACDE and recently proposed optimizers on CEC2017.

	Dims	MPA	FOX	POA	OOA	EVO	COA	FLA	RIME	DEA ² H ²	CDE
+/- summary	30-D	23/1/5	28/1/0	23/4/2	28/1/0	26/2/1	29/0/0	25/2/2	18/4/7	18/6/5	23/4/2
+/- summary	50-D	23/1/5	25/3/1	24/2/3	28/1/0	26/2/1	29/0/0	23/4/2	17/7/5	18/6/5	22/6/1

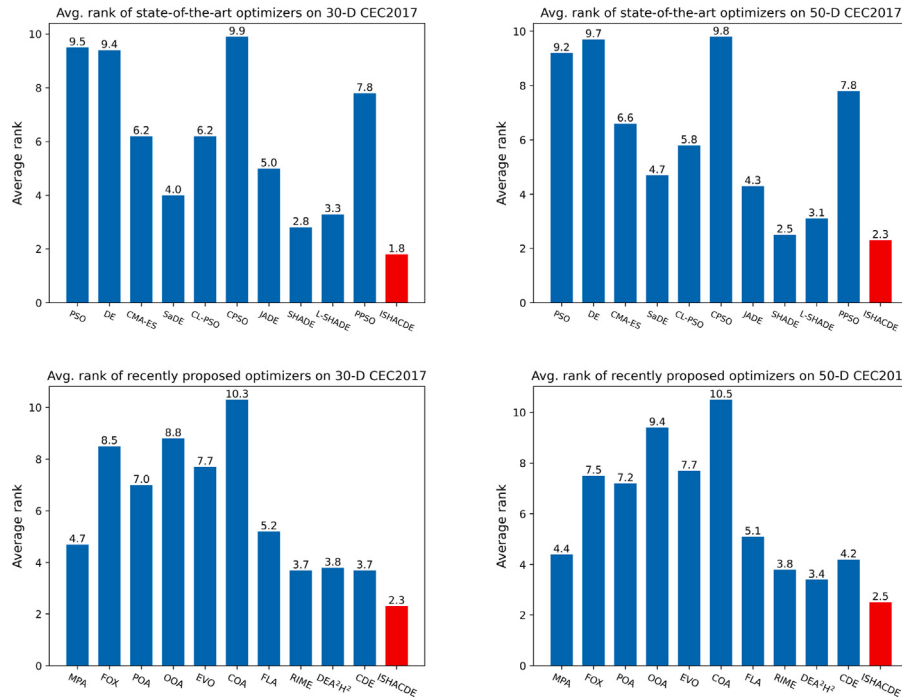


Fig. 5. Average ranks of optimizers on CEC2017.

Here, we present the summary of statistical analysis on CEC2017 in Tables 4 and 5. Fig. 5 presents the average ranks of competitor optimizers on CEC2017. Convergence curves, exploration-exploitation proportions of ISHACDE, and boxplots of optimizers on CEC2017 representative functions (i.e., f_1 : Unimodal function; f_6 : Multimodal function; f_{12} and f_{17} : Hybrid functions; f_{24} and f_{30} : Composite functions) are presented in Figs. 6 and 7, where the proportion between exploration and exploitation is defined Eq. (17) [63].

$$\begin{aligned} Div^t &= \frac{1}{D} \sum_{d=1}^D \frac{1}{N} \sum_{i=1}^N |\mathbf{X}_{mean,d}^t - \mathbf{X}_{i,d}^t| \\ Exploration &= \frac{Div^t}{Div_{max}} \\ Exploitation &= \frac{|Div^t - Div_{max}|}{Div_{max}} \end{aligned} \quad (17)$$

where D is the dimension size and N denotes the population size. \mathbf{X}_{mean}^t represents the mean of the population in the t th iteration and \mathbf{X}_i^t is the i th individual in the t th iteration. Similar to the definition of standard deviation, Div^t describes the dispersion of the population to the mean.

The experimental results and statistical analysis confirm the efficiency and superiority of our proposed ISHACDE on median-scale CEC2017 benchmark functions. This is particularly evident from the summary of statistical significance in Tables 4 and 5 and the average ranks presented in Fig. 5. Compared to state-of-the-art optimizers such as CMA-ES, JADE, SHADE, and L-SHADE, ISHACDE performs

significantly better. Specifically, it outperforms CMA-ES on 24 and 25 instances in 30-D and 50-D; JADE on 25 and 22 instances in 30-D and 50-D; SHADE on 22 and 17 instances in 30-D and 50-D; and L-SHADE on 22 and 18 instances in 30-D and 50-D. When compared to recently proposed optimizers such as MPA, RIME, DEA²H², and the original CDE, ISHACDE significantly outperforms MPA on 23 instances in both 30-D and 50-D; RIME on 18 and 17 instances in 30-D and 50-D; DEA²H² on 18 instances in both 30-D and 50-D; and CDE on 23 and 22 instances in 30-D and 50-D. Although ISHACDE is significantly worse than specific optimizers in some instances, the metric of the average ranks further highlights the state-of-the-art performance of our proposed ISHACDE.

The rapid convergence speed of ISHACDE is clearly demonstrated by the convergence curves presented in Figs. 6 and 7, where ISHACDE quickly converges toward elite solutions. This accelerated convergence highlights the effectiveness of the integrated independent success history adaptation scheme in ISHACDE in guiding the evolution direction in the solution space. Moreover, the remarkable robustness and stability of ISHACDE are visually evident from the boxplots. These plots show the consistent performance of ISHACDE across multiple independent runs, with narrow interquartile ranges and few outliers, indicating minimal variance in results. Such stability is crucial for practical applications, where reliable performance over a range of conditions is often more valuable than exceptional performance in single cases.

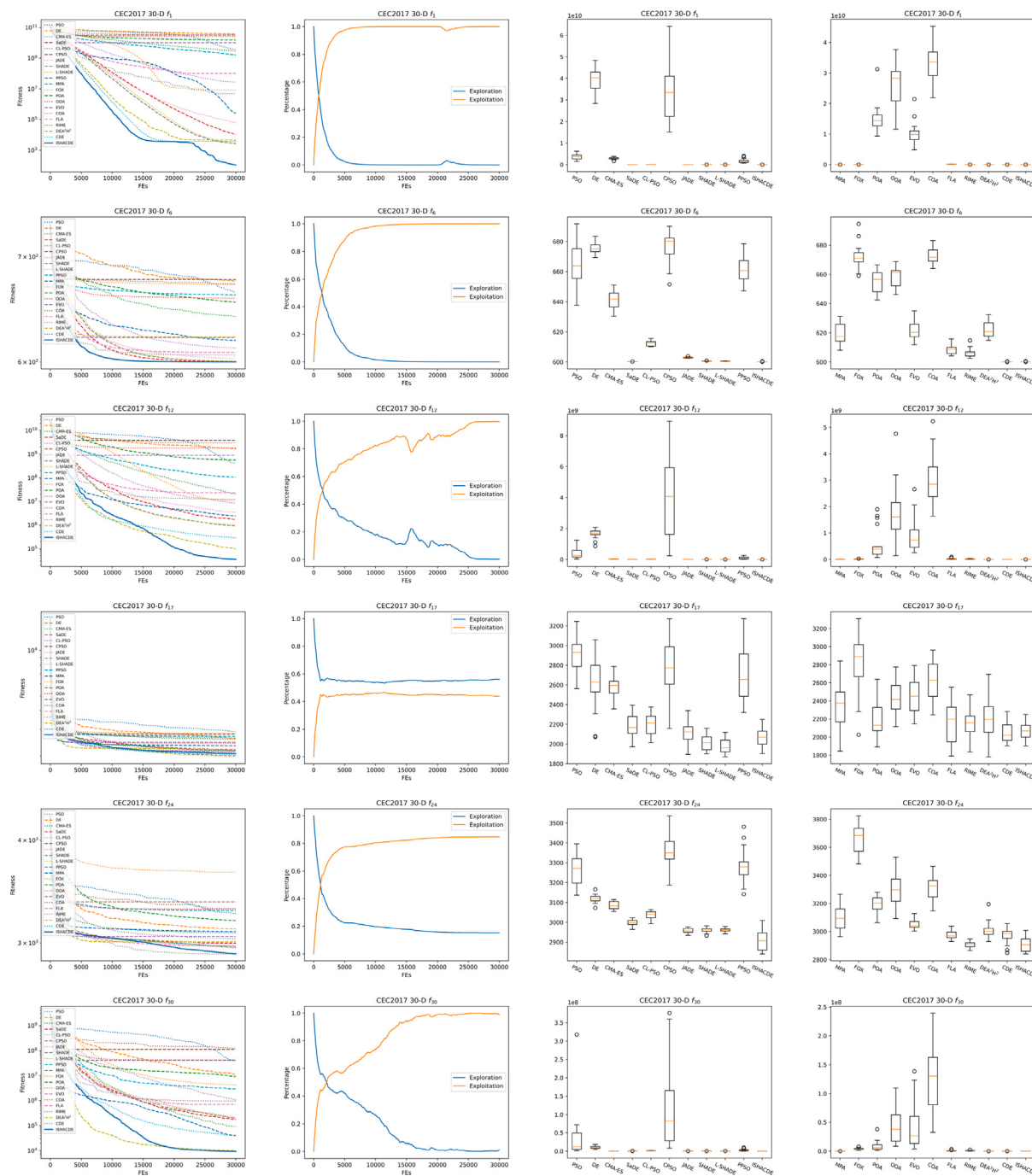


Fig. 6. Convergence curves, exploration-exploitation proportions of ISHACDE, and boxplots of optimizers on 30-D CEC2017 representative functions.

Additionally, the balanced exploration and exploitation behaviors of ISHACDE presented in Figs. 6 and 7 affirm the efficiency and effectiveness of its search operator design and parameter adaptation scheme. These figures show how ISHACDE adeptly navigates the search space and avoids premature convergence while still maintaining focus on promising regions. In simple functions such as \$f_1\$ and \$f_4\$, the rapid switch focusing on exploitation accelerates the optimization and approach to the near-optimum, while in complex functions such as \$f_{15}\$ and \$f_{30}\$, the careful balance between global exploration and local exploitation ensures that ISHACDE not only explores a wide range of potential solutions but also refines its search in high-quality areas, which achieves more accurate convergence.

4.2.2. Experimental results on CEC2020

The detailed experimental results and statistical analysis of ISHACDE and competitor algorithms on CEC2020 are summarized in Appendix C. Here we summarize the statistical analysis between ISHACDE and competitor optimizers on CEC2020 in Tables 6 and 7. Fig. 8 presents the average ranks of competitor optimizers on CEC2020, while convergence curves, exploration-exploitation proportions of ISHACDE, and boxplots of optimizers on CEC2020 representative functions (i.e., \$f_1\$: Unimodal function; \$f_4\$: Multimodal function; \$f_6\$ and \$f_7\$: Hybrid functions; \$f_9\$ and \$f_{10}\$: Composite functions) are demonstrated in Figs. 9 and 10.

The superior performance of ISHACDE is observable on CEC2020 benchmark functions from the summarized experimental results and

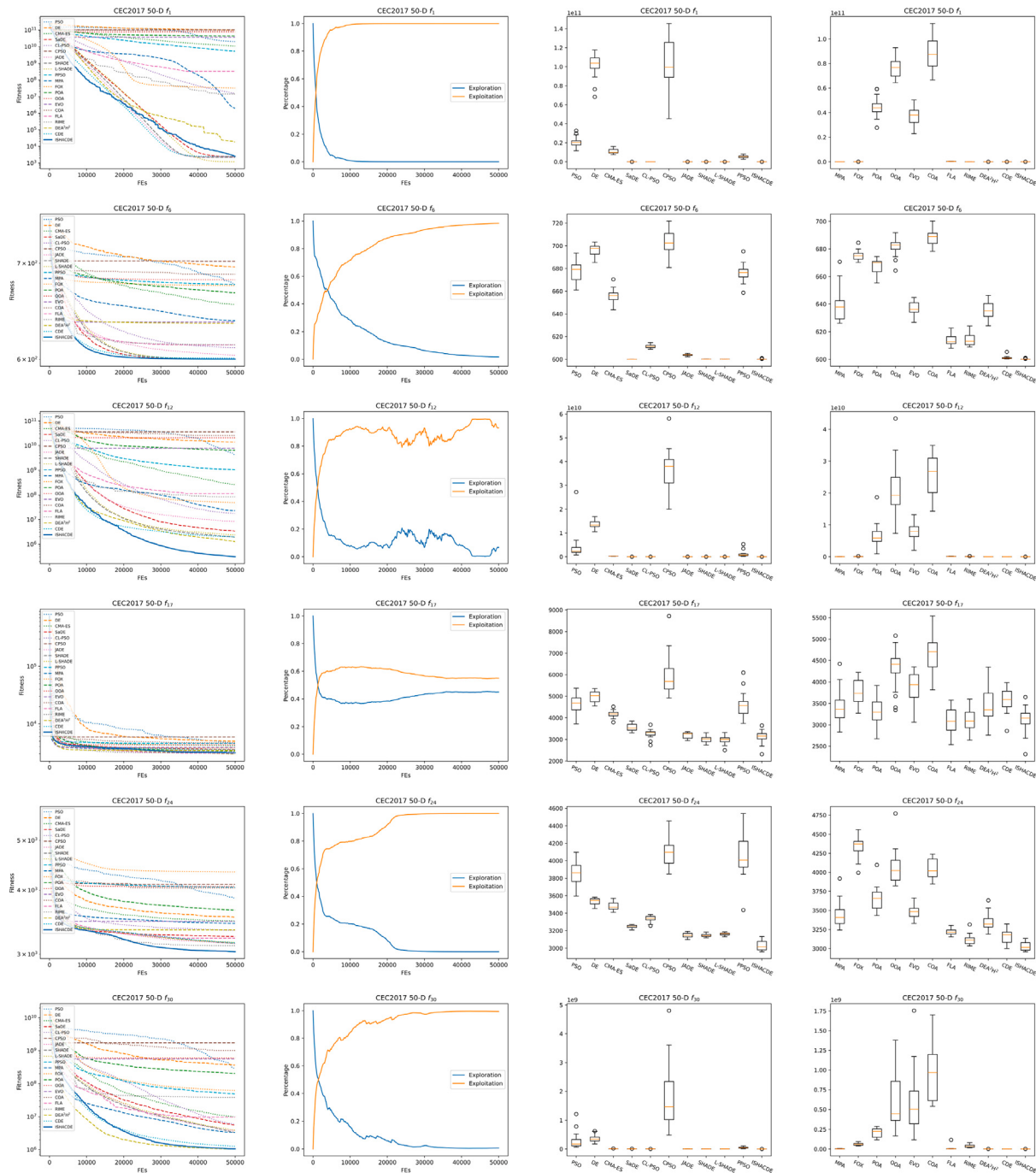


Fig. 7. Convergence curves, exploration-exploitation proportions of ISHACDE, and boxplots of optimizers on 50-D CEC2017 representative functions.

Table 6

The summary of statistical analysis between ISHACDE and state-of-the-art optimizers on CEC2020.

	Dims	PSO	DE	CMA-ES	SaDE	CL-PSO	CPSO	JADE	SHADE	L-SHADE	PPSO
+/- summary	50-D	10/0/0	10/0/0	10/0/0	6/3/1	9/1/0	10/0/0	6/2/2	7/2/1	7/2/1	10/0/0
+/- summary	100-D	10/0/0	10/0/0	10/0/0	5/4/1	9/0/1	10/0/0	5/2/3	5/4/1	6/3/1	10/0/0

Table 7

The summary of statistical analysis between ISHACDE and recently proposed optimizers on CEC2020.

	Dims	MPA	FOX	POA	OOA	EVO	COA	FLA	RIME	DEA ² H ²	CDE
+/- summary	50-D	10/0/0	10/0/0	10/0/0	10/0/0	10/0/0	10/0/0	10/0/0	10/0/0	9/0/1	9/1/0
+/- summary	100-D	10/0/0	10/0/0	10/0/0	10/0/0	10/0/0	10/0/0	10/0/0	10/0/0	10/0/0	10/0/0

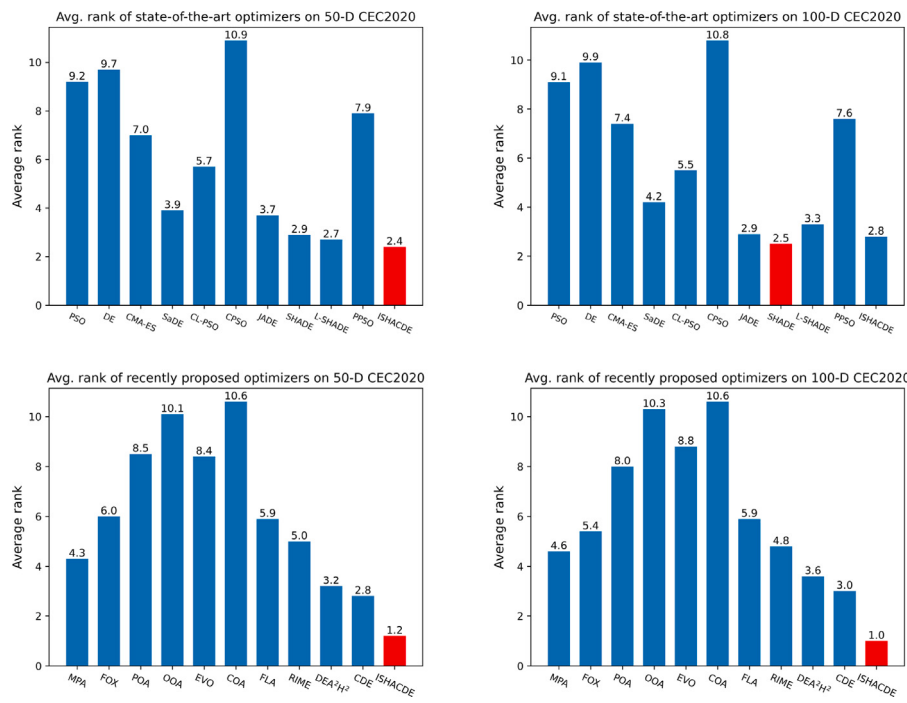


Fig. 8. Average ranks of optimizers on CEC2020.

statistical analysis. Compared to state-of-the-art optimizers such as CMA-ES, JADE, SHADE, and L-SHADE, ISHACDE outperforms CMA-ES on 10 instances in both 50-D and 100-D; JADE on 6 and 5 instances in 50-D and 100-D; SHADE on 7 and 5 instances in 50-D and 100-D; and L-SHADE on 7 and 6 instances in 50-D and 100-D. When compared to recently proposed optimizers such as MPA, RIME, DEA²H², and the original CDE, ISHACDE significantly outperforms MPA on 10 instances in both 50-D and 100-D; RIME on 10 instances in both 50-D and 100-D; DEA²H² on 9 and 10 instances in 50-D and 100-D; and CDE on 9 and 10 instances in 50-D and 100-D.

Meanwhile, we observe that as the dimension of the optimization problem increases from 50 to 100, the competitiveness of algorithms such as SaDE, JADE, SHADE, and L-SHADE also improves. This trend is also evident in CEC2017 benchmark functions the dimension increasing from 30 to 50, where these algorithms demonstrate enhanced scalability in higher-dimensional problem spaces.

This improvement in performance with the increasing dimension suggests that these algorithms adapt well to the complexity of high-dimensional landscapes. In contrast, we infer that the scalability and adaptability of the proposed ISHACDE are relatively weaker compared to SaDE, JADE, SHADE, and L-SHADE in handling high-dimensional problems. The reduced competitiveness of ISHACDE in these cases may be attributed to the inherent design of CDE, which might not fully utilize the historical experiences and knowledge efficiently.

Although the relative weakness in the scalability of ISHACDE is observed, ISHACDE still outperforms these state-of-the-art optimizers on the more challenging high-dimensional CEC2020 benchmark functions generally. This indicates that while SaDE, JADE, SHADE, and L-SHADE have remarkable performance in some instances, the effective searchability of ISHACDE maintains its competitiveness in complex optimization tasks.

4.2.3. Experimental results on CEC2022

The detailed experimental results and statistical analysis of ISHACDE and competitor algorithms on CEC2022 are summarized in Appendix D. Here we summarize the statistical analysis between ISHACDE and competitor optimizers on CEC2022 in Tables 8 and 9. Fig. 11 presents the average ranks of competitor optimizers on

CEC2022. Convergence curves, exploration-exploitation proportions of ISHACDE, and boxplots of optimizers on CEC2022 representative functions (i.e., f_1 : Unimodal function; f_2 and f_3 : Multimodal functions; f_7 : Hybrid function; f_9 and f_{12} : Composite functions) are presented in Figs. 12 and 13.

The excellent optimization results of ISHACDE in CEC2022 confirm its efficiency, effectiveness, and scalability. Compared to state-of-the-art optimizers CMA-ES, JADE, SHADE, and L-SHADE, ISHACDE performs significantly better than CMA-ES on 10 instances in both 10-D and 20-D; JADE on 9 and 10 instances in 10-D and 20-D; SHADE on 9 instances in both 10-D and 20-D; and L-SHADE on 9 instances in both 10-D and 20-D; Compared to recently proposed optimizers MPA, RIME, DEA²H², and the original CDE, ISHACDE outperforms MPA on 9 and 8 instances in 10-D and 20-D; RIME on 8 and 11 instances in 10-D and 20-D; DEA²H² on 6 and 5 instances in 10-D and 20-D; and CDE on 2 and 7 instances in 10-D and 20-D.

However, the original CDE outperforms ISHACDE on the 10-dimensional CEC2022 benchmark functions, as reflected in both the statistical analysis and the average rank metrics. This performance discrepancy can be attributed to the principles outlined by the No Free Lunch Theorem (NFLT) [64]. According to the NFLT, no single optimization algorithm can consistently outperform all others across the full spectrum of optimization problems. In essence, NFLT asserts that if an optimizer excels on one class of problems, it will inevitably perform worse on others, as each problem landscape demands different search strategies for optimal performance.

In 10-D CEC2022 benchmarks, the original design of CDE might be more naturally aligned with the problem characteristics, which allows CDE to perform more efficiently. The simple search operators without complex adaptive mechanisms may offer an advantage in lower-dimensional challenges where exploitation of the solution space tends to be more effective than exploration. On the other hand, ISHACDE, with its efficient independent success history adaptation scheme, is designed to perform well on a wider variety of complex problems. However, this enhancement might introduce unnecessary complexity in simpler, low-dimensional problems, potentially leading to diminished efficiency. This aligns with the trade-offs highlighted by the NFLT. This observation further reinforces the essence of the NFLT:

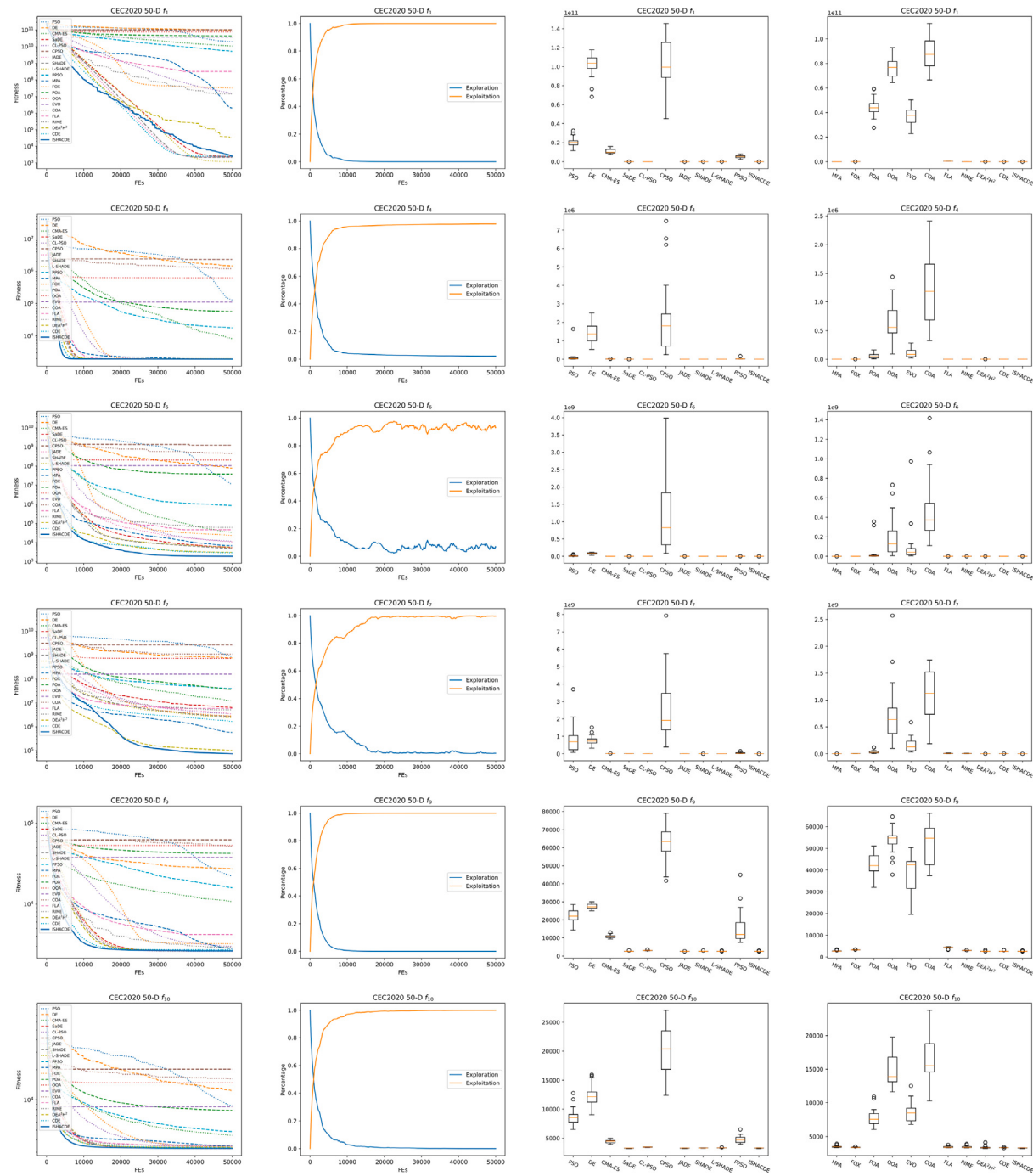


Fig. 9. Convergence curves, exploration-exploitation proportions of ISHACDE, and boxplots of optimizers on 50-D CEC2020 representative functions.

Table 8

The summary of statistical analysis between ISHACDE and state-of-the-art optimizers on CEC2022.

	Dims	PSO	DE	CMA-ES	SaDE	CL-PSO	CPSO	JADE	SHADE	L-SHADE	PPSO
+/- summary	10-D	12/0/0	12/0/0	10/1/1	9/2/1	11/1/0	11/1/0	9/2/1	9/2/1	9/1/2	11/0/1
+/- summary	20-D	12/0/0	11/1/0	10/1/1	9/3/0	11/1/0	11/0/1	10/2/0	9/3/0	9/3/0	11/1/0

Table 9

The summary of statistical analysis between ISHACDE and recently proposed optimizers on CEC2022.

	Dims	MPA	FOX	POA	OOA	EVO	COA	FLA	RIME	DEA ² H ²	CDE
+/- summary	10-D	9/1/2	11/0/1	10/1/1	11/0/1	11/0/1	11/1/0	9/2/1	8/2/2	6/0/6	2/7/3
+/- summary	20-D	8/2/2	11/0/1	11/0/1	11/1/0	11/0/1	12/0/0	11/0/1	11/0/1	5/4/3	7/4/1

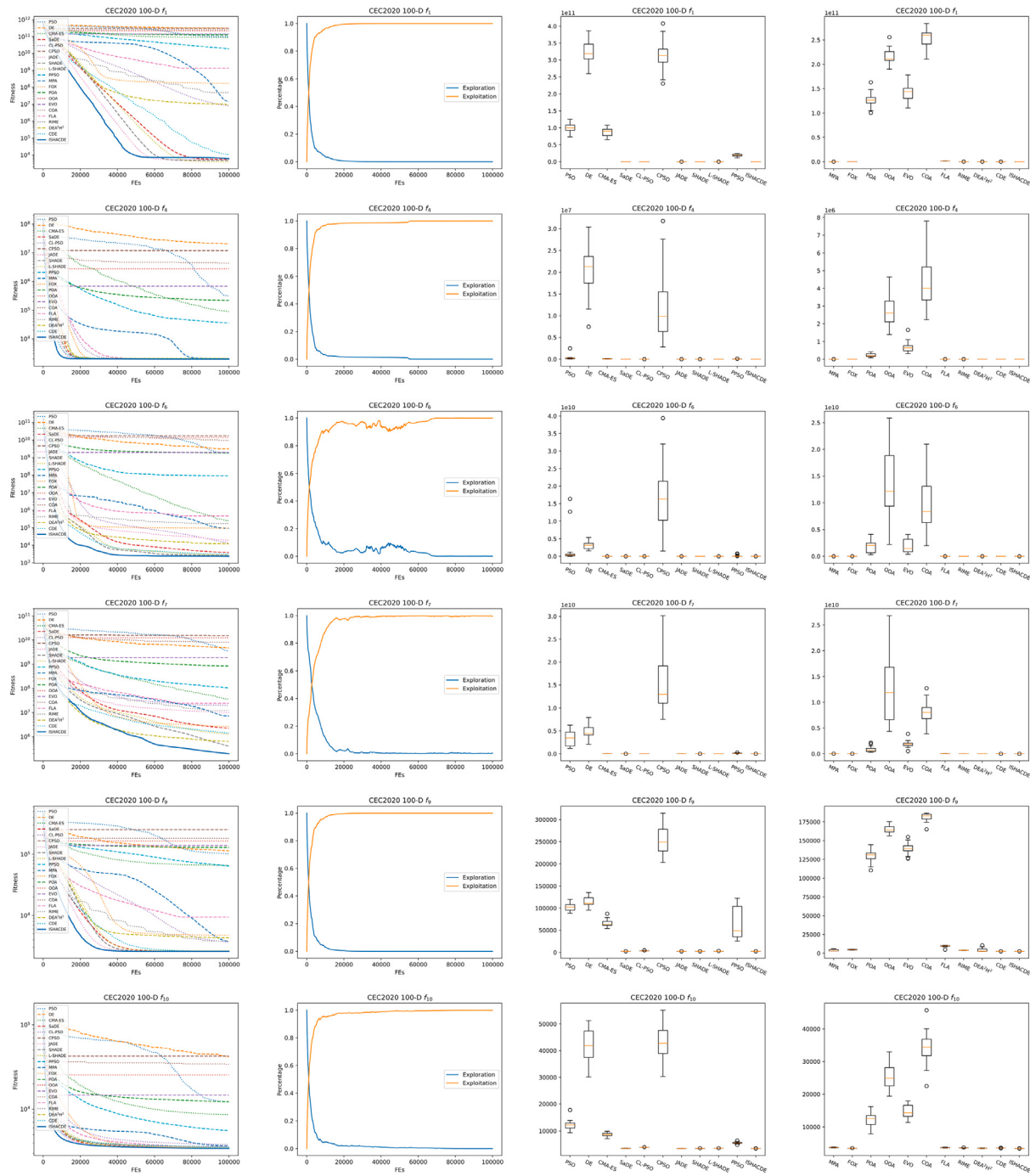


Fig. 10. Convergence curves, exploration-exploitation proportions of ISHACDE, and boxplots of optimizers on 100-D CEC2020 representative functions.

the design of an optimizer must be problem-specific, and no single algorithm can universally dominate across all optimization tasks.

4.2.4. Ablation experiments on CEC benchmarks

This section presents the ablation experiments on CEC benchmarks to investigate the practical effectiveness of our hypothesis that the independent success history adaptation scheme. We initially define the abbreviation of optimizers in these experiments: SHACDE: CDE + success history adaptation and ISHACDE: CDE + independent success history adaptation. Tables 10 and 11 summarize the statistical analysis and average ranks of these optimizers on CEC benchmarks, and the detailed results are presented in Appendix E.

Table 10
The summary of statistical analysis for ablation experiments on CEC benchmarks.

Bench	Dims	SHACDE	ISHACDE
CEC2017	30-D	—	1/16/12
	50-D	—	0/19/10
CEC2020	50-D	—	0/5/5
	100-D	—	0/6/4
CEC2022	10-D	—	0/5/7
	20-D	—	0/5/7

It is evident that the independent evolution significantly accelerates the optimization convergence. Decoupling these scaling parameters

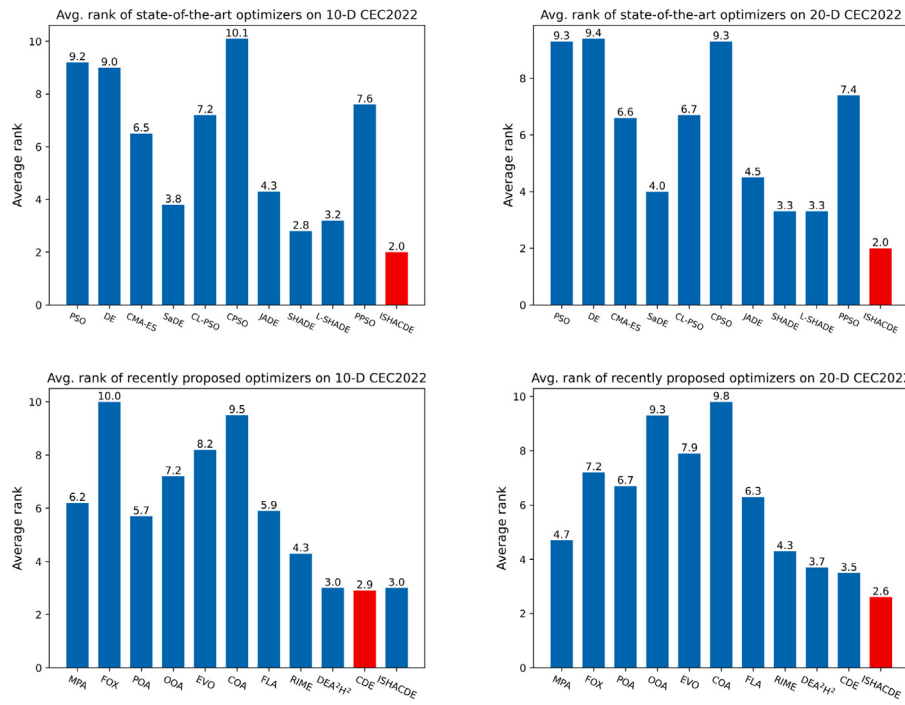


Fig. 11. Average ranks of optimizers on CEC2022.

Table 11

The summary of average ranks for ablation experiments on CEC benchmarks.

Bench	Dims	SHACDE	ISHACDE
CEC2017	30-D	1.8	1.2
	50-D	1.8	1.2
CEC2020	50-D	1.8	1.2
	100-D	1.6	1.4
CEC2022	10-D	1.8	1.2
	20-D	1.8	1.2

allows for more flexible and adaptive search dynamics, which leads to enhanced exploitation and exploration capabilities within CDE.

In the majority of cases, SHACDE performs either approximately equal to or significantly worse than ISHACDE with only one exception in 30-D CEC2017. This case does not affect the broader trend, where the comprehensive experimental results support the superiority of the independent success history adaptation scheme. Therefore, the hypothesis proposed in this research that the independent success history adaptation scheme can accelerate optimization convergence is both theoretically reasonable and practically effective. The independent evolution mechanism offers more nuanced control over the balance between exploration and exploitation and enables ISHACDE to adapt more effectively to varying problem landscapes.

4.2.5. Optimization experiments on GTOPX

We first present the average rank of our proposed ISHACDE compared with optimizers on the GTOPX benchmark in Fig. 14. The detailed experimental results and statistical analysis on instances are detailed in the subsequent contexts.

Cassini1: Tables 12 and 13 summarize the experimental results and statistical analysis on Cassini1, and the convergence curves and boxplots are presented in Fig. 15.

In the Cassini1, ISHACDE as the top-performing optimizer consistently outperforms a range of state-of-the-art optimizers as well as several recently proposed optimization approaches. This superior performance highlights the capacity of ISHACDE to tackle complex real-world problems with high efficiency and precision. The advanced

Table 12

The experimental results and statistical analysis between ISHACDE and state-of-the-art optimizers on Cassini1.

	mean	std	Best	Worst
PSO	1.969776e+01	+ 7.391204e+00	1.015584e+01	3.683723e+01
DE	1.109413e+01	+ 2.895353e+00	5.303423e+00	1.254197e+01
CMA-ES	1.254148e+01	+ 4.45375e-05	1.254142e+01	1.254155e+01
SaDE	9.491824e+00	+ 2.752610e+00	5.309217e+00	1.256270e+01
CL-PSO	1.060040e+01	+ 1.919182e+00	6.838625e+00	1.409163e+01
CPSO	1.441962e+01	+ 6.134119e+00	6.040525e+00	2.564052e+01
JADE	1.051807e+01	+ 2.685738e+00	5.303424e+00	1.254155e+01
SHADE	1.032842e+01	+ 2.598484e+00	5.303421e+00	1.254141e+01
L-SHADE	1.105579e+01	+ 2.047606e+00	5.303421e+00	1.254145e+01
PPSO	2.703028e+01	+ 1.189952e+01	1.440250e+01	5.820972e+01
ISHACDE	7.030301e+00	2.619726e+00	5.303421e+00	1.103198e+01

Table 13

The experimental results and statistical analysis between ISHACDE and recently proposed optimizers on Cassini1.

	mean	std	Best	Worst
MPA	1.583439e+01	+ 3.698561e+00	1.099678e+01	2.321670e+01
FOX	3.191786e+01	+ 1.146271e+01	1.780469e+01	6.061007e+01
POA	9.750388e+00	+ 3.820098e+00	5.303744e+00	1.679111e+01
OOA	1.773272e+01	+ 5.846684e+00	6.545241e+00	2.844931e+01
EVO	2.551876e+01	+ 6.530781e+00	1.811068e+01	3.737458e+01
COA	1.093465e+01	+ 2.053794e+00	7.742056e+00	1.336818e+01
FLA	1.303608e+01	+ 4.074902e+00	5.952496e+00	1.954155e+01
RIME	1.111090e+01	+ 4.280519e+00	5.319147e+00	1.644100e+01
DEA ² H ²	1.701778e+01	+ 1.333662e+01	5.303469e+00	5.566573e+01
CDE	1.245845e+01	+ 4.141712e+00	5.303423e+00	1.672367e+01
ISHACDE	7.030301e+00	2.619726e+00	5.303421e+00	1.103198e+01

adaptive mechanisms in ISHACDE enable it to explore the solution space more effectively and yield high-quality solutions that dominate other optimizers.

Furthermore, the remarkable convergence behavior of ISHACDE is visible in the convergence curves presented in Fig. 15, where ISHACDE swiftly approaches elite individuals, which significantly reduces the objective function values within a relatively small number of iterations. In addition to convergence speed, the robustness of ISHACDE is also

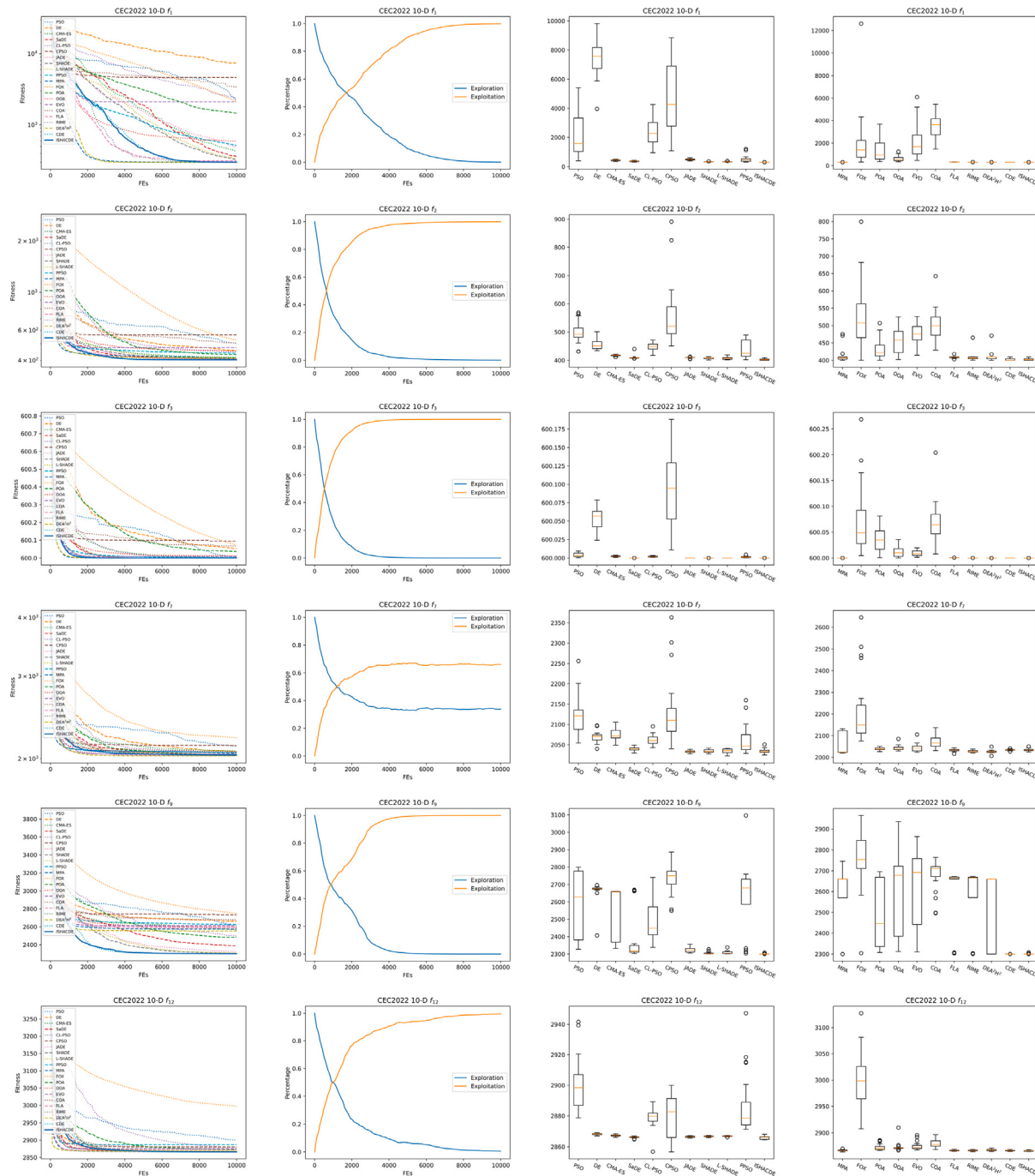


Fig. 12. Convergence curves, exploration-exploitation proportions of ISHACDE, and boxplots of optimizers on 10-D CEC2022 representative functions.

evident from the boxplots, which reveal the consistency of ISHACDE across multiple independent runs. The narrow interquartile ranges and the absence of significant outliers confirm the stability of ISHACDE.

Cassini2: Tables 14 and 15 summarize the experimental results and statistical analysis on Cassini2, and the convergence curves and boxplots are presented in Fig. 16.

In Cassini2, the dominance of ISHACDE against other competitors remains observable, which reinforces the excellent performance of ISHACDE across diverse optimization challenges. While the convergence speed of ISHACDE is not always the fastest and occasionally trails behind DEA²H² during the early and middle stages of optimization, it compensates with its exceptional exploitative search capability and an impressive ability to escape local optima. This balance between

exploitation and exploration enables ISHACDE to continue refining the solution, ultimately achieving a better global optimum by the conclusion of the optimization process. Moreover, the capacity to escape the local optima of ISHACDE is crucial in Cassini2, which allows ISHACDE to approach near-optimal solutions in the late stage of optimization for handling the complex Cassini2 challenge.

Messenger (reduced): Tables 16 and 17 summarize the experimental results and statistical analysis on Messenger (reduced), and the convergence curves and boxplots are presented in Fig. 17.

In Messenger (reduced), ISHACDE demonstrates remarkable performance as in the previous challenges that ranked as the top optimizer among state-of-the-art methods and placed as the second-best when

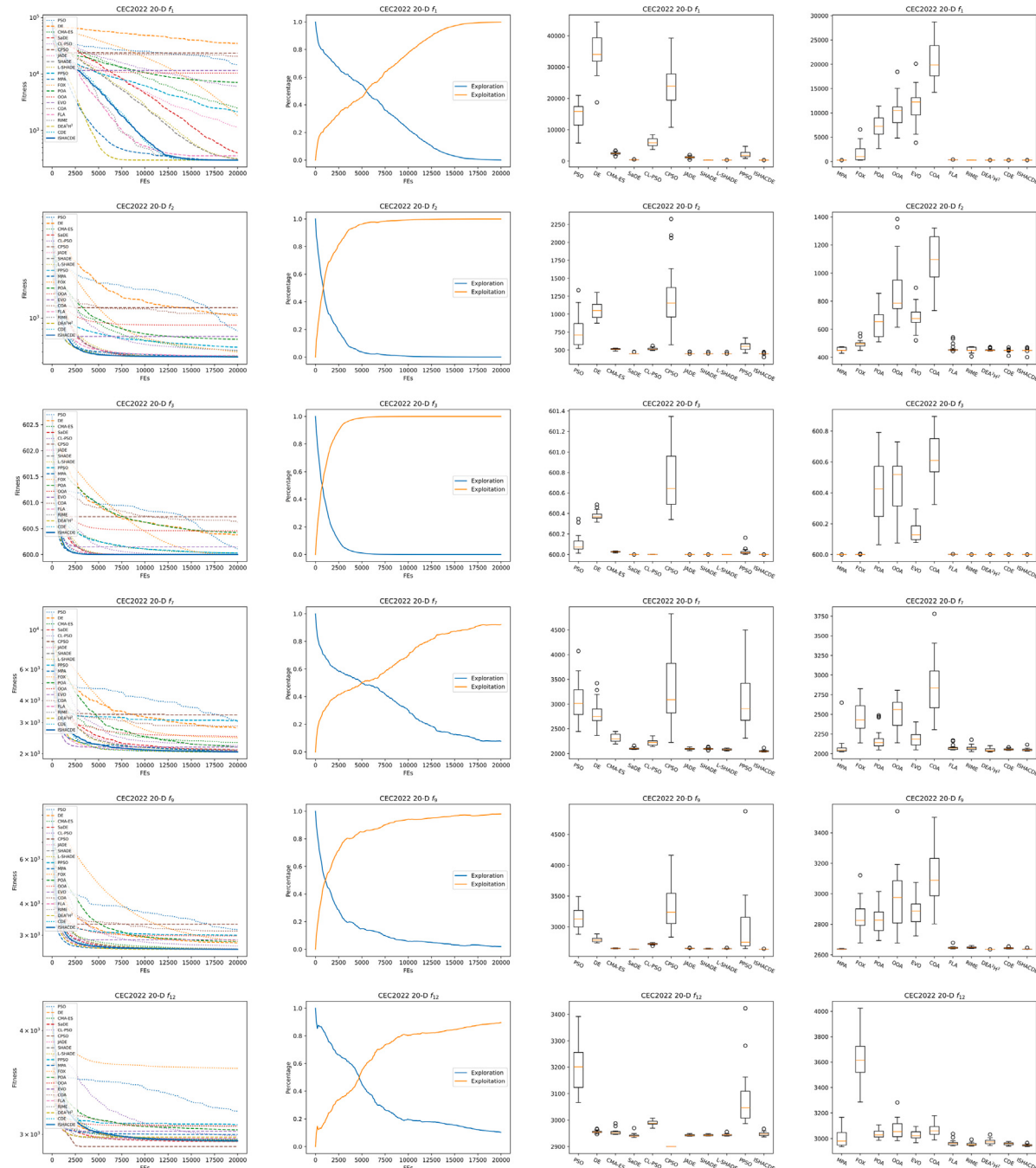


Fig. 13. Convergence curves, exploration-exploitation proportions of ISHACDE, and boxplots of optimizers on 20-D CEC2022 representative functions.

compared to recently proposed approaches. The impressive competitiveness in Messenger (reduced) highlights the versatility and effectiveness of ISHACDE. Notably, despite ISHACDE being numerically worse than CDE, the statistical significance between CDE and ISHACDE does not exist, which indicates that ISHACDE is highly competitive and comparable to the best-performing algorithm in this instance.

Moreover, the robustness of ISHACDE is particularly noteworthy. The standard deviation metrics summarized in Tables 16 and 17 indicate that ISHACDE maintains a consistent level of performance across multiple independent runs. This consistency is further strengthened by the boxplots in Fig. 17, which illustrate the stability of ISHACDE compared to its competitors.

Messenger (full): Tables 18 and 19 summarize the experimental results and statistical analysis on Messenger (full), and the convergence curves and boxplots are presented in Fig. 18.

In Messenger (full), CDE emerges as the best-performing optimizer while the statistical significance does not exist. Nevertheless, ISHACDE demonstrates competitive performance and consistently outperforms all other optimizers evaluated in this instance. Additionally, Messenger (full) formulates a complete space mission to Mercury, where the travel sequence is Earth–Venus–Venus–Mercury–Mercury–Mercury, which shows the complexity of this challenge. These experimental results and statistical analysis highlight the robustness and adaptability of ISHACDE.

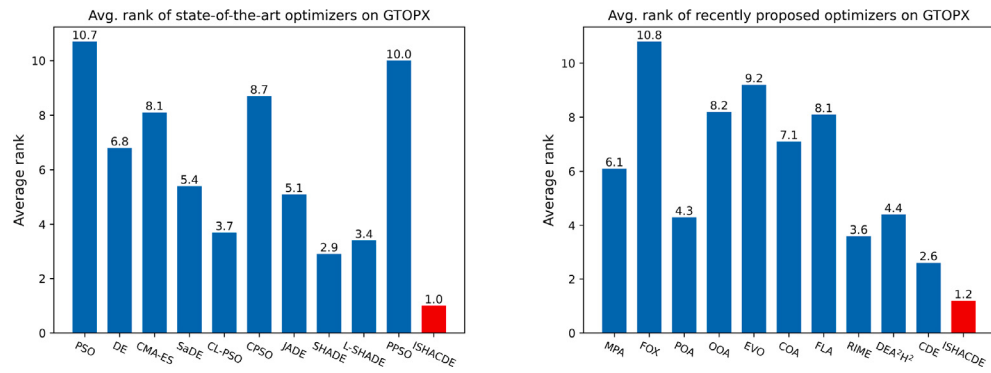


Fig. 14. Average ranks of optimizers on GTOPX.

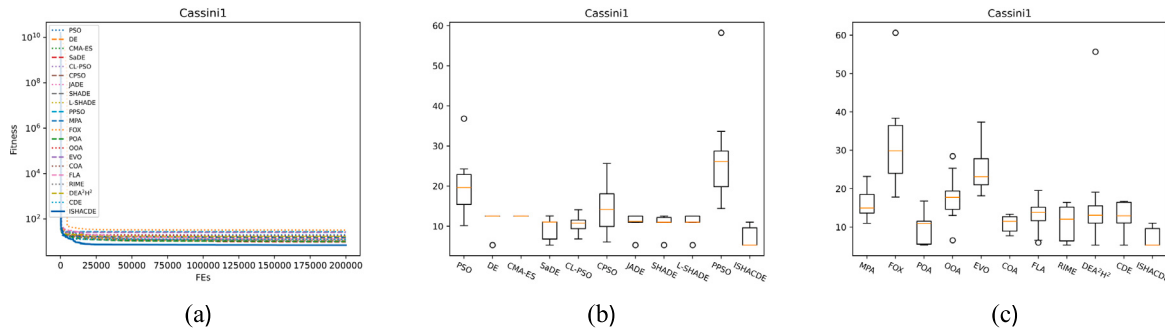


Fig. 15. The convergence curves and boxplots on Cassini1.

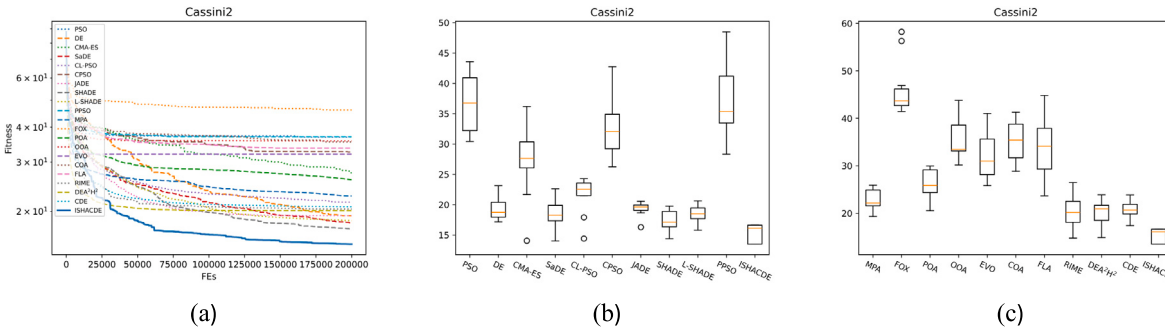


Fig. 16. The convergence curves and boxplots on Cassini2.

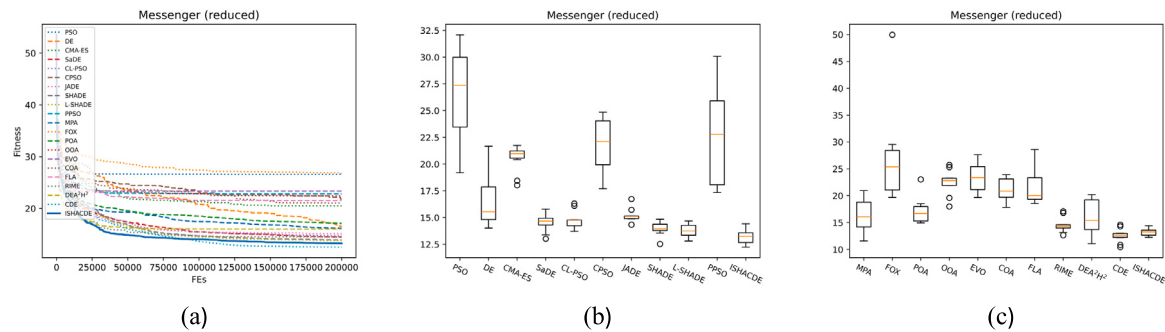


Fig. 17. The convergence curves and boxplots on Messenger (reduced).

GTOC1: Tables 20 and 21 summarize the experimental results and statistical analysis on GTOC1, and the convergence curves and boxplots are presented in Fig. 19.

In GTOC1, our proposed ISHACDE demonstrates remarkable reliability and consistency in the constrained optimization challenge. Unlike

several state-of-the-art optimizers such as PSO, CPSO, and PPSO which occasionally fail to find feasible solutions, ISHACDE consistently finds feasible solutions in every independent trial run. This success highlights the robustness of ISHACDE. Moreover, ISHACDE achieves the best average performance across all trials, which outperforms a range of

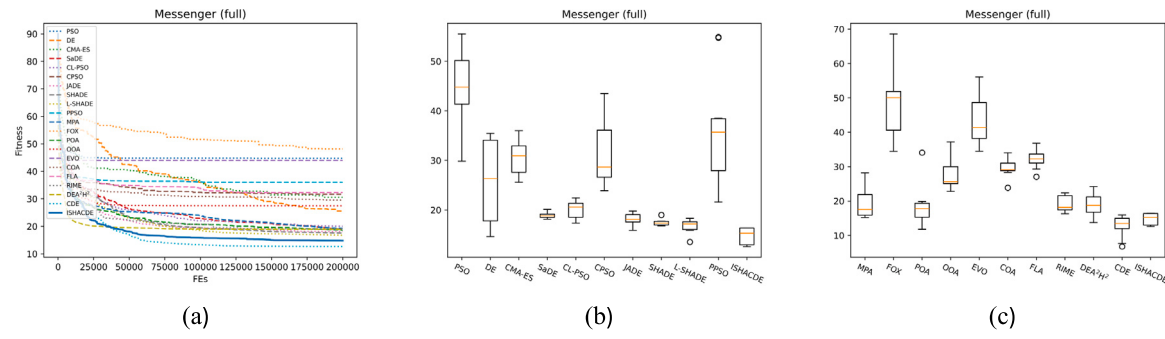


Fig. 18. The convergence curves and boxplots on Messenger (full).

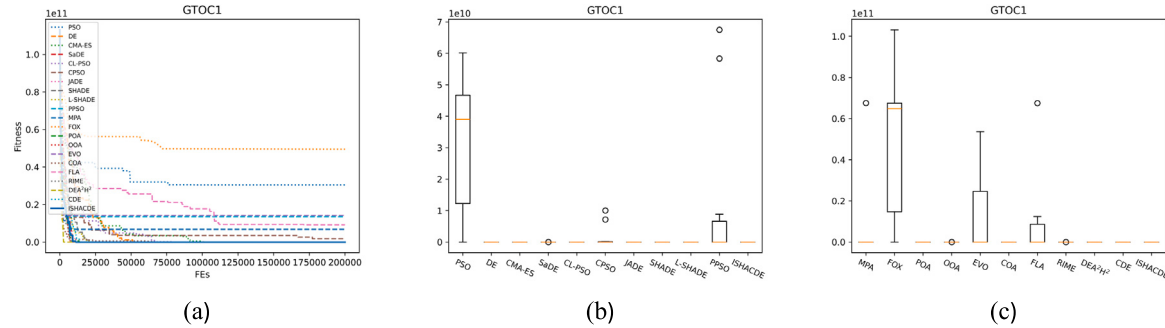


Fig. 19. The convergence curves and boxplots on GTOC1.

Table 14

The experimental results and statistical analysis between ISHACDE and state-of-the-art optimizers on Cassini2.

	mean	std	Best	Worst
PSO	3.687448e+01	4.758799e+00	3.041325e+01	4.357246e+01
DE	1.930419e+01	1.845082e+00	1.717698e+01	2.311928e+01
CMA-ES	2.745477e+01	5.983244e+00	1.407117e+01	3.617613e+01
SaDE	1.822368e+01	2.560050e+00	1.400700e+01	2.262507e+01
CL-PSO	2.157939e+01	2.966211e+00	1.441469e+01	2.430028e+01
CPSO	3.259466e+01	4.520625e+00	2.625669e+01	4.275556e+01
JADE	1.931761e+01	1.138237e+00	1.629739e+01	2.057195e+01
SHADE	1.732205e+01	1.717158e+00	1.439585e+01	1.976516e+01
L-SHADE	1.848652e+01	1.411753e+00	1.577127e+01	2.063051e+01
PPSO	3.696039e+01	6.239248e+00	2.832438e+01	4.849957e+01
ISHACDE	1.528080e+01	1.472284e+00	1.351002e+01	1.665853e+01

Table 15

The experimental results and statistical analysis between ISHACDE and recently proposed optimizers on Cassini2.

	mean	std	Best	Worst
MPA	2.271417e+01	2.193433e+00	1.931121e+01	2.591693e+01
FOX	4.614191e+01	5.769422e+00	4.143286e+01	5.823732e+01
POA	2.596979e+01	3.276168e+00	2.054217e+01	2.996331e+01
OOA	3.572593e+01	4.130661e+00	3.017713e+01	4.380734e+01
EVO	3.205941e+01	4.598902e+00	2.581195e+01	4.102295e+01
COA	3.541648e+01	4.219876e+00	2.885050e+01	4.130271e+01
FLA	3.368935e+01	5.876266e+00	2.366481e+01	4.480402e+01
RIME	2.039136e+01	3.190693e+00	1.474881e+01	2.647094e+01
DEA ² H ²	2.011782e+01	2.547339e+00	1.488413e+01	2.386764e+01
CDE	2.078879e+01	1.869795e+00	1.740478e+01	2.385257e+01
ISHACDE	1.528080e+01	1.472284e+00	1.351002e+01	1.665853e+01

well-known competitor algorithms. Compared with recently proposed methods such as MPA, FOX, EVO, and FLA, all of which fail to find feasible solutions at least once across multiple runs. Further statistical analysis underscores the superiority and effectiveness of ISHACDE in constrained environments.

Table 16

The experimental results and statistical analysis between ISHACDE and state-of-the-art optimizers on Messenger (reduced).

	mean	std	Best	Worst
PSO	2.659372e+01	4.032875e+00	1.919745e+01	3.209575e+01
DE	1.654689e+01	2.348950e+00	1.403037e+01	2.167515e+01
CMA-ES	2.053812e+01	1.200423e+00	1.803171e+01	2.174434e+01
SaDE	1.452637e+01	7.676218e-01	1.302548e+01	1.579933e+01
CL-PSO	1.474594e+01	8.309837e-01	1.370959e+01	1.632154e+01
CPSO	2.185188e+01	2.475303e+00	1.768777e+01	2.486644e+01
JADE	1.515563e+01	6.524716e-01	1.433958e+01	1.673947e+01
SHADE	1.396058e+01	6.140050e-01	1.254094e+01	1.484467e+01
L-SHADE	1.379891e+01	5.862541e-01	1.280659e+01	1.468544e+01
PPSO	2.283009e+01	4.705961e+00	1.734824e+01	3.008711e+01
ISHACDE	1.326370e+01	7.499011e-01	1.224641e+01	1.443090e+01

Table 17

The experimental results and statistical analysis between ISHACDE and recently proposed optimizers on Messenger (reduced).

	mean	std	Best	Worst
MPA	1.619855e+01	2.941808e+00	1.159125e+01	2.097049e+01
FOX	2.681381e+01	8.436867e+00	1.968272e+01	4.996542e+01
POA	1.712814e+01	2.316084e+00	1.493436e+01	2.303591e+01
OOA	2.245760e+01	2.214925e+00	1.800729e+01	2.573472e+01
EVO	2.338089e+01	2.571296e+00	1.963881e+01	2.763339e+01
COA	2.105598e+01	2.041470e+00	1.782095e+01	2.391335e+01
FLA	2.154872e+01	3.069867e+00	1.856390e+01	2.860091e+01
RIME	1.455698e+01	1.341017e+00	1.265471e+01	1.710928e+01
DEA ² H ²	1.604725e+01	3.053173e+00	1.106674e+01	2.018834e+01
CDE	1.256753e+01	1.226797e+00	1.043962e+01	1.460270e+01
ISHACDE	1.326370e+01	7.499011e-01	1.224641e+01	1.443090e+01

Rosetta: Tables 22 and 23 summarize the experimental results and statistical analysis on Rosetta, and the convergence curves and boxplots are presented in Fig. 20.

Rosetta formulates the multi-gravity assist space mission where the travel sequence is Earth–Earth–Mars–Earth–Earth–67P. In this task, the competitiveness and superiority of ISHACDE are clearly demonstrated

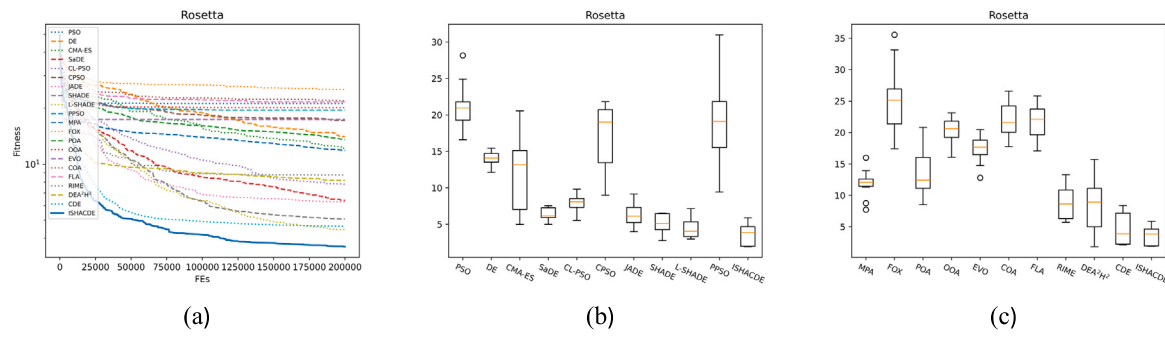


Fig. 20. The convergence curves and boxplots on Rosetta.

Table 18

The experimental results and statistical analysis between ISHACDE and state-of-the-art optimizers on Messenger (full).

	mean	std	Best	Worst
PSO	4.472286e+01 +	7.192854e+00	2.983417e+01	5.554463e+01
DE	2.559178e+01 +	8.292524e+00	1.462544e+01	3.544832e+01
CMA-ES	3.056516e+01 +	3.377069e+00	2.558580e+01	3.600316e+01
SaDE	1.892374e+01 +	5.708799e-01	1.814674e+01	2.011008e+01
CL-PSO	2.001076e+01 +	1.697892e+00	1.735038e+01	2.243127e+01
CPSO	3.171082e+01 +	6.606709e+00	2.389839e+01	4.348986e+01
JADE	1.812823e+01 +	1.125990e+00	1.587640e+01	1.977859e+01
SHADE	1.757625e+01 +	7.719949e-01	1.678269e+01	1.900740e+01
L-SHADE	1.675000e+01 +	1.312801e+00	1.354685e+01	1.832262e+01
PPSO	3.599797e+01 +	1.089378e+01	2.160901e+01	5.491136e+01
ISHACDE	1.480685e+01	1.587775e+00	1.261164e+01	1.637744e+01

Table 19

The experimental results and statistical analysis between ISHACDE and recently proposed optimizers on Messenger (full).

	mean	std	Best	Worst
MPA	1.934161e+01 +	4.112676e+00	1.522288e+01	2.815974e+01
FOX	4.813642e+01 +	9.926831e+00	3.446332e+01	6.861550e+01
POA	1.860491e+01 +	5.687657e+00	1.180655e+01	3.408685e+01
OOA	2.746880e+01 +	4.296002e+00	2.284407e+01	3.721835e+01
EVO	4.393588e+01 +	7.276549e+00	3.446793e+01	5.606707e+01
COA	2.954585e+01 +	2.582775e+00	2.387543e+01	3.406482e+01
FLA	3.233408e+01 +	2.823878e+00	2.705337e+01	3.679896e+01
RIME	1.914588e+01 +	2.203462e+00	1.631406e+01	2.237107e+01
DEA ² H ²	1.896307e+01 +	3.063870e+00	1.374146e+01	2.418820e+01
CDE	1.265393e+01 ≈	2.992812e+00	6.768666e+00	1.598101e+01
ISHACDE	1.480685e+01	1.587775e+00	1.261164e+01	1.637744e+01

Table 20

The experimental results and statistical analysis between ISHACDE and state-of-the-art optimizers on GTOC1.

	mean	std	Best	Worst
PSO	3.045328e+10 +	2.108287e+10	-9.649717e+04	6.020797e+10
DE	-6.846880e+05 ≈	4.079558e+05	-1.193119e+06	-3.000548e+02
CMA-ES	-8.213583e+04 +	4.027150e+04	-1.691185e+05	-2.758173e+04
SaDE	-7.334950e+05 ≈	1.253186e+05	-9.780909e+05	-4.932465e+05
CL-PSO	-4.714242e+05 +	1.911057e+05	-7.956573e+05	-2.102736e+05
CPSO	1.737134e+09 +	3.494585e+09	-3.668427e+05	1.004359e+10
JADE	-6.224707e+05 +	9.072962e+04	-8.001274e+05	-4.814040e+05
SHADE	-8.334478e+05 ≈	9.103382e+04	-1.007716e+06	-7.036838e+05
L-SHADE	-8.245670e+05 ≈	9.639661e+04	-1.043306e+06	-7.208583e+05
PPSO	1.347321e+10 +	2.495836e+10	-3.154121e+05	6.751466e+10
ISHACDE	-8.348549e+05	9.718440e+04	-9.962286e+05	-7.112155e+05

through both the experimental results and the statistical analysis presented in Tables 22 and 23. These results highlight the outstanding performance of ISHACDE which significantly outperforms all competitor algorithms except for L-SHADE and CDE. Another strength of ISHACDE in the Rosetta instance is its remarkable robustness, which is consistently observable through the std and the corresponding boxplots. The low variance in performance indicates that ISHACDE achieves

Table 21

The experimental results and statistical analysis between ISHACDE and recently proposed optimizers on GTOC1.

	mean	std	Best	Worst
MPA	6.752415e+09 +	2.025884e+10	-8.926708e+05	6.752893e+10
FOX	4.943421e+10 +	3.430498e+10	-1.091966e+05	1.031665e+11
POA	-7.273582e+05 ≈	1.880684e+05	-1.040003e+06	-4.509043e+05
OOA	-2.840856e+05 +	1.685866e+05	-6.651977e+05	-9.729939e-01
EVO	1.419798e+10 +	2.167293e+10	-4.628030e+05	5.367601e+10
COA	-2.225535e+05 +	1.490765e+05	-5.144207e+05	-2.508860e+04
FLA	9.209546e+09 +	1.997875e+05	-3.011575e+05	6.752862e+10
RIME	-6.740185e+05 +	1.6033300e+05	-1.060868e+06	-5.227693e+05
DEA ² H ²	-6.284534e+05 +	2.127933e+05	-9.870601e+05	-2.574126e+05
CDE	-7.490474e+05 ≈	1.450661e+05	-9.491559e+05	-5.479580e+05
ISHACDE	-8.348549e+05	9.718440e+04	-9.962286e+05	-7.112155e+05

Table 22

The experimental results and statistical analysis between ISHACDE and state-of-the-art optimizers on Rosetta.

	mean	std	Best	Worst
PSO	2.120114e+01 +	3.220382e+00	1.660294e+01	2.815494e+01
DE	1.405663e+01 +	8.996501e-01	1.211470e+01	1.544209e+01
CMA-ES	1.207636e+01 +	5.067854e+00	4.951300e+00	2.055630e+01
SaDE	6.394915e+00 +	8.606701e-01	4.978140e+00	7.541151e+00
CL-PSO	7.794987e+00 +	1.219329e+00	5.522672e+00	9.819181e+00
CPSO	1.718245e+01 +	4.507356e+00	8.968448e+00	2.182016e+01
JADE	6.296594e+00 +	1.503177e+00	3.973145e+00	9.131991e+00
SHADE	5.064347e+00 +	1.320620e+00	2.755007e+00	6.504686e+00
L-SHADE	4.432129e+00 ≈	1.340749e+00	2.964159e+00	7.142300e+00
PPSO	1.952796e+01 +	6.047466e+00	9.428758e+00	3.100028e+01
ISHACDE	3.597113e+00	1.496283e+00	1.908155e+00	5.865088e+00

Table 23

The experimental results and statistical analysis between ISHACDE and state-of-the-art optimizers on Rosetta.

	mean	std	Best	Worst
MPA	1.187193e+01 +	2.225614e+00	7.710812e+00	1.598597e+01
FOX	2.525083e+01 +	5.448334e+00	1.740686e+01	3.555433e+01
POA	1.357459e+01 +	3.717854e+00	8.537556e+00	2.081931e+01
OOA	2.014516e+01 +	2.205883e+00	1.606829e+01	2.314466e+01
EVO	1.742443e+01 +	2.313246e+00	1.279538e+01	2.046706e+01
COA	2.196404e+01 +	2.698768e+00	1.775252e+01	2.659651e+01
FLA	2.167137e+01 +	2.7388214e+00	1.706862e+01	2.582203e+01
RIME	8.750572e+00 +	2.617476e+00	5.720910e+00	1.328940e+01
DEA ² H ²	8.185927e+00 +	4.117642e+00	1.826546e+00	1.569939e+01
CDE	4.638937e+00 ≈	2.490509e+00	2.126073e+00	8.400114e+00
ISHACDE	3.597113e+00	1.496283e+00	1.908155e+00	5.865088e+00

stable results across multiple independent runs.

Sagas: Tables 24 and 25 summarize the experimental results and statistical analysis on Sagas, and the convergence curves and boxplots are presented in Fig. 21.

Sagas models the space mission of Earth–Earth–Jupiter. In this task, ISHACDE performs comparably with SaDE, CL-PSO, POA, RIME, DEA²H², and CDE, while significantly outperforming the remaining

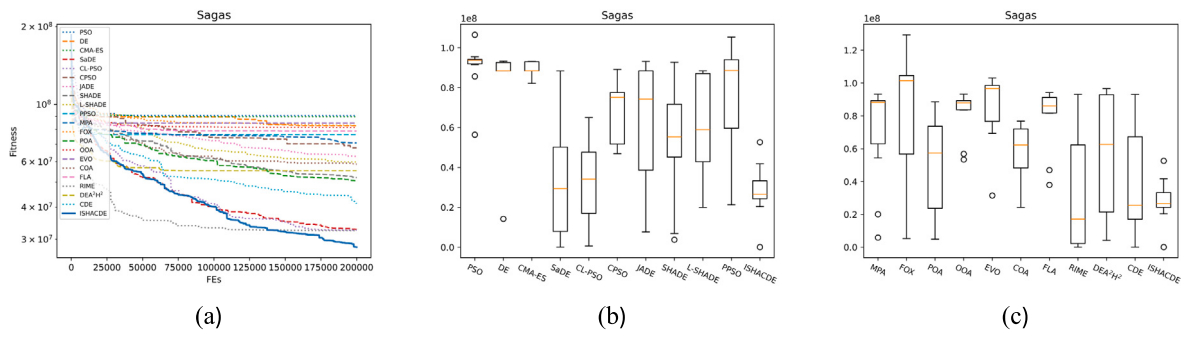


Fig. 21. The convergence curves and boxplots on Sagas.

Table 24

The experimental results and statistical analysis between ISHACDE and state-of-the-art optimizers on Sagas.

	mean	std	Best	Worst
PSO	9.038437e+07	+ 1.231824e+07	5.641577e+07	1.064673e+08
DE	8.273544e+07	+ 2.293381e+07	1.422446e+07	9.319366e+07
CMA-ES	8.961900e+07	+ 3.310748e+06	8.216177e+07	9.314025e+07
SaDE	3.274416e+07	≈ 2.799741e+07	1.000000e+05	8.837564e+07
CL-PSO	3.256025e+07	≈ 2.026569e+07	6.790997e+05	6.499365e+07
CPSO	6.790415e+07	+ 1.472998e+07	4.690187e+07	8.910263e+07
JADE	6.282769e+07	+ 3.041061e+07	7.698401e+06	9.311749e+07
SHADE	5.197022e+07	+ 2.722838e+07	3.765627e+06	9.268364e+07
L-SHADE	5.977414e+07	+ 2.512371e+07	1.995528e+07	8.839465e+07
PPSO	7.646533e+07	+ 2.535769e+07	2.128985e+07	1.053094e+08
ISHACDE	2.800412e+07	1.310120e+07	1.000000e+05	5.264729e+07

Table 25

The experimental results and statistical analysis between ISHACDE and recently proposed optimizers on Sagas.

	mean	std	Best	Worst
MPA	7.090548e+07	+ 3.098059e+07	5.909286e+06	9.320642e+07
FOX	8.302590e+07	+ 3.688395e+07	5.266253e+06	1.294072e+08
POA	5.050122e+07	≈ 3.047984e+07	4.887495e+06	8.856297e+07
OOA	8.144147e+07	+ 1.344140e+07	5.339501e+07	9.324943e+07
EVO	8.465506e+07	+ 2.098260e+07	3.149689e+07	1.030998e+08
COA	5.864055e+07	+ 1.583672e+07	2.428632e+07	7.679745e+07
FLA	7.886408e+07	+ 1.877744e+07	3.795064e+07	9.427286e+07
RIME	3.243306e+07	≈ 3.577227e+07	1.000000e+05	9.310695e+07
DEA ² H ²	5.533703e+07	≈ 3.836844e+07	4.177366e+06	9.654177e+07
CDE	4.125601e+07	≈ 3.345747e+07	1.000000e+05	9.309403e+07
ISHACDE	2.800412e+07	1.310120e+07	1.000000e+05	5.264729e+07

optimizers. These detailed experimental results demonstrate the capacity of ISHACDE to tackle complex optimization challenges effectively. Nevertheless, an important observation is that the optima found by all optimizers are considerably distant from the theoretical optimum listed in Table 1. This gap highlights the intrinsic difficulty of the Sagas problem, which is recognized as a strongly constrained optimization problem.

The characteristics of these strong constraints present a substantial challenge for most optimization techniques. To further validate the complexity and constraint intensity of the Sagas instance, we applied a random search technique with 200,000 FEs within the problem space. This experiment is repeated 30 times to ensure statistical reliability. The pseudocode for this random search is detailed in Algorithm 2. The convergence curve of random search presented in Fig. 22 reveals that the random search struggles to find feasible solutions within the allocated FEs, which further confirms the statement that the Sagas instance is a strong-constrained optimization challenge.

Additionally, considering that the random search technique cannot find a feasible solution within limited FEs, we infer that the initialization technique in swarm intelligence approaches may play an important role. Future research will focus on developing advanced initialization

The convergence curve of the random search

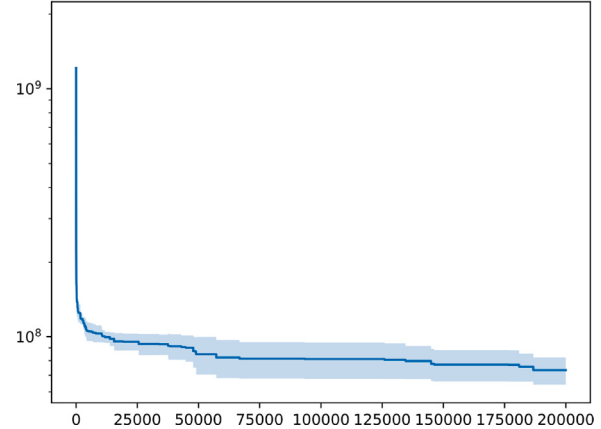


Fig. 22. The convergence curve of random search.

methods that can improve the chances of finding feasible and high-quality solutions early in the optimization process. Smart initialization techniques, such as using data-driven or constraint-aware approaches, may significantly enhance the ability of algorithms to avoid infeasible regions.

Algorithm 2: Random search

```

Input: Dimension:  $D$ , Sampling times:  $T$ , Lower and upper bound:  $LB$  and  $UB$ 
Output: Optimum:  $X_{best}$ 
1 Function RS( $D, T, LB, UB$ ):
2    $t = 0$ 
3   Initialize the fitness of  $X_{best}^t$  as a large number
4   while  $t < T$  do
5     for  $i = 0$  to  $D$  do
6        $X_i^t = \text{rand}(LB_i, UB_i)$  if  $X_i^t$  is better than  $X_{best}^t$  then
7          $X_{best}^t = X_i^t$ 
8       end
9     end
10     $t = t + 1$ 
11  end
12  return  $X_{best}^t$ 

```

In summary, the experimental results and comprehensive statistical analysis presented through tables, convergence curves, and boxplots, clearly demonstrate the competitiveness and superiority of the proposed ISHACDE on the GTOPX benchmark. Across a wide range of test instances, ISHACDE consistently outperforms or remains comparatively with state-of-the-art and recently proposed optimization techniques, affirming its effectiveness in handling complex optimization tasks.

Table 26
The computational complexity of representative MAs.

Alg.	Computational complexity
GA [65]	$O(T \times N \times D)$
DE [11]	$O(T \times N \times D)$
PSO [46]	$O(T \times N \times D)$
GWO [66]	$O(T \times N \times \log(N) \times D)$
WOA [67]	$O(T \times N \times D)$

The convergence curves highlight the convergence speed and accuracy of ISHACDE, while the remarkable exploitative searchability allows ISHACDE to refine solutions and achieve better optima as the evolution progresses. This is further supported by the boxplots, which demonstrate the robustness and stability of ISHACDE across multiple independent trials and are reflected in the lower variance of optimal solutions compared to competitor algorithms.

The statistical analysis further validates the strength of ISHACDE in finding high-quality solutions and balancing exploration and exploitation – enhanced by its adaptive mechanisms – allowing ISHACDE as a highly competitive optimizer for the GTOPX benchmark.

5. Discussion

This section discusses the proposed ISHACDE. Section 5.1 analyzes the computational complexity of ISHACDE, and Section 5.2 provides some open topics for future research.

5.1. Computational complexity analysis

The computational complexity analysis of ISHACDE begins by defining some related variables. Assuming the population size is N , the dimension size is D , and the maximum iteration is T . The main steps of ISHACDE are listed as follows:

- Population and parameters initialization: $O(N \times D)$.
- Construct the mutant vector using DE/winner-to-best/1: $O(T \times N \times D)$.
- Construct the offspring individual using binomial crossover: $O(T \times N \times D)$.
- Select the survival individuals: $O(T \times N)$.
- Update μ_F and μ_{Cr} : Best situation $O(1)$ and worst situation $O(T \times N)$

In summary, the computational complexity of ISHACDE is $O(N \times D + 2 \times T \times (N \times D + N)) := O(T \times N \times D)$. Meanwhile, we summarize the computational complexity of representative MAs in Table 26 for an intuitive comparison. In this study, our proposed ISHACDE demonstrates equivalent computational complexity to many metaheuristic algorithms, highlighting its flexibility and ease of implementation.

5.2. Open topics for future research

Through the above experiments and analysis, ISHACDE achieved satisfactory performance. Here, we list a few open topics for future research.

5.2.1. Extending ISHACDE to various optimization tasks

The effectiveness and robustness of ISHACDE are clear, and ISHACDE has great potential to address various optimization tasks such as multi-objective optimization [68], large-scale optimization [69], and optimization with uncertainty [70]. Additionally, ISHACDE is also promising in real-world applications such as parameter identification of the photovoltaic model [10], image denoising [71], and sound composition [72].

5.2.2. Integrating independent success history adaptation scheme to other optimizers

The independent success history adaptation scheme proposed in ISHACDE is an effective and efficient method for hyperparameter adaptation. Many MAs have explicit or implicit hyperparameters that can significantly impact their performance. Therefore, introducing the independent success history adaptation scheme to various metaheuristic algorithms to enhance their optimization performance is a promising topic for future research.

6. Conclusion

This paper proposes a novel ISHACDE. Based on the skeleton of CDE, we further introduce an independent success history adaptation scheme. We design comprehensive and fair numerical experiments on CEC2017, CEC2020, and CEC2022 benchmark functions. Ten state-of-the-art optimizers and ten recently proposed optimization approaches are employed as competitors. The experimental results and statistical analysis conducted by the Holm multiple comparison test confirm the efficiency and effectiveness of our proposed ISHACDE in functional optimization tasks.

Additionally, we further adopt the proposed ISHACDE to address the challenge of SMT0, which is provided by the GTOPX benchmark. The rigorous statistical analysis also confirms the remarkable robustness, adaptability, and scalability of our proposed ISHACDE.

In future research, we will continue to develop problem-specific optimization algorithms based on ISHACDE for solving real-world applications efficiently.

CRediT authorship contribution statement

Rui Zhong: Writing – review & editing, Writing – original draft, Software, Methodology, Data curation, Conceptualization. **Abdelazim G. Hussien:** Writing – review & editing, Supervision, Project administration. **Shilong Zhang:** Writing – review & editing, Formal analysis. **Yuefeng Xu:** Writing – review & editing, Validation. **Jun Yu:** Writing – review & editing, Project administration, Conceptualization.

Declaration of competing interest

The authors declare that they have no known competing financial interests or personal relationships that could have appeared to influence the work reported in this paper.

Acknowledgment

This work was supported by JST SPRING Grant Number JPMJSP2119.

Appendix A. CEC benchmark details

The details of CEC2017, CEC2020, and CEC2022 benchmark functions are summarized in Tables 27, 28, and 29.

Appendix B. Experimental details on CEC2017

Tables 30, 31, 32, and 33 summarize the experimental results and statistical analysis between ISHACDE and state-of-the-art optimizers on CEC2017 benchmark functions. Tables 34, 35, 36, and 37 summarize the experimental results and statistical analysis between ISHACDE and recently proposed optimizers on CEC2017 benchmark functions. Symbols +, ≈, and – denote that ISHACDE is significantly better, without statistical significance, and significantly worse than the specific competitor optimizer. The best values in the Tables are in bold.

Table 27

Summary of the CEC2017 benchmark functions: Uni. = Unimodal function, Multi. = Simple multimodal function, Hybrid. = Hybrid function, Comp. = Composition function.

No.	Func.	Feature	Optimum
f_1	Shifted and Rotated Bent Cigar function	Uni.	100
f_3	Shifted and Rotated Rosenbrock's function		300
f_4	Shifted and Rotated Rastrigin's function		400
f_5	Shifted and Rotated Expanded Schaffer's F6 function		500
f_6	Shifted and Rotated Lunacek Bi_Rastrigin function	Multi.	600
f_7	Shifted and Rotated Non-Continuous Rastrigin's function		700
f_8	Shifted and Rotated Levy function		800
f_9	Shifted and Rotated Schwefel's function		900
f_{10}	Hybrid function 1 (N = 3)		1000
f_{11}	Hybrid function 2 (N = 3)		1100
f_{12}	Hybrid function 3 (N = 3)		1200
f_{13}	Hybrid function 4 (N = 4)		1300
f_{14}	Hybrid function 5 (N = 4)	Hybrid.	1400
f_{15}	Hybrid function 6 (N = 4)		1500
f_{16}	Hybrid function 6 (N = 5)		1600
f_{17}	Hybrid function 6 (N = 5)		1700
f_{18}	Hybrid function 6 (N = 5)		1800
f_{19}	Hybrid function (N = 6)		1900
f_{20}	Composition function 1 (N = 3)		2000
f_{21}	Composition function 2 (N = 3)		2100
f_{22}	Composition function 3 (N = 4)		2200
f_{23}	Composition function 4 (N = 4)		2300
f_{24}	Composition function 5 (N = 5)		2400
f_{25}	Composition function 6 (N = 5)	Comp.	2500
f_{26}	Composition function 7 (N = 6)		2600
f_{27}	Composition function 8 (N = 6)		2700
f_{28}	Composition function 9 (N = 3)		2800
f_{29}	Composition function 10 (N = 3)		2900
f_{30}	Composition function 11 (N = 3)		3000

Search range: $[-100, 100]^D$

Table 28

Summary of the CEC2020 benchmark functions: Uni. = Unimodal function, Multi. = Multimodal function, Hybrid. = Hybrid function, Comp. = Composition function.

No.	Func.	Feature	Optimum
f_1	Shifted and Rotated Bent Cigar Function	Uni.	100
f_2	Shifted and Rotated Schwefel's function		1100
f_3	Shifted and Rotated Lunacek bi-Rastrigin function	Multi.	700
f_4	Expanded Rosenbrock's plus Griewangk's function		1900
f_5	Hybrid function 1 (N = 3)		1700
f_6	Hybrid function 2 (N = 4)	Hybrid.	1600
f_7	Hybrid function 3 (N = 5)		2100
f_8	Composition function 1 (N = 3)		2200
f_9	Composition function 2 (N = 4)	Comp.	2400
f_{10}	Composition function 3 (N = 5)		2500

Search range: $[-100, 100]^D$

Table 29

Summary of the CEC2022 benchmark functions: Uni. = Unimodal function, Basic. = Basic function, Hybrid. = Hybrid function, Comp. = Composition function.

Func.	Description	Feature	Optimum
f_1	Shifted and full Rotated Zakharov	Uni.	300
f_2	Shifted and full Rotated Rosenbrock		400
f_3	Shifted and full Rotated Expanded Schaffer f_6	Basic.	600
f_4	Shifted and full Rotated Non-Continuous Rastrigin		800
f_5	Shifted and full Rotated Levy		900
f_6	Hybrid function 1 (N = 3)		1800
f_7	Hybrid function 2 (N = 6)	Hybrid.	2000
f_8	Hybrid function 3 (N = 5)		2200
f_9	Composition function 1 (N = 5)		2300
f_{10}	Composition function 2 (N = 4)	Comp.	2400
f_{11}	Composition function 3 (N = 5)		2600
f_{12}	Composition function 3 (N = 6)		2700

Search range: $[-100, 100]^D$

Table 30

Experimental results and statistical analysis between ISHACDE and state-of-the-art optimizers on 30-D CEC2017.

Func.	PSO	DE	CMA-ES	SaDE	CL-PSO	CPSO	JADE	SHADE	L-SHADE	PPSO	ISHACDE	
f_1	mean std	3.610e+09 + 1.348e+09	3.897e+10 + 5.431e+09	2.817e+09 + 4.598e+08	1.051e+04 + 6.231e+03	2.683e+07 + 6.425e+06	3.250e+10 + 1.223e+10	6.016e+04 + 6.017e+04	2.710e+03 + 2.001e+03	2.913e+03 + 2.755e+03	1.620e+09 + 9.308e+08	1.091e+02 1.371e+01
f_3	mean std	1.059e+05 + 2.131e+04	2.491e+05 + 3.102e+04	9.933e+04 + 1.601e+04	1.030e+05 + 1.463e+04	1.001e+05 + 1.254e+04	1.340e+05 + 1.876e+04	7.353e+04 + 2.098e+04	7.063e+04 + 2.780e+04	6.841e+04 + 2.815e+04	6.615e+04 + 2.980e+04	5.200e+04 2.980e+04
f_4	mean std	2.177e+03 + 1.363e+03	3.812e+03 + 5.996e+02	7.141e+02 + 4.651e+01	4.956e+02 + 1.236e+01	5.585e+02 + 1.544e+01	7.920e+03 + 3.537e+03	5.084e+02 + 1.268e+01	4.972e+02 + 1.858e+01	5.097e+02 + 1.149e+01	7.310e+02 + 8.712e+01	4.709e+02 3.320e+01
f_5	mean std	8.324e+02 + 5.166e+01	9.000e+02 + 1.696e+01	7.628e+02 + 1.608e+01	6.783e+02 + 1.526e+01	6.956e+02 + 1.359e+01	8.750e+02 + 1.010e+01	6.305e+02 + 9.631e+00	6.375e+02 + 1.096e+01	6.408e+02 + 4.013e+01	7.436e+02 + 2.124e+01	6.081e+02 2.124e+01
f_6	mean std	6.648e+02 + 1.420e+01	6.756e+02 + 3.947e+00	6.411e+02 + 5.426e+00	6.002e+02 + 3.528e-02	6.125e+02 + 1.704e+00	6.770e+02 + 9.748e+00	6.029e+02 + 3.519e-01	6.005e+02 + 1.181e-01	6.621e+02 + 1.106e-01	6.005e+02 + 8.870e+00	6.000e+02 1.053e-01
f_7	mean std	1.138e+03 + 6.678e+01	2.449e+03 + 2.567e+02	1.146e+03 + 2.165e+01	9.198e+02 + 1.190e+01	9.483e+02 + 1.511e+01	1.681e+03 + 1.653e+02	8.690e+02 + 1.139e+01	8.670e+02 + 9.341e+00	8.754e+02 + 7.483e+00	1.256e+03 + 8.975e+01	8.562e+02 2.282e+01
f_8	mean std	1.098e+03 + 3.890e+01	1.187e+03 + 2.396e+01	1.066e+03 + 1.112e+01	9.879e+02 + 1.151e+01	9.871e+02 + 1.330e+01	1.133e+03 + 4.677e+01	9.309e+02 + 9.277e+00	9.363e+02 + 8.905e+00	9.357e+02 + 1.239e+01	1.002e+03 + 3.429e+01	9.270e+02 1.904e+01
f_9	mean std	1.039e+04 + 4.293e+03	1.730e+04 + 1.887e+03	5.031e+03 + 5.904e+02	9.016e+02 ≈ 9.512e-01	4.606e+03 + 8.929e+02	1.354e+04 + 3.354e+03	1.471e+03 + 2.519e+02	9.519e+02 + 3.254e+01	9.896e+02 + 8.253e+01	7.927e+03 + 1.832e+03	9.045e+02 + 5.228e+00
f_{10}	mean std	8.885e+03 + 2.341e+02	8.231e+03 + 3.091e+02	8.522e+03 + 3.109e+02	8.143e+03 + 3.079e+02	6.932e+03 + 2.229e+02	8.555e+03 ≈ 5.804e+02	6.174e+03 ≈ 2.559e+02	6.238e+03 ≈ 3.774e+02	6.368e+03 ≈ 2.561e+02	6.622e+03 ≈ 9.105e+02	6.307e+03 ≈ 6.485e+02
f_{11}	mean std	3.803e+03 + 1.419e+03	2.103e+03 + 3.533e+02	1.344e+03 + 2.342e+01	1.265e+03 + 2.818e+01	1.652e+03 + 1.951e+02	8.071e+03 + 2.937e+03	1.630e+03 + 1.558e+02	1.255e+03 + 1.970e+01	1.262e+03 + 1.780e+01	1.650e+03 + 1.994e+02	1.167e+03 1.022e+02
f_{12}	mean std	3.900e+08 + 3.278e+08	1.659e+09 + 2.767e+08	2.046e+07 + 3.998e+06	1.706e+06 + 8.114e+05	8.379e+06 + 2.660e+06	3.883e+09 + 2.488e+09	3.452e+06 + 1.008e+06	9.110e+05 + 4.592e+05	9.950e+05 + 3.523e+05	1.039e+08 + 8.111e+07	3.482e+04 2.320e+04
f_{13}	mean std	3.417e+07 + 1.020e+08	1.104e+08 + 3.678e+07	7.545e+03 ≈ 1.251e+03	2.287e+05 + 1.808e+05	6.410e+05 + 4.204e+05	1.798e+09 + 1.277e+09	1.519e+06 + 8.618e+05	1.081e+05 + 4.678e+04	8.106e+04 + 2.711e+04	8.106e+06 + 1.869e+07	1.538e+04 + 3.371e+04
f_{14}	mean std	3.891e+05 + 3.792e+05	9.851e+03 + 3.253e+03	1.504e+03 − 5.618e+00	9.752e+03 + 3.359e+03	2.169e+05 + 1.335e+05	8.197e+05 + 7.156e+05	2.018e+05 + 1.024e+05	2.170e+03 − 8.176e+02	3.358e+03 − 3.290e+03	8.293e+04 + 1.322e+05	9.527e+03 + 2.180e+04
f_{15}	mean std	9.104e+05 + 3.275e+06	4.108e+05 + 1.503e+05	1.821e+03 − 5.393e+01	4.071e+04 + 1.910e+04	1.903e+05 + 1.873e+05	1.454e+08 + 1.950e+08	4.691e+05 + 2.462e+05	9.736e+03 + 3.882e+03	1.054e+04 + 5.005e+03	4.376e+04 + 5.282e+04	3.640e+03 + 7.982e+03
f_{16}	mean std	4.195e+03 + 2.675e+02	3.819e+03 + 1.921e+02	3.525e+03 + 1.962e+02	3.046e+03 + 1.750e+02	2.952e+03 + 1.736e+02	4.342e+03 + 3.550e+02	2.850e+03 + 1.851e+02	2.758e+03 ≈ 1.235e+02	2.683e+03 ≈ 1.507e+02	3.577e+03 + 3.967e+02	2.729e+03 + 3.318e+02

Table 31

Experimental results and statistical analysis between ISHACDE and state-of-the-art optimizers on 30-D CEC2017 (Continued).

Func.	PSO	DE	CMA-ES	SaDE	CL-PSO	CPSO	JADE	SHADE	L-SHADE	PPSO	ISHACDE	
f_{17}	mean std	2.909e+03 + 1.793e+02	2.624e+03 + 2.667e+02	2.584e+03 + 9.776e+01	2.178e+03 + 1.214e+02	2.202e+03 + 1.059e+02	2.797e+03 + 2.676e+02	2.112e+03 ≈ 1.175e+02	2.012e+03 ≈ 7.611e+01	1.978e+03 ≈ 7.014e+01	2.697e+03 + 2.773e+02	2.079e+03 + 9.101e+01
f_{18}	mean std	1.517e+07 + 1.072e+07	4.257e+06 + 2.037e+06	4.413e+03 − 9.710e+02	1.257e+06 + 4.484e+05	8.734e+05 + 4.277e+05	1.709e+07 + 1.180e+07	9.877e+05 + 4.082e+05	3.147e+05 + 1.382e+05	3.356e+05 + 1.746e+05	3.121e+06 + 5.273e+06	2.043e+05 + 3.481e+05
f_{19}	mean std	2.453e+07 + 8.768e+07	8.400e+06 + 2.669e+06	2.154e+03 − 5.625e+01	3.782e+04 − 1.749e+04	2.052e+05 + 1.244e+05	1.866e+08 + 1.548e+08	3.057e+05 + 1.512e+05	1.313e+04 − 7.329e+03	1.484e+04 − 7.270e+03	2.901e+05 + 7.359e+05	7.535e+04 + 3.199e+05
f_{20}	mean std	2.928e+03 + 1.492e+02	2.580e+03 + 1.365e+02	2.915e+03 + 1.109e+02	2.547e+03 ≈ 9.181e+01	2.579e+03 + 8.049e+01	2.852e+03 + 1.721e+02	2.478e+03 ≈ 9.154e+01	2.405e+03 ≈ 7.399e+01	2.424e+03 ≈ 7.153e+01	2.847e+03 + 1.948e+02	2.482e+03 + 1.391e+02
f_{21}	mean std	2.605e+03 + 5.560e+01	2.664e+03 + 2.056e+01	2.552e+03 + 1.890e+01	2.480e+03 + 9.927e+00	2.485e+03 + 1.782e+01	2.656e+03 + 4.537e+01	2.430e+03 + 1.131e+01	2.438e+03 + 1.228e+01	2.438e+03 + 7.525e+00	2.538e+03 + 4.512e+01	2.411e+03 + 2.955e+01
f_{22}	mean std	4.611e+03 + 2.550e+03	9.920e+03 + 2.088e+02	4.006e+04 + 2.471e+02	2.834e+03 + 1.610e+03	3.329e+03 + 4.492e+02	7.928e+03 + 1.852e+03	2.680e+03 + 2.718e+01	2.319e+03 + 2.696e+01	2.325e+03 + 2.696e+01	6.708e+03 + 2.209e+03	2.300e+03 + 1.012e+00
f_{23}	mean std	3.043e+03 + 5.029e+01	2.987e+03 + 1.876e+01	2.920e+03 + 1.505e+01	2.833e+03 + 9.662e+00	2.853e+03 + 1.432e+01	3.216e+03 + 6.585e+01	2.781e+03 + 9.979e+00	2.790e+03 + 1.058e+01	2.786e+03 + 1.199e+01	3.129e+03 + 1.025e+02	2.760e+03 + 2.663e+01
f_{24}	mean std	3.258e+03 + 7.990e+01	3.119e+03 + 1.869e+01	3.086e+03 + 1.841e+01	2.997e+03 + 2.040e+01	3.037e+03 + 1.7979e+01	3.365e+03 + 1.2131e+01	2.957e+03 + 1.2299e+01	2.962e+03 + 9.182e+00	3.283e+03 + 8.201e+01	3.283e+03 + 5.042e+01	2.909e+03 + 5.042e+01
f_{25}	mean std	3.189e+03 + 1.295e+02	6.380e+03 + 5.306e+02	3.139e+03 + 3.978e+01	2.887e+03 ≈ 1.234e+01	2.954e+03 + 5.165e+03	2.888e+03 ≈ 4.854e+00	2.888e+03 ≈ 6.016e+00	2.889e+03 ≈ 2.809e+00	3.119e+03 + 1.478e+02	2.889e+03 + 9.614e+00	2.889e+03 + 8.112e+00
f_{26}	mean std	7.877e+03 + 8.510e+02	7.594e+03 + 1.790e+02	6.304e+03 + 1.429e+02	5.385e+03 + 9.584e+01	5.978e+03 + 1.588e+02	9.137e+03 + 8.630e+02	9.137e+03 + 1.067e+02	9.137e+03 + 9.730e+01	9.137e+03 + 1.261e+02	8.190e+03 + 7.550e+02	4.301e+03 + 5.494e+02
f_{27}	mean std	3.632e+03 + 1.306e+02	3.281e+03 + 1.673e+01	3.242e+03 + 1.425e+01	3.219e+03 ≈ 7.791e+00	3.258e+03 + 5.913e+00	3.228e+03 + 8.283e-05	3.228e+03 + 4.854e+00	3.224e+03 + 6.016e+00	3.224e+03 + 2.809e+00	3.459e+03 + 1.478e+02	3.220e+03 + 9.614e+00
f_{28}	mean std	3.941e+03 + 2.832e+02	4.713e+03 + 6.023e+02	3.421e+03 + 4.123e+01	3.230e+03 + 1.720e+01	3.359e+03 + 1.698e+01	3.300e+03 + 9.374e-03	3.230e+03 + 2.002e+01	3.226e+03 + 1.535e+01	3.234e+03 + 2.071e+01	3.524e+03 + 1.061e+02	3.197e+03 + 3.291e+01
f_{29}	mean std	5.393e+03 + 3.418e+02	4.305e+03 + 2.405e+02	4.363e+03 + 2.024e+02	4.084e+03 + 1.107e+02	4.031e+03 + 1.311e+02	5.336e+03 + 4.479e+02	3.726e+03 + 9.809e+01	3.769e+03 + 7.056e+01	3.803e+03 + 9.872e+01	5.221e+03 + 3.981e+02	3.551e+03 + 8.170e+01
f_{30}	mean std	3.792e+07 + 6.822e+07	1.088e+07 + 3.849e+06	8.942e+04 + 3.062e+04	1.750e+05 + 1.259e+05	1.062e+06 + 4.046e+05	1.125e+08 + 1.055e+08	1.998e+05 + 9.235e+04	1.925e+05 + 8.764e+04	1.863e+05 + 9.431e+04	2.866e+06 + 2.712e+06	9.192e+03 + 2.828e+03
+/-		29/0/0	29/0/0	24/1/4	24/4/1	29/0/0	28/0/1	25/4/0	22/5/2	22/4/3	28/1/0	-
Avg. ranks		9.5	9.4	6.2	4.0	6.2	9.9	5.0	2.8	3.3	7.8	1.8

Table 32

Experimental results and statistical analysis between ISHACDE and state-of-the-art optimizers on 50-D CEC2017.

Func.	PSO	DE	CMA-ES	SaDE	CL-PSO	CPSO	JADE	SHADE	L-SHADE	PPSO	ISHACDE	
f_1	mean std	2.049e+10 + 5.450e+09	1.017e+11 + 1.196e+10	1.093e+10 + 2.491e+09	2.405e+03 ≈ 2.448e+03	1.565e+07 + 3.425e+06	1.041e+11 + 2.605e+10	2.282e+03 ≈ 4.019e+03	2.182e+03 ≈ 1.809e+03	1.195e+03 ≈ 1.121e+03	5.232e+09 + 1.331e+09	2.493e+03 2.654e+03
f_3	mean std	2.358e+05 + 2.291e+04	4.577e+05 + 4.188e+04	2.442e+05 + 2.852e+04	2.341e+05 + 2.306e+04	2.175e+05 + 2.116e+04	2.781e+05 + 3.012e+04	1.727e+05 ≈ 2.492e+04	1.085e+05 ≈ 7.678e+04	1.051e+05 ≈ 7.130e+04	1.791e+05 ≈ 4.925e+04	1.483e+05 6.234e+04
f_4	mean std	5.999e+03 + 4.170e+03	1.546e+04 + 3.047e+03	1.670e+03 + 3.037e+02	5.566e+02 ≈ 5.093e+01	6.550e+02 + 3.133e+01	2.658e+04 + 7.647e+03	5.207e+02 ≈ 4.704e+01	5.398e+02 ≈ 4.909e+01	5.212e+02 ≈ 4.590e+01	1.459e+03 + 2.952e+02	5.411e+02 5.692e+01
f_5	mean std	1.105e+03 + 1.014e+02	1.272e+03 + 4.455e+01	1.022e+03 + 2.066e+01	8.561e+02 + 1.379e+01	8.775e+02 + 2.071e+01	1.246e+03 + 5.047e+01	7.563e+02 + 2.120e+01	7.553e+02 + 1.125e+01	7.677e+02 + 1.440e+01	9.600e+02 + 7.180e+01	7.200e+02 6.052e+01
f_6	mean std	6.763e+02 + 9.408e+00	6.961e+02 + 5.101e+00	6.552e+02 + 6.054e+00	6.001e+02 ≈ 1.184e−02	6.114e+02 + 1.552e+00	7.024e+02 + 1.021e+01	6.038e+02 + 6.755e−01	6.001e+02 ≈ 3.504e−02	6.001e+02 ≈ 2.635e−02	6.764e+02 + 7.194e+00	6.001e+02 2.403e−01
f_7	mean std	1.608e+03 + 1.016e+02	4.709e+03 + 2.855e+02	1.504e+03 + 4.744e+01	1.108e+03 + 1.490e+01	1.150e+03 + 2.084e+01	3.111e+03 + 3.307e+02	1.013e+03 + 1.286e+01	1.011e+03 + 1.432e+01	1.016e+03 + 1.576e+01	1.989e+03 + 1.472e+02	9.889e+02 3.230e+01
f_8	mean std	1.371e+03 + 7.305e+01	1.579e+03 + 2.702e+01	1.307e+03 + 1.751e+01	1.157e+03 + 1.488e+01	1.171e+03 + 1.939e+01	1.543e+03 + 6.951e+01	1.056e+03 + 1.468e+01	1.052e+03 + 1.753e+01	1.063e+03 + 1.779e+01	1.279e+03 + 4.976e+01	1.008e+03 4.744e+01
f_9	mean std	2.815e+04 + 7.490e+03	5.065e+04 + 4.160e+03	1.400e+04 + 2.655e+03	9.014e+02 − 1.008e+00	1.658e+04 + 2.436e+03	4.410e+04 + 7.989e+03	3.211e+03 + 1.319e+03	9.255e+02 − 5.326e+01	9.619e+02 − 5.272e+01	2.294e+04 + 5.615e+03	1.055e+03 1.299e+02
f_{10}	mean std	1.498e+04 + 3.149e+02	1.470e+04 + 4.215e+02	1.502e+04 + 3.914e+02	1.439e+04 + 3.940e+02	1.147e+04 + 3.289e+02	1.494e+04 + 6.806e+02	1.063e+04 + 4.641e+02	1.012e+04 ≈ 3.222e+02	1.034e+04 + 3.489e+02	1.151e+04 ≈ 1.404e+03	1.025e+04 7.786e+02
f_{11}	mean std	1.236e+04 + 5.326e+03	2.029e+04 + 3.948e+03	1.659e+03 + 6.963e+01	1.457e+03 + 3.681e+01	3.108e+03 + 7.033e+02	2.839e+04 + 6.270e+03	5.038e+03 + 1.419e+03	1.447e+03 + 6.234e+01	1.473e+03 + 4.884e+01	3.683e+03 + 1.191e+03	1.447e+03 4.691e+02
f_{12}	mean std	4.072e+09 + 5.590e+09	1.371e+10 + 1.542e+09	2.609e+08 + 3.784e+07	3.396e+06 + 2.304e+06	1.788e+07 + 3.381e+06	3.611e+10 + 8.827e+09	8.363e+06 + 5.932e+06	1.935e+06 + 7.520e+05	2.378e+06 + 8.722e+05	1.052e+09 + 1.190e+09	3.119e+05 3.168e+05
f_{13}	mean std	7.948e+08 + 2.444e+09	2.168e+09 + 4.156e+08	2.248e+05 + 6.549e+04	6.027e+04 + 5.746e+04	1.015e+05 + 4.029e+04	1.140e+10 + 5.607e+09	1.047e+06 + 6.031e+05	2.784e+04 + 8.513e+03	2.566e+04 + 1.036e+04	2.059e+07 + 1.766e+07	3.125e+03 2.130e+03
f_{14}	mean std	7.029e+06 + 4.532e+06	1.057e+06 + 4.801e+05	1.622e+03 − 1.702e+01	1.905e+05 + 5.626e+04	1.482e+06 + 5.423e+05	1.375e+07 + 8.270e+06	1.134e+06 + 6.202e+05	2.198e+03 + 1.959e+03	5.367e+03 − 1.188e+04	2.398e+06 + 4.924e+06	1.391e+05 2.975e+05
f_{15}	mean std	1.212e+08 + 4.448e+08	2.997e+07 + 1.671e+07	3.531e+03 − 2.775e+02	5.311e+04 + 3.212e+04	3.090e+04 + 1.981e+04	2.400e+09 + 1.560e+09	5.427e+05 + 2.792e+05	7.854e+03 + 6.190e+03	1.310e+04 + 6.637e+03	1.383e+06 + 1.895e+06	5.369e+03 2.466e+03
f_{16}	mean std	6.252e+03 + 7.005e+02	6.172e+03 + 2.945e+02	5.422e+03 + 1.951e+02	4.516e+03 + 3.117e+02	3.583e+03 ≈ 2.812e+02	6.804e+03 + 6.803e+02	3.817e+03 + 1.675e+02	3.570e+03 ≈ 1.928e+02	3.488e+03 ≈ 2.153e+02	4.873e+03 + 6.314e+02	3.553e+03 4.484e+02

Table 33

Experimental results and statistical analysis between ISHACDE and state-of-the-art optimizers on 50-D CEC2017 (Continued).

Func.	PSO	DE	CMA-ES	SaDE	CL-PSO	CPSO	JADE	SHADE	L-SHADE	PPSO	ISHACDE	
f_{17}	mean std	4.667e+03 + 3.968e+02	4.993e+03 + 2.527e+02	4.178e+03 + 1.571e+02	3.556e+03 + 1.542e+02	3.264e+03 + 1.918e+02	5.922e+03 + 9.336e+02	3.179e+03 + 1.397e+02	3.010e+03 − 1.514e+02	2.964e+03 − 1.744e+02	4.567e+03 + 5.743e+02	3.118e+03 2.763e+02
f_{18}	mean std	4.688e+07 + 3.470e+07	2.359e+07 + 7.780e+06	6.234e+04 ≈ 2.462e+04	3.623e+06 + 1.362e+06	3.906e+06 + 2.223e+06	6.952e+07 + 3.329e+07	5.008e+06 + 1.503e+06	1.435e+06 + 1.001e+06	1.292e+06 + 1.118e+06	5.543e+06 + 4.257e+06	6.995e+05 1.950e+06
f_{19}	mean std	1.830e+06 + 5.709e+06	4.152e+07 + 1.583e+07	5.742e+03 ≈ 1.351e+03	2.596e+04 + 1.134e+04	3.791e+04 + 1.433e+04	1.281e+09 + 8.810e+08	1.303e+05 + 6.435e+04	9.488e+03 + 6.026e+03	1.735e+04 + 7.980e+03	1.196e+06 + 1.686e+06	5.945e+03 4.632e+03
f_{20}	mean std	4.171e+03 + 1.671e+02	4.401e+03 + 1.873e+02	4.215e+03 + 1.342e+02	3.818e+03 + 1.576e+02	3.281e+03 ≈ 1.481e+02	4.230e+03 + 1.889e+02	3.442e+03 + 1.388e+02	3.171e+03 − 1.457e+02	3.241e+03 − 1.494e+02	3.703e+03 + 2.861e+02	3.356e+03 1.405e+02
f_{21}	mean std	2.939e+03 + 8.639e+01	3.059e+03 + 2.474e+01	2.824e+03 + 2.703e+01	2.650e+03 + 2.007e+01	2.658e+03 + 2.140e+01	3.045e+03 + 8.157e+01	2.563e+03 + 1.875e+01	2.551e+03 + 1.389e+01	2.557e+03 + 1.341e+01	2.858e+03 + 6.569e+01	2.495e+03 6.831e+01
f_{22}	mean std	1.667e+04 + 5.328e+02	1.667e+04 + 3.030e+02	1.641e+04 + 2.572e+02	1.585e+04 + 3.724e+02	1.217e+04 + 3.026e+03	1.617e+04 + 1.590e+03	1.120e+04 + 2.578e+03	9.978e+03 ≈ 2.963e+03	1.101e+04 + 2.258e+03	1.384e+04 + 1.260e+03	1.125e+04 3.406e+03
f_{23}	mean std	3.726e+03 + 1.705e+02	3.489e+03 + 3.905e+01	3.319e+03 + 3.168e+01	3.078e+03 + 1.457e+01	3.136e+03 + 2.529e+01	3.940e+03 + 1.519e+02	3.002e+03 + 1.737e+01	2.982e+03 + 1.540e+01	2.989e+03 + 1.338e+01	3.855e+03 + 2.115e+02	2.940e+03 5.263e+01
f_{24}	mean std	3.861e+03 + 1.321e+02	3.537e+03 + 3.457e+01	3.479e+03 + 4.456e+01	3.248e+03 + 1.766e+01	3.338e+03 + 3.267e+01	4.105e+03 + 1.544e+02	3.148e+03 + 2.519e+01	3.147e+03 + 1.789e+01	3.163e+03 + 1.407e+01	4.053e+03 + 2.304e+02	3.033e+03 5.422e+01
f_{25}	mean std	5.432e+03 + 6.790e+02	1.964e+04 + 3.346e+03	4.187e+03 + 3.657e+02	3.046e+03 ≈ 2.106e+01	3.183e+03 + 1.693e+01	1.710e+04 + 4.549e+03	3.045e+03 ≈ 2.538e+01	3.080e+03 + 2.521e+01	3.088e+03 + 2.289e+01	3.890e+03 + 3.376e+02	3.050e+03 4.196e+01
f_{26}	mean std	1.301e+04 + 1.178e+03	1.182e+04 + 4.656e+02	9.263e+03 + 2.870e+02	7.027e+03 + 2.195e+02	7.752e+03 + 2.180e+02	1.698e+04 + 1.674e+03	6.263e+03 + 1.552e+02	6.240e+03 + 2.173e+02	6.403e+03 + 1.976e+02	1.372e+04 + 1.108e+03	5.540e+03 7.310e+02
f_{27}	mean std	4.978e+03 + 4.483e+02	3.649e+03 + 7.083e+01	3.493e+03 + 6.309e+01	3.278e+03 − 3.989e+01	3.566e+03 + 3.320e+01	3.200e+03 ≈ 5.019e−05	3.399e+03 ≈ 3.242e+01	3.302e+03 ≈ 3.902e+01	3.332e+03 ≈ 4.417e+01	4.464e+03 + 3.719e+02	3.384e+03 5.523e+01
f_{28}	mean std	6.429e+03 + 8.434e+02	8.815e+03 + 3.417e+02	3.961e+03 + 2.709e+02	3.323e+03 + 1.775e+01	3.608e+03 + 3.966e+01	3.300e+03 − 1.043e−04	3.319e+03 ≈ 1.255e+01	3.334e+03 + 2.740e+01	3.350e+03 + 1.726e+01	4.417e+03 + 3.175e+02	3.311e+03 2.266e+01
f_{29}	mean std	8.366e+03 + 1.487e+03	6.729e+03 + 3.716e+02	5.936e+03 + 1.989e+02	4.914e+03 + 1.596e+02	4.593e+03 + 1.885e+02	1.112e+04 + 3.032e+03	4.097e+03 + 1.673e+02	4.101e+03 + 1.277e+02	4.164e+03 + 1.154e+02	7.410e+03 + 1.076e+03	3.827e+03 2.368e+02
f_{30}	mean std	2.918e+08 + 2.776e+08	3.669e+08 + 1.241e+08	9.908e+06 + 2.939e+06	5.555e+06 + 1.881e+06	5.778e+06 + 9.817e+05	1.737e+09 + 1.101e+09	3.791e+06 + 9.992e+05	3.358e+06 + 7.304e+05	3.887e+06 + 8.498e+05	4.913e+07 + 2.897e+07	1.065e+06 3.454e+05
+/-/-	29/0/0	29/0/0	25/2/2	23/4/2	27/2/0	27/0/2	22/7/0	17/8/4	18/7/4	27/2/0	-	
Avg. ranks	9.2	9.7	6.6	4.7	5.8	9.8	4.3	2.5	3.1	7.8	2.3	

Table 34

Experimental results and statistical analysis between ISHACDE and recently proposed optimizers on 30-D CEC2017.

Func.	MPA	FOX	POA	OOA	EVO	COA	FLA	RIME	DEA ² H ²	CDE	ISHACDE	
f_1	mean std	2.573e+05 + 1.877e+05	8.319e+06 + 1.480e+06	1.516e+10 + 4.377e+09	2.606e+10 + 7.278e+09	9.958e+09 + 3.746e+09	3.358e+10 + 6.488e+09	1.026e+08 + 2.434e+07	4.812e+06 + 1.606e+06	4.497e+03 + 3.796e+03	3.762e+03 + 3.879e+03	1.091e+02 1.371e+01
f_3	mean std	4.405e+03 - 2.430e+03	6.673e+04 + 2.342e+04	4.341e+04 ≈ 7.908e+03	5.168e+04 ≈ 1.048e+04	1.554e+05 + 4.623e+04	8.912e+04 + 7.211e+03	2.105e+04 - 5.625e+03	2.791e+04 - 1.071e+04	4.901e+02 - 5.206e+02	6.583e+04 + 4.841e+02	5.200e+04 + 4.938e+02 + 4.709e+02
f_4	mean std	5.058e+02 + 2.847e+01	5.158e+02 + 1.466e+01	1.791e+03 + 1.400e+03	4.703e+03 + 1.756e+03	2.290e+03 + 7.946e+02	6.236e+03 + 6.269e+02	5.245e+02 + 8.422e+02	5.206e+02 + 6.500e+02	4.938e+02 + 5.932e+02 ≈	4.938e+02 + 6.449e+02 +	4.709e+02 + 6.822e+02 + 6.081e+02
f_5	mean std	6.816e+02 + 4.927e+01	7.763e+02 + 2.211e+01	7.569e+02 + 3.778e+01	7.946e+02 + 3.354e+01	6.269e+02 + 1.668e+01	8.422e+02 + 1.917e+01	6.500e+02 + 2.636e+01	5.932e+02 + 2.449e+01	6.449e+02 + 3.679e+01	6.822e+02 + 1.908e+01	6.000e+02 ≈ 2.124e+01
f_6	mean std	6.193e+02 + 6.909e+00	6.721e+02 + 7.873e+00	6.550e+02 + 7.496e+00	6.588e+02 + 6.733e+00	6.219e+02 + 6.415e+00	6.728e+02 + 5.099e+00	6.087e+02 + 3.158e+00	6.062e+02 + 2.748e+00	6.223e+02 + 5.615e+00	6.000e+02 + 9.007e-02	6.000e+02 + 1.053e-01
f_7	mean std	9.978e+02 + 6.971e+01	1.320e+03 + 4.673e+01	1.190e+03 + 5.684e+01	1.185e+03 + 7.796e+01	9.609e+02 + 4.639e+01	1.325e+03 + 7.214e+01	9.420e+02 + 2.852e+01	8.514e+02 ≈ 3.246e+01	9.851e+02 + 5.198e+01	9.229e+02 + 1.208e+01	8.562e+02 + 2.282e+01
f_8	mean std	9.566e+02 + 4.182e+01	9.830e+02 + 2.239e+01	9.831e+02 + 2.437e+01	1.041e+03 + 2.004e+01	9.252e+02 ≈ 2.926e+01	1.105e+03 + 1.920e+01	9.462e+02 + 2.287e+01	8.840e+02 - 1.866e+01	9.416e+02 ≈ 3.503e+01	9.782e+02 + 1.471e+01	9.270e+02 + 1.904e+01
f_9	mean std	3.280e+03 + 1.091e+03	8.127e+03 + 4.354e+02	5.639e+03 + 5.101e+02	5.931e+03 + 1.320e+03	3.348e+03 + 8.012e+02	8.616e+03 + 1.725e+03	3.528e+03 + 1.863e+03	1.662e+03 + 5.951e+02	3.153e+03 + 9.237e+02	9.081e+02 + 8.307e+00	9.045e+02 + 5.228e+00
f_{10}	mean std	4.750e+03 - 7.396e+02	5.984e+03 ≈ 6.450e+02	5.074e+03 - 3.605e+02	7.191e+03 + 7.275e+02	5.327e+03 - 6.208e+02	8.090e+03 + 3.425e+02	4.977e+03 - 6.830e+02	4.532e+03 - 5.098e+02	5.102e+03 - 7.739e+02	8.232e+03 + 3.113e+02	6.307e+03 + 6.485e+02
f_{11}	mean std	1.319e+03 + 6.095e+01	1.371e+03 + 6.404e+01	1.826e+03 + 3.878e+02	2.323e+03 + 7.114e+02	4.711e+03 + 1.533e+03	5.891e+03 + 1.292e+03	1.304e+03 + 1.304e+01	1.262e+03 + 6.338e+01	1.215e+03 + 4.652e+01	3.679e+01 + 3.679e+01	1.167e+03 + 1.022e+02
f_{12}	mean std	2.444e+06 + 1.873e+06	1.072e+07 + 6.522e+06	5.647e+08 + 5.498e+08	1.778e+09 + 1.058e+09	8.949e+08 + 6.080e+08	3.045e+09 + 9.205e+08	2.318e+07 + 2.131e+07	1.216e+07 + 8.638e+06	9.790e+04 + 8.432e+04	2.849e+05 + 1.914e+05	3.482e+04 + 2.320e+04
f_{13}	mean std	7.863e+04 + 3.746e+04	5.109e+05 + 1.679e+04	4.131e+06 + 5.971e+06	8.821e+07 + 1.327e+08	6.042e+08 + 5.175e+08	6.016e+08 + 2.978e+08	2.284e+06 + 1.701e+06	1.250e+05 + 6.301e+04	2.146e+04 + 2.020e+04	2.088e+04 + 1.027e+04	1.538e+04 + 3.371e+04
f_{14}	mean std	2.221e+03 - 1.217e+03	4.400e+04 + 3.594e+04	4.643e+03 - 6.030e+03	1.962e+04 + 2.731e+04	1.479e+06 + 1.713e+06	2.780e+05 + 1.726e+05	8.137e+04 + 4.473e+04	6.760e+04 + 5.052e+04	1.616e+03 - 7.407e+01	4.910e+03 - 2.370e+03	9.527e+03 - 2.180e+04
f_{15}	mean std	1.218e+04 + 1.161e+04	7.581e+04 + 5.121e+04	4.653e+04 + 5.350e+04	4.303e+04 + 4.144e+04	2.059e+07 + 4.873e+07	7.125e+06 + 3.746e+06	3.945e+05 + 2.737e+05	2.975e+04 + 2.027e+04	8.202e+03 + 1.138e+04	8.434e+03 + 4.872e+03	3.640e+03 + 7.982e+03
f_{16}	mean std	2.832e+03 ≈ 4.465e+02	3.956e+03 + 3.460e+02	2.898e+03 ≈ 2.683e+02	3.537e+03 + 2.844e+02	3.524e+03 + 3.007e+02	3.881e+03 + 2.706e+02	2.680e+03 ≈ 2.895e+02	2.510e+03 - 3.194e+02	2.691e+03 ≈ 3.628e+02	3.139e+03 + 3.030e+02	2.729e+03 + 2.030e+02

Table 35

Experimental results and statistical analysis between ISHACDE and recently proposed optimizers on 30-D CEC2017 (Continued).

Func.	MPA	FOX	POA	OOA	EVO	COA	FLA	RIME	DEA ² H ²	CDE	ISHACDE	
f_{17}	mean std	2.343e+03 + 2.623e+02	2.827e+03 + 3.386e+02	2.167e+03 + 1.886e+02	2.437e+03 + 1.800e+02	2.468e+03 + 2.041e+02	2.633e+03 + 2.082e+02	2.166e+03 + 2.248e+02	2.143e+03 + 1.549e+02	2.224e+03 + 2.348e+02	2.051e+03 ≈ 1.055e+02	2.079e+03 + 9.101e+01
f_{18}	mean std	6.702e+04 - 3.881e+04	6.400e+05 + 4.624e+05	1.470e+05 ≈ 5.871e+05	3.494e+05 + 9.644e+06	9.644e+06 + 3.083e+06	9.040e+05 + 9.040e+05	1.034e+06 + 1.034e+04	3.055e+04 - 2.137e+04	6.025e+05 + 3.370e+05	2.043e+05 + 3.481e+05	
f_{19}	mean std	1.683e+04 - 1.494e+04	1.351e+06 + 7.895e+05	1.536e+06 + 1.330e+06	2.291e+06 + 2.628e+06	4.064e+07 + 5.054e+07	2.242e+07 + 1.703e+07	3.706e+05 + 4.878e+05	3.284e+04 - 2.741e+04	4.357e+03 - 4.890e+03	1.121e+04 - 9.042e+03	7.535e+04 + 3.199e+05
f_{20}	mean std	2.619e+03 + 1.983e+02	3.021e+03 + 2.741e+02	2.405e+03 ≈ 1.030e+02	2.601e+03 + 1.367e+02	2.555e+03 ≈ 1.655e+02	2.777e+03 + 9.406e+01	2.397e+03 ≈ 1.376e+02	2.425e+03 ≈ 1.323e+02	2.597e+03 ≈ 2.249e+02	2.555e+03 ≈ 1.148e+02	2.482e+03 + 1.391e+02
f_{21}	mean std	2.449e+03 + 2.785e+01	2.641e+03 + 4.463e+01	2.510e+03 + 7.750e+01	2.588e+03 + 3.159e+01	2.468e+03 + 3.278e+01	2.619e+03 + 2.652e+01	2.451e+03 + 1.952e+01	2.379e+03 - 1.493e+01	2.429e+03 ≈ 3.482e+01	2.478e+03 + 1.451e+01	2.411e+03 + 2.955e+01
f_{22}	mean std	5.129e+03 + 1.711e+03	7.683e+03 + 7.154e+02	4.493e+03 + 1.201e+03	6.281e+03 + 1.129e+03	3.598e+03 + 1.166e+03	6.445e+03 + 7.113e+02	5.892e+03 + 1.863e+03	4.442e+03 + 1.827e+03	5.601e+03 + 1.697e+03	2.300e+03 ≈ 1.196e+00	2.300e+03 + 1.012e+00
f_{23}	mean std	2.853e+03 + 4.612e+01	3.405e+03 + 1.361e+02	2.990e+03 + 8.517e+01	3.113e+03 + 8.302e+01	2.867e+03 + 5.509e+01	3.136e+03 + 5.723e+01	2.801e+03 + 3.097e+01	2.750e+03 - 2.574e+01	2.851e+03 + 4.169e+01	2.776e+03 + 5.028e+01	2.760e+03 + 2.663e+01
f_{24}	mean std	3.096e+03 + 8.575e+01	3.658e+03 + 1.019e+02	3.193e+03 + 1.209e+02	3.299e+03 + 3.597e+01	3.055e+03 + 8.214e+01	3.303e+03 + 2.903e+01	2.977e+03 + 2.074e+01	2.908e+03 ≈ 5.274e+01	3.009e+03 + 5.568e+01	2.971e+03 + 5.272e+01	2.909e+03 + 5.042e+01
f_{25}	mean std	2.902e+03 + 1.667e+01	2.934e+03 + 1.616e+01	3.274e+03 + 1.640e+02	3.636e+03 + 1.774e+02	3.361e+03 + 1.396e+02	4.317e+03 + 3.738e+02	2.921e+03 + 2.731e+01	2.903e+03 + 2.381e+01	2.900e+03 + 2.310e+01	2.890e+03 + 1.837e+01	2.889e+03 + 8.112e+00
f_{26}	mean std	5.569e+03 + 1.039e+03	9.415e+03 + 1.150e+03	6.716e+03 + 1.641e+03	8.402e+03 + 7.279e+02	6.564e+03 + 6.304e+02	8.472e+03 + 5.951e+02	5.219e+03 + 3.173e+02	4.531e+03 + 4.399e+02	6.125e+03 + 6.156e+02	4.547e+03 + 8.485e+02	4.301e+03 + 5.494e+02
f_{27}	mean std	3.253e+03 + 2.651e+01	3.920e+03 + 3.055e+02	3.357e+03 + 6.167e+01	3.534e+03 + 1.384e+02	3.478e+03 + 5.291e+01	3.237e+03 + 5.902e+01	3.228e+03 + 1.547e+01	3.228e+03 + 7.475e+00	3.235e+03 + 2.371e+01	3.220e+03 + 1.053e+01	3.220e+03 + 9.614e-00
f_{28}	mean std	3.260e+03 + 4.423e+01	3.270e+03 + 5.269e+00	3.900e+03 + 2.911e+02	4.838e+03 + 4.649e+02	4.105e+03 + 2.186e+02	5.545e+03 + 4.172e+02	3.307e+03 + 7.586e+01	3.295e+03 + 4.792e+01	3.207e+03 ≈ 3.056e+01	3.221e+03 + 1.575e+01	3.197e+03 + 3.291e+01
f_{29}	mean std	4.030e+03 + 2.000e+02	5.173e+03 + 4.605e+02	4.390e+03 + 2.600e+02	5.194e+03 + 4.037e+02	4.419e+03 + 3.043e+02	4.952e+03 + 3.208e+02	3.836e+03 + 1.925e+02	3.907e+03 + 1.608e+02	4.134e+03 + 3.480e+02	3.814e+03 + 1.615e+02	3.551e+03 + 8.170e+01
f_{30}	mean std	4.020e+04 + 1.986e+04	4.149e+06 + 1.879e+06	9.057e+06 + 8.513e+06	4.228e+07 + 2.842e+07	4.070e+07 + 3.775e+07	1.260e+08 + 5.864e+07	6.864e+05 + 7.957e+05	9.565e+05 + 6.181e+05	1.002e+04 ≈ 3.885e+03	3.937e+04 + 1.833e+04	9.192e+03 + 2.828e+03
+/-/-	Avg. ranks	23/1/5	28/1/0	23/4/2	28/1/0	26/2/1	29/0/0	25/2/2	18/4/7	18/6/5	23/4/2	
Avg. ranks		4.7	8.5	7.0	8.8	7.7	10.3	5.2	3.7	3.8	3.7	

Table 36

Experimental results and statistical analysis between ISHACDE and recently proposed optimizers on 50-D CEC2017.

Func.	MPA	FOX	POA	OOA	EVO	COA	FLA	RIME	DEA ² H ²	CDE	ISHACDE	
f_1	mean std	2.018e+06 + 6.460e+05	3.252e+07 + 3.232e+06	4.425e+10 + 7.771e+09	7.640e+10 + 7.598e+09	3.715e+10 + 6.766e+09	8.814e+10 + 1.411e+10	3.238e+08 + 4.279e+07	1.455e+07 + 6.243e+06	1.870e+04 + 3.677e+046	2.470e+03 ≈ 2.423e+03	2.493e+03 2.654e+03
f_3	mean std	2.822e+04 – 1.060e+04	1.360e+05 ≈ 4.033e+04	1.054e+05 – 1.287e+04	1.447e+05 ≈ 1.331e+04	3.262e+05 + 1.062e+05	1.860e+05 + 1.866e+04	7.536e+04 – 1.563e+04	9.368e+04 – 2.247e+04	4.784e+03 – 2.352e+03	1.488e+05 ≈ 2.202e+04	1.483e+05 6.234e+04
f_4	mean std	5.919e+02 + 5.692e+01	5.829e+02 + 4.093e+01	6.382e+03 + 2.127e+03	1.603e+04 + 3.055e+03	6.084e+03 + 1.570e+03	2.102e+04 + 5.484e+03	6.459e+02 + 4.166e+01	5.395e+02 ≈ 5.855e+01	5.361e+02 ≈ 5.878e+01	5.411e+02 5.662e+01	5.411e+02 5.692e+01
f_5	mean std	8.454e+02 + 5.718e+01	8.803e+02 + 1.701e+01	9.045e+02 + 3.012e+01	1.054e+03 + 3.039e+01	8.012e+02 + 3.184e+01	1.140e+03 + 3.126e+01	8.483e+02 + 5.372e+01	6.641e+02 + 3.603e+01	8.108e+02 + 4.587e+01	8.515e+02 + 6.078e+01	7.200e+02 6.052e+01
f_6	mean std	6.384e+02 + 1.124e+01	6.753e+02 + 3.421e+00	6.678e+02 + 5.668e+00	6.818e+02 + 6.356e+00	6.370e+02 + 4.655e+00	6.878e+02 + 5.724e+00	6.139e+02 + 3.688e+00	6.142e+02 + 4.242e+00	6.356e+02 + 6.275e+00	6.010e+02 + 1.103e+00	6.001e+02 2.403e-01
f_7	mean std	1.507e+03 + 1.352e+02	1.875e+03 + 6.276e+01	1.727e+03 + 9.763e+01	1.790e+03 + 6.352e+01	1.374e+03 + 9.343e+01	1.990e+03 + 7.342e+01	1.219e+03 + 5.676e+01	1.002e+03 ≈ 3.281e+01	1.357e+03 + 1.589e+02	1.151e+03 + 3.284e+01	9.889e+02 ≈ 3.230e+01
f_8	mean std	1.154e+03 + 5.333e+01	1.194e+03 + 2.042e+01	1.248e+03 + 3.461e+01	1.365e+03 + 3.906e+01	1.115e+03 + 3.555e+01	1.435e+03 + 3.412e+01	1.132e+03 + 3.578e+01	9.719e+02 – 3.389e+01	1.109e+03 + 6.742e+01	1.161e+03 + 3.733e+01	1.008e+03 4.744e+01
f_9	mean std	9.354e+03 + 3.855e+03	2.998e+04 + 1.378e+03	1.761e+04 + 1.034e+03	2.319e+04 + 2.983e+03	9.873e+03 + 1.461e+03	3.122e+04 + 2.990e+03	1.461e+04 + 4.804e+03	3.714e+03 + 1.760e+03	9.047e+03 + 2.787e+03	1.918e+03 + 8.220e+02	1.055e+03 1.299e+02
f_{10}	mean std	7.264e+03 – 7.508e+02	9.197e+03 ≈ 9.165e+02	8.679e+03 – 8.735e+02	1.243e+04 + 1.086e+03	8.835e+03 – 9.653e+02	1.408e+04 + 6.040e+02	9.146e+03 ≈ 6.960e+02	7.610e+03 – 9.071e+02	7.917e+03 – 8.088e+02	1.446e+04 + 3.383e+02	1.025e+04 7.786e+02
f_{11}	mean std	1.497e+03 + 7.412e+01	1.587e+03 + 7.808e+01	6.677e+03 + 2.703e+03	1.290e+04 + 2.805e+03	1.638e+04 + 6.515e+03	1.943e+04 + 2.689e+03	1.507e+03 + 9.195e+01	1.598e+03 + 1.195e+02	1.370e+03 + 4.590e+01	1.297e+03 ≈ 5.982e+01	1.447e+03 4.691e+02
f_{12}	mean std	2.308e+07 + 1.254e+07	4.882e+07 + 3.655e+07	6.536e+09 + 3.707e+09	2.102e+10 + 8.081e+09	7.815e+09 + 2.760e+09	2.566e+10 + 6.491e+09	1.145e+08 + 3.390e+07	8.333e+07 + 4.583e+07	1.270e+06 + 1.093e+06	1.990e+06 + 1.004e+06	3.119e+05 3.168e+05
f_{13}	mean std	2.468e+05 + 1.062e+05	2.339e+06 + 3.952e+05	1.420e+09 + 2.743e+09	5.965e+09 + 3.713e+09	3.285e+09 + 1.797e+09	6.827e+09 + 2.433e+09	9.976e+06 + 7.462e+06	3.431e+05 + 2.334e+05	1.329e+04 + 7.927e+03	3.974e+03 + 2.370e+03	3.125e+03 2.130e+03
f_{14}	mean std	1.392e+04 – 1.120e+04	1.148e+05 – 7.744e+04	3.021e+05 + 4.727e+05	9.774e+05 + 1.005e+06	8.771e+06 + 8.546e+06	2.636e+06 + 1.224e+06	4.298e+05 + 2.749e+05	2.720e+05 + 1.737e+05	5.319e+03 – 4.566e+03	1.016e+05 – 6.187e+04	1.391e+05 2.975e+05
f_{15}	mean std	4.533e+04 + 1.588e+04	6.311e+05 + 1.395e+05	7.009e+06 + 1.712e+07	2.893e+08 + 4.006e+08	4.423e+08 + 2.959e+08	6.298e+08 + 2.963e+08	1.293e+06 + 7.314e+05	8.970e+04 + 5.326e+04	9.610e+03 + 6.199e+03	7.388e+03 + 3.513e+03	5.369e+03 2.466e+03
f_{16}	mean std	3.588e+03 ≈ 4.196e+02	4.789e+03 + 5.802e+02	4.141e+03 + 5.457e+02	5.344e+03 + 3.755e+02	4.622e+03 + 6.209e+02	6.113e+03 + 4.498e+02	3.593e+03 ≈ 3.427e+02	3.448e+03 ≈ 5.165e+02	3.347e+03 ≈ 3.400e+02	4.113e+03 + 4.376e+02	3.553e+03 4.484e+02

Table 37

Experimental results and statistical analysis between ISHACDE and recently proposed optimizers on 50-D CEC2017 (Continued).

Func.	MPA	FOX	POA	OOA	EVO	COA	FLA	RIME	DEA ² H ²	CDE	ISHACDE	
f_{17}	mean std	3.423e+03 + 3.551e+02	3.763e+03 + 2.932e+02	3.328e+03 ≈ 3.593e+02	4.324e+03 + 4.617e+02	3.879e+03 + 3.618e+02	4.659e+03 + 4.138e+02	3.074e+03 ≈ 3.048e+02	3.097e+03 ≈ 2.631e+02	3.443e+03 + 4.353e+02	3.574e+03 + 2.573e+02	3.118e+03 2.763e+02
f_{18}	mean std	1.763e+05 – 1.313e+05	1.935e+06 + 1.265e+06	1.881e+06 + 2.302e+06	7.984e+06 + 1.258e+07	3.252e+07 + 2.801e+07	1.272e+07 + 6.703e+06	3.482e+06 + 2.564e+06	3.599e+06 + 1.948e+06	7.940e+04 – 3.476e+04	2.411e+06 + 3.476e+04	6.995e+05 1.950e+06
f_{19}	mean std	2.422e+04 + 1.174e+04	2.696e+06 + 2.121e+06	1.051e+07 + 1.308e+07	6.209e+07 + 7.754e+07	2.117e+08 + 2.287e+08	3.597e+08 + 1.766e+08	4.091e+05 + 2.784e+05	1.686e+05 + 1.497e+05	2.266e+04 + 1.294e+04	1.524e+04 + 6.553e+03	5.945e+03 4.632e+03
f_{20}	mean std	3.208e+03 ≈ 3.297e+02	2.956e+03 – 2.854e+02	3.552e+03 ≈ 2.672e+02	3.311e+03 ≈ 2.773e+02	3.763e+03 + 2.003e+02	3.007e+03 + 2.977e+02	3.192e+03 ≈ 2.450e+02	3.307e+03 ≈ 2.924e+02	3.827e+03 + 1.301e+02	3.356e+03 + 1.405e+02	3.356e+03 1.405e+02
f_{21}	mean std	2.661e+03 + 4.929e+01	3.006e+03 + 5.891e+01	2.798e+03 + 5.180e+01	2.944e+03 + 7.356e+01	2.671e+03 + 5.744e+01	2.991e+03 + 4.200e+01	2.640e+03 + 4.373e+01	2.488e+03 ≈ 3.502e+01	2.582e+03 + 6.362e+01	2.649e+03 + 3.252e+01	2.495e+03 6.831e+01
f_{22}	mean std	9.234e+03 – 1.110e+03	1.137e+04 ≈ 8.650e+02	1.076e+04 ≈ 1.454e+03	1.425e+04 + 8.532e+02	1.106e+04 ≈ 2.224e+03	1.581e+04 + 3.313e+02	1.089e+04 ≈ 9.139e+02	9.294e+03 + 8.432e+02	9.798e+03 – 1.089e+03	1.429e+04 + 4.346e+03	1.125e+04 3.406e+03
f_{23}	mean std	3.183e+03 + 7.891e+01	4.128e+03 + 2.057e+02	3.435e+03 + 1.084e+02	3.849e+03 + 1.254e+02	3.272e+03 + 8.090e+01	3.877e+03 + 1.562e+02	3.081e+03 + 3.891e+01	2.951e+03 + 3.906e+01	3.245e+03 + 3.906e+01	2.997e+03 ≈ 1.154e+02	2.940e+03 1.148e+02
f_{24}	mean std	3.444e+03 + 1.643e+02	4.340e+03 + 1.303e+02	3.655e+03 + 1.505e+02	4.066e+03 + 2.180e+02	3.476e+03 + 7.615e+01	4.038e+03 + 1.166e+02	3.221e+03 + 4.389e+01	3.116e+03 + 6.455e+01	3.345e+03 + 1.041e+02	3.157e+03 + 8.929e+01	3.033e+03 5.422e+01
f_{25}	mean std	3.110e+03 + 3.741e+01	3.103e+03 + 9.835e+00	6.286e+03 + 9.609e+02	1.015e+04 + 9.938e+02	6.968e+03 + 7.280e+02	1.290e+04 + 1.676e+03	1.290e+03 + 3.895e+01	3.135e+03 + 3.446e+01	3.071e+03 ≈ 3.446e+01	3.093e+03 + 3.538e+01	3.050e+03 2.524e+01
f_{26}	mean std	8.496e+03 + 1.150e+03	1.234e+04 + 1.297e+03	1.209e+04 + 2.235e+03	1.437e+04 + 1.184e+03	1.157e+04 + 1.311e+03	1.444e+04 + 9.636e+02	7.477e+03 + 4.859e+02	6.018e+03 ≈ 4.248e+02	9.339e+03 + 1.110e+03	5.820e+03 ≈ 4.815e+02	5.540e+03 7.310e+02
f_{27}	mean std	3.628e+03 + 1.291e+02	5.305e+03 + 7.675e+02	4.106e+03 + 2.134e+02	4.595e+03 + 2.956e+02	4.092e+03 + 3.296e+02	4.523e+03 + 2.284e+02	3.508e+03 + 1.247e+02	3.466e+03 + 2.705e+02	3.646e+03 + 1.761e+02	3.481e+03 + 8.005e+01	3.384e+03 5.523e+01
f_{28}	mean std	3.388e+03 + 3.695e+01	3.344e+03 + 2.793e+01	6.283e+03 + 7.251e+02	8.669e+03 + 6.570e+02	6.548e+03 + 5.299e+02	1.007e+04 + 8.147e+02	3.378e+03 + 2.662e+01	3.403e+03 + 5.217e+01	3.314e+03 ≈ 3.628e+01	3.370e+03 + 2.804e+01	3.311e+03 2.266e+01
f_{29}	mean std	4.877e+03 + 3.247e+02	6.586e+03 + 5.412e+02	6.525e+03 + 6.491e+02	9.811e+03 + 1.860e+03	6.067e+03 + 6.470e+02	8.847e+03 + 8.385e+02	4.425e+03 + 3.152e+02	4.492e+03 + 3.709e+02	5.020e+03 + 4.075e+02	4.291e+03 + 3.981e+02	3.827e+03 2.368e+02
f_{30}	mean std	3.374e+06 + 1.398e+06	6.224e+07 + 1.446e+07	2.044e+08 + 5.366e+08	6.030e+08 + 3.496e+08	5.618e+08 + 3.726e+08	1.011e+09 + 3.921e+08	9.694e+06 + 2.473e+07	3.849e+07 + 1.838e+07	1.053e+06 ≈ 2.970e+05	1.278e+06 + 2.771e+05	1.065e+06 3.454e+05
+/-/-	Avg. ranks	23/1/5	25/3/1	24/2/3	28/1/0	26/2/1	29/0/0	23/4/2	17/7/5	18/6/5	22/6/1	-
Avg. ranks		4.4	7.5	7.2	9.4	7.7	10.5	5.1	3.8	3.4	4.2	2.5

Table 38

Experimental results and statistical analysis between ISHACDE and state-of-the-art optimizers on 50-D CEC2020.

Func.	PSO	DE	CMA-ES	SaDE	CL-PSO	CPSO	JADE	SHADE	L-SHADE	PPSO	ISHACDE	
f_1	mean std	2.049e+10 + 5.450e+09	1.017e+11 + 1.196e+10	1.093e+10 + 2.491e+09	2.405e+03 \approx 2.448e+03	1.565e+07 + 3.425e+06	1.041e+11 + 2.605e+10	2.282e+03 \approx 4.019e+03	2.182e+03 \approx 1.809e+03	1.195e+03 \approx 1.121e+03	5.232e+09 + 1.331e+09	2.493e+03 2.654e+03
f_2	mean std	2.703e+12 + 5.197e+11	1.166e+13 + 1.382e+12	1.117e+12 + 3.103e+11	3.420e+05 + 3.347e+08	1.243e+13 + 2.640e+12	5.647e+05 + 4.247e+05	4.613e+05 + 3.961e+05	4.146e+05 + 3.039e+05	6.726e+11 + 3.168e+11	2.127e+05 2.685e+05	
f_3	mean std	7.440e+11 + 1.973e+11	4.350e+12 + 4.199e+11	4.141e+11 + 8.799e+10	9.563e+04 + 9.221e+04	4.737e+08 + 8.872e+07	3.678e+12 + 6.853e+11	6.679e+04 + 8.792e+04	4.150e+04 + 7.561e+04	5.391e+04 + 6.141e+04	2.091e+11 + 7.595e+10	4.008e+03 1.321e+04
f_4	mean std	1.301e+05 + 3.494e+05	1.430e+06 + 5.894e+05	8.392e+03 + 5.394e+03	1.931e+03 + 2.076e+00	1.943e+03 + 2.639e+00	2.348e+06 + 2.064e+06	1.927e+03 + 2.632e+00	1.926e+03 + 1.704e+00	1.929e+03 + 2.425e+00	1.804e+04 + 3.303e+04	1.918e+03 9.852e+00
f_5	mean std	7.353e+07 + 3.944e+07	5.959e+07 + 1.545e+07	2.208e+06 + 2.875e+05	4.271e+06 + 1.355e+06	4.047e+06 + 9.557e+05	1.272e+08 + 6.694e+07	4.288e+06 + 1.264e+06	1.560e+06 + 4.831e+05	1.420e+06 + 4.933e+05	1.660e+07 + 1.264e+07	2.822e+05 8.107e+05
f_6	mean std	1.159e+07 + 1.471e+07	7.886e+07 + 2.538e+07	3.276e+04 + 6.116e+03	5.498e+03 + 2.541e+03	1.182e+04 + 1.968e+03	1.241e+09 + 1.147e+09	1.094e+04 + 2.960e+03	4.885e+03 + 2.108e+03	5.630e+03 + 1.825e+03	8.624e+05 + 9.653e+05	1.887e+03 1.701e+02
f_7	mean std	8.783e+08 + 8.365e+08	7.715e+08 + 2.745e+08	1.223e+07 + 4.750e+06	6.495e+06 + 2.184e+06	3.458e+06 + 1.155e+06	2.653e+09 + 1.846e+09	3.420e+06 + 1.317e+06	2.706e+06 + 9.463e+05	2.422e+06 + 8.761e+05	4.071e+07 + 3.783e+07	7.430e+04 4.542e+04
f_8	mean std	4.142e+03 + 6.428e+02	3.182e+03 + 1.050e+02	2.630e+03 + 2.927e+01	2.405e+03 - 5.547e+00	2.412e+03 \approx 6.580e+00	6.667e+03 + 1.319e+03	2.399e+03 - 3.358e+00	2.398e+03 - 5.399e+00	2.397e+03 - 5.173e+00	5.672e+03 + 2.685e+03	2.421e+03 9.753e+00
f_9	mean std	2.209e+04 + 3.688e+03	2.746e+04 + 1.495e+03	1.078e+04 + 9.307e+02	2.625e+03 \approx 1.089e+02	2.994e+03 + 1.670e+02	6.262e+04 + 1.046e+04	2.600e+03 - 4.058e-01	2.642e+03 + 1.247e+02	2.622e+03 \approx 9.727e+01	1.601e+04 + 9.332e+03	2.630e+03 9.247e+01
f_{10}	mean std	8.724e+03 + 1.442e+03	1.235e+04 + 1.724e+03	4.441e+03 + 2.859e+02	3.270e+03 \approx 2.608e+01	3.459e+03 + 4.151e+01	2.028e+04 + 4.499e+03	3.282e+03 \approx 2.786e+01	3.301e+03 \approx 2.396e+01	3.335e+03 + 6.051e+01	4.833e+03 + 6.609e+02	3.289e+03 3.150e+01
+/-	10/0/0	10/0/0	10/0/0	6/3/1	9/1/0	10/0/0	6/2/2	7/2/1	7/2/1	10/0/0	-	
Avg. ranks	9.2	9.7	7.0	3.9	5.7	10.9	3.7	2.9	2.7	7.9	2.4	

Table 39

Experimental results and statistical analysis between ISHACDE and state-of-the-art optimizers on 100-D CEC2020.

Func.	PSO	DE	CMA-ES	SaDE	CL-PSO	CPSO	JADE	SHADE	L-SHADE	PPSO	ISHACDE	
f_1	mean std	9.957e+10 + 1.167e+10	3.228e+11 + 3.067e+10	8.768e+10 + 1.271e+10	5.661e+03 \approx 5.242e+03	8.133e+06 + 2.628e+06	3.112e+11 + 4.221e+10	5.233e+03 \approx 4.985e+03	4.911e+03 \approx 4.059e+03	4.047e+03 \approx 3.494e+03	1.887e+10 + 3.414e+09	6.236e+03 6.388e+03
f_2	mean std	1.130e+13 + 1.076e+12	3.143e+13 + 1.895e+12	8.986e+12 + 1.570e+12	3.698e+05 \approx 3.794e+05	1.371e+09 + 3.502e+08	3.384e+13 + 5.344e+12	2.215e+05 \approx 1.973e+05	2.656e+05 \approx 3.394e+05	2.531e+05 \approx 1.886e+05	1.982e+12 + 3.859e+11	3.158e+05 2.524e+05
f_3	mean std	3.612e+12 + 5.063e+11	1.125e+13 + 8.208e+11	3.179e+12 + 5.205e+11	4.674e+04 \approx 4.633e+04	4.099e+08 + 1.041e+08	1.172e+13 + 1.935e+12	1.821e+04 - 2.704e+04	1.979e+04 \approx 1.851e+04	2.973e+04 \approx 4.127e+04	6.553e+11 + 1.505e+11	7.047e+04 1.099e+05
f_4	mean std	3.148e+05 + 5.078e+05	2.045e+07 + 5.403e+06	8.938e+04 + 3.688e+04	1.982e+03 + 4.592e+00	2.012e+03 + 6.886e+00	1.181e+07 + 7.797e+06	1.966e+03 + 7.933e+00	1.970e+03 + 4.106e+00	1.985e+03 + 8.048e+00	3.573e+04 + 2.730e+04	1.960e+03 1.259e+01
f_5	mean std	7.687e+08 + 3.596e+08	7.370e+08 + 1.482e+08	2.737e+07 + 7.707e+06	2.168e+07 + 6.195e+06	4.779e+07 + 8.546e+06	8.035e+08 + 2.682e+08	3.451e+07 + 8.590e+06	8.494e+06 + 5.863e+06	1.605e+07 + 4.777e+06	7.299e+07 + 2.462e+07	4.932e+05 2.436e+05
f_6	mean std	1.772e+09 + 4.306e+09	3.128e+09 + 1.036e+09	2.490e+05 + 6.306e+04	3.874e+03 + 2.927e+03	1.302e+04 + 1.032e+04	1.769e+10 + 9.085e+09	1.953e+04 + 2.700e+04	2.647e+03 + 2.858e+02	2.799e+03 + 4.795e+02	9.187e+07 + 2.249e+08	2.330e+03 3.894e+02
f_7	mean std	3.474e+09 + 1.710e+09	4.786e+09 + 1.614e+09	3.484e+07 + 1.105e+07	2.213e+06 + 1.083e+06	1.967e+07 + 3.680e+06	1.541e+10 + 6.370e+09	1.006e+07 + 6.097e+06	4.051e+05 + 2.052e+05	1.252e+06 + 4.622e+05	1.056e+08 + 6.009e+07	1.948e+05 1.314e+05
f_8	mean std	9.737e+03 + 2.609e+03	4.315e+03 + 4.104e+02	3.549e+03 + 2.489e+02	2.440e+03 - 8.390e+00	4.779e+07 + 7.378e+00	8.035e+08 + 4.921e+03	3.451e+07 + 5.309e+00	8.494e+06 + 1.100e+01	1.605e+07 + 7.855e+00	7.299e+07 + 5.204e+03	4.932e+05 2.309e+01
f_9	mean std	1.028e+05 + 8.120e+03	1.142e+05 + 1.153e+04	6.602e+04 + 8.016e+03	2.600e+03 + 3.431e-02	3.708e+03 + 3.627e+02	2.540e+05 + 2.985e+04	2.600e+03 + 1.993e-04	2.644e+03 + 6.550e-04	2.644e+03 + 1.912e+02	6.458e+04 + 3.429e+04	2.600e+03 1.139e-04
f_{10}	mean std	1.214e+04 + 1.722e+03	4.188e+04 + 6.420e+03	8.593e+03 + 8.045e+02	3.456e+03 \approx 3.993e+01	3.850e+03 + 3.872e+01	4.249e+04 + 7.075e+03	3.420e+03 - 2.118e+01	3.438e+03 \approx 2.860e+01	3.485e+03 + 2.489e+01	5.567e+03 + 3.356e+02	3.444e+03 2.769e+01
+/-	10/0/0	10/0/0	10/0/0	5/4/1	9/0/1	10/0/0	5/2/3	5/4/1	6/3/1	10/0/0	-	
Avg. ranks	9.1	9.9	7.4	4.2	5.5	10.8	2.9	2.5	3.3	7.6	2.8	

Table 40

Experimental results and statistical analysis between ISHACDE and recently proposed optimizers on 50-D CEC2020.

Func.	MPA	FOX	POA	OOA	EVO	COA	FLA	RIME	DEA ² H ²	CDE	ISHACDE	
f_1	mean std	2.018e+06 + 6.460e+05	3.252e+07 + 3.232e+06	4.425e+10 + 7.771e+09	7.640e+10 + 7.598e+09	3.715e+10 + 6.766e+09	8.814e+10 + 1.411e+10	3.238e+08 + 4.279e+07	1.455e+07 + 6.243e+06	3.143e+04 + 6.578e+04	2.470e+03 ≈ 2.423e+03	2.493e+03 2.654e+03
f_2	mean std	4.988e+08 + 5.372e+08	3.755e+09 + 7.087e+08	4.696e+12 + 1.110e+12	8.205e+12 + 1.137e+12	3.867e+12 + 6.898e+11	1.014e+13 + 1.243e+12	3.896e+10 + 5.609e+09	2.169e+09 + 1.374e+09	5.448e+06 + 1.176e+07	4.039e+05 + 3.800e+05	2.127e+05 2.685e+05
f_3	mean std	7.322e+07 + 3.399e+07	1.232e+09 + 1.743e+08	1.323e+12 + 3.985e+11	2.575e+12 + 3.132e+11	1.228e+12 + 4.062e+11	3.341e+12 + 4.183e+11	1.233e+10 + 1.935e+09	5.382e+08 + 2.079e+08	1.778e+06 + 6.498e+06	1.012e+05 + 1.010e+05	4.008e+03 1.321e+04
f_4	mean std	1.947e+03 + 1.352e+01	1.973e+03 + 1.681e+01	5.730e+04 + 4.564e+04	6.344e+05 + 3.315e+05	1.111e+05 + 7.984e+04	1.202e+06 + 6.008e+05	1.941e+03 + 2.588e+00	1.930e+03 + 4.732e+00	1.959e+03 + 1.629e+01	1.944e+03 + 6.563e+00	1.918e+03 9.852e+00
f_5	mean std	3.758e+05 + 1.895e+05	1.516e+06 + 3.992e+05	7.389e+06 + 5.712e+06	4.231e+07 + 2.285e+07	1.614e+07 + 1.097e+07	6.177e+07 + 2.209e+07	4.157e+06 + 2.450e+06	3.798e+06 + 1.954e+06	2.116e+05 – 6.972e+04	2.208e+06 + 1.088e+06	2.822e+05 8.107e+05
f_6	mean std	6.798e+03 + 3.713e+03	2.331e+04 + 7.351e+03	3.825e+07 + 1.001e+08	2.045e+08 + 2.123e+08	1.070e+08 + 2.118e+08	4.720e+08 + 3.236e+08	4.668e+04 + 4.289e+04	6.212e+04 + 2.191e+04	3.033e+03 + 6.042e+02	2.919e+03 + 5.600e+02	1.887e+03 1.701e+02
f_7	mean std	5.843e+05 + 3.719e+05	2.832e+06 + 1.491e+06	3.766e+07 + 3.030e+07	7.302e+08 + 5.755e+08	1.613e+08 + 1.367e+08	1.103e+09 + 4.639e+08	5.969e+06 + 3.822e+06	5.214e+06 + 2.603e+06	1.035e+05 + 4.346e+04	1.694e+06 + 1.205e+06	7.430e+04 4.542e+04
f_8	mean std	2.609e+03 + 5.236e+02	8.916e+03 + 1.145e+03	5.209e+03 + 2.201e+03	7.176e+03 + 2.175e+03	2.848e+03 + 1.255e+02	4.657e+03 + 8.553e+02	2.441e+03 + 7.259e+00	2.468e+03 + 1.275e+01	2.688e+03 + 1.176e+02	2.445e+03 + 1.561e+01	2.421e+03 9.753e+00
f_9	mean std	2.819e+03 + 2.357e+02	3.222e+03 + 1.091e+02	4.254e+04 + 4.881e+03	5.348e+04 + 5.960e+03	3.802e+04 + 9.632e+03	5.223e+04 + 9.557e+03	4.196e+03 + 3.572e+02	2.925e+03 + 8.226e+01	2.635e+03 + 1.336e+02	2.713e+03 + 2.254e+02	2.630e+03 9.247e+01
f_{10}	mean std	3.504e+03 + 1.526e+02	3.385e+03 + 4.813e+01	7.855e+03 + 1.221e+03	1.485e+04 + 2.402e+03	8.553e+03 + 1.457e+03	1.627e+04 + 3.399e+03	3.464e+03 + 1.472e+02	3.459e+03 + 1.733e+02	3.373e+03 + 2.023e+02	3.337e+03 + 4.128e+01	3.289e+03 3.150e+01
+/-	10/0/0	10/0/0	10/0/0	10/0/0	10/0/0	10/0/0	10/0/0	10/0/0	9/0/1	9/1/0	-	
Avg. ranks	4.3	6.0	8.5	10.1	8.4	10.6	5.9	5.0	3.2	2.8	1.2	

Table 41

Experimental results and statistical analysis between ISHACDE and recently proposed optimizers on 100-D CEC2020.

Func.	MPA	FOX	POA	OOA	EVO	COA	FLA	RIME	DEA ² H ²	CDE	ISHACDE	
f_1	mean std	1.441e+07 + 4.944e+06	1.701e+08 + 1.352e+07	1.268e+11 + 1.452e+10	2.162e+11 + 1.535e+10	1.425e+11 + 1.557e+10	2.535e+11 + 1.902e+10	1.357e+09 + 1.792e+08	4.907e+07 + 1.036e+07	9.516e+06 + 1.644e+07	1.069e+04 + 1.585e+04	6.236e+03 6.388e+03
f_2	mean std	1.491e+09 + 5.352e+08	1.679e+10 + 1.747e+09	1.446e+13 + 2.411e+12	2.505e+13 + 1.939e+12	1.490e+13 + 1.863e+12	2.816e+13 + 2.024e+12	1.302e+11 + 1.668e+10	5.176e+09 + 1.256e+09	4.774e+08 + 6.756e+08	1.989e+06 + 5.227e+06	3.158e+05 2.524e+05
f_3	mean std	5.212e+08 + 1.587e+08	6.198e+09 + 4.734e+08	4.492e+12 + 6.048e+11	8.350e+12 + 6.815e+11	4.915e+12 + 6.330e+11	9.508e+12 + 9.921e+11	4.923e+10 + 6.849e+09	1.902e+09 + 6.500e+08	1.147e+08 + 1.107e+08	4.863e+05 + 1.445e+06	7.047e+04 1.099e+05
f_4	mean std	2.063e+03 + 2.580e+01	2.048e+03 + 1.823e+01	2.163e+05 + 9.616e+04	2.757e+06 + 8.449e+05	6.816e+05 + 3.032e+05	4.347e+06 + 1.396e+06	2.003e+03 + 8.238e+00	2.004e+03 + 2.314e+01	2.088e+03 + 4.434e+01	2.052e+03 + 2.253e+01	1.960e+03 1.259e+01
f_5	mean std	4.609e+06 + 1.589e+06	9.635e+06 + 2.594e+06	7.542e+07 + 3.190e+07	4.454e+08 + 1.766e+08	1.920e+08 + 5.506e+07	5.204e+08 + 1.122e+08	2.941e+07 + 8.201e+06	2.074e+07 + 6.628e+06	1.072e+06 + 4.657e+05	4.634e+06 + 1.251e+06	4.932e+05 2.436e+05
f_6	mean std	9.292e+04 + 5.705e+04	9.455e+04 + 2.799e+04	1.848e+09 + 1.223e+09	1.433e+10 + 6.605e+09	1.944e+09 + 1.270e+09	9.638e+09 + 4.953e+09	4.619e+05 + 6.936e+05	1.737e+05 + 7.020e+04	1.202e+04 + 1.011e+04	3.104e+03 + 5.646e+02	2.330e+03 3.894e+02
f_7	mean std	7.178e+06 + 4.019e+06	2.660e+06 + 9.874e+05	8.526e+08 + 5.387e+08	1.266e+10 + 6.464e+09	1.891e+09 + 6.250e+08	8.195e+09 + 2.145e+09	2.443e+07 + 1.093e+07	1.223e+07 + 3.738e+06	6.374e+05 + 2.979e+05	1.409e+06 + 8.190e+05	1.948e+05 1.314e+05
f_8	mean std	3.562e+03 + 2.834e+03	1.658e+04 + 8.003e+02	1.400e+04 + 4.562e+03	2.037e+04 + 3.142e+03	4.066e+03 + 3.877e+02	1.611e+04 + 3.620e+03	2.494e+03 + 8.154e+00	2.528e+03 + 2.141e+01	3.104e+03 + 1.606e+02	2.575e+03 + 5.417e+01	2.494e+03 2.309e+01
f_9	mean std	3.811e+03 + 9.958e+02	4.743e+03 + 4.446e+02	1.298e+05 + 8.016e+03	1.651e+05 + 5.025e+03	1.398e+05 + 7.511e+03	1.815e+05 + 5.139e+03	9.402e+03 + 1.130e+03	3.830e+03 + 1.305e+02	4.308e+03 + 2.381e+03	2.601e+03 + 8.363e-01	2.600e+03 1.139e-04
f_{10}	mean std	3.707e+03 + 1.051e+02	3.479e+03 + 2.863e+01	1.225e+04 + 2.071e+03	2.548e+04 + 3.969e+03	1.465e+04 + 1.911e+03	3.415e+04 + 5.012e+03	3.653e+03 + 9.151e+01	3.599e+03 + 6.968e+01	3.485e+03 + 5.340e+01	3.595e+03 + 6.437e+01	3.444e+03 2.769e+01
+/-	10/0/0	10/0/0	10/0/0	10/0/0	10/0/0	10/0/0	9/1/0	10/0/0	10/0/0	10/0/0	-	
Avg. ranks	4.6	5.4	8.0	10.3	8.8	10.6	5.9	4.8	3.6	3.0	1.0	

Table 42

Experimental results and statistical analysis between ISHACDE and state-of-the-art optimizers on 10-D CEC2022.

Func.	PSO	DE	CMA-ES	SaDE	CL-PSO	CPSO	JADE	SHADE	L-SHADE	PPSO	ISHACDE	
f_1	mean	2.218e+03 + 7.447e+03 + 4.335e+02 + 3.609e+02 + 2.321e+03 + 4.645e+03 + 4.793e+02 + 3.281e+02 + 3.330e+02 + 5.144e+02 +	3.001e+02									
	std	1.543e+03 1.366e+03 4.238e+01 2.605e+01 8.635e+02 2.431e+03 5.762e+01 1.161e+01 1.654e+01 2.420e+02 4.132e-01										
f_2	mean	4.993e+02 + 4.564e+02 + 4.166e+02 + 4.099e+02 + 4.480e+02 + 5.637e+02 + 4.094e+02 + 4.072e+02 + 4.073e+02 + 4.396e+02 +	4.027e+02									
	std	3.798e+01 1.851e+01 2.299e+00 7.046e+00 1.500e+01 1.093e+02 1.810e+00 3.147e+00 4.481e+00 3.018e+01 2.893e+00										
f_3	mean	6.000e+02 + 6.001e+02 + 6.000e+02 + 6.000e+02 + 6.001e+02 + 6.000e+02 + 6.000e+02 + 6.000e+02 + 6.000e+02 + 6.000e+02 +	6.000e+02									
	std	2.647e-03 1.402e-02 7.346e-04 1.710e-07 6.411e-04 5.344e-02 8.082e-07 2.751e-07 2.491e-07 1.053e-03 7.661e-10										
f_4	mean	8.010e+02 + 8.011e+02 + 8.011e+02 + 8.008e+02 ≈ 8.006e+02 ≈ 8.008e+02 ≈ 8.005e+02 ≈ 8.005e+02 ≈ 8.004e+02 -	8.004e+02	-	8.004e+02	-	8.004e+02	-	8.004e+02	-	8.007e+02	
	std	1.546e-01 2.182e-01 1.873e-01 1.564e-01 1.407e-01 2.739e-01 1.083e-01 8.296e-02 8.445e-02 2.502e-01 1.524e-01										
f_5	mean	9.012e+02 + 9.026e+02 + 9.004e+02 + 9.000e+02 + 9.005e+02 + 9.010e+02 + 9.001e+02 + 9.001e+02 + 9.001e+02 +	9.000e+02									
	std	6.004e-01 6.050e-01 7.398e-02 4.525e-04 2.301e-01 6.359e-01 4.371e-02 3.585e-02 5.364e-02 9.728e-01 8.101e-07										
f_6	mean	4.913e+05 + 1.263e+05 + 4.134e+03 ≈ 2.792e+04 + 1.218e+05 + 2.203e+06 + 3.187e+04 + 1.959e+04 + 1.759e+04 +	3.770e+04	+ 6.497e+03								
	std	7.766e+05 4.504e+04 6.596e+02 6.660e+03 7.011e+04 4.330e+06 1.297e+04 6.856e+03 5.832e+03 1.628e+04 4.687e+03										
f_7	mean	2.122e+03 + 2.076e+03 + 2.040e+03 + 2.063e+03 + 2.134e+03 + 2.033e+03 ≈ 2.034e+03 ≈ 2.034e+03 ≈ 2.063e+03 +	2.034e+03	≈ 2.034e+03 ≈ 2.034e+03 + 2.034e+03 ≈ 2.034e+03 +								
	std	4.604e+01 1.441e+01 1.395e+01 4.676e+00 1.225e+01 8.232e+01 2.688e+00 4.038e+00 5.331e+00 3.588e+01 5.539e+00										
f_8	mean	3.140e+03 + 2.255e+03 + 2.229e+03 + 2.229e+03 + 2.310e+03 + 2.943e+03 + 2.233e+03 + 2.229e+03 + 2.227e+03 + 2.663e+03 +	2.224e+03									
	std	1.300e+03 9.876e+00 1.668e+00 3.810e+00 5.829e+01 6.377e+02 3.298e+00 2.025e+00 2.586e+00 5.575e+02 5.362e+00										
+/≈/-		12/0/0	12/0/0	10/1/1	9/2/1	11/1/0	11/1/0	9/2/1	9/2/1	9/1/2	11/0/1	-
Avg. ranks		9.2	9.0	6.5	3.8	7.2	10.1	4.3	2.8	3.2	7.6	2.0

Table 43

Experimental results and statistical analysis between ISHACDE and state-of-the-art optimizers on 20-D CEC2022.

Func.	PSO	DE	CMA-ES	SaDE	CL-PSO	CPSO	JADE	SHADE	L-SHADE	PPSO	ISHACDE	
f_1	mean	1.453e+04 + 3.475e+04 + 2.447e+03 + 4.007e+02 + 5.888e+03 + 2.344e+04 + 1.161e+03 + 3.145e+02 + 3.171e+02 + 2.143e+03 +	3.002e+02									
	std	4.076e+03 5.844e+03 4.689e+02 4.811e+01 1.435e+03 7.260e+03 4.233e+02 6.784e+00 8.545e+00 1.089e+03 6.851e-01										
f_2	mean	7.724e+02 + 1.058e+03 + 5.112e+02 + 4.516e+02 + 5.151e+02 + 1.240e+03 + 4.518e+02 + 4.518e+02 + 4.506e+02 + 5.509e+02 +	4.502e+02									
	std	2.251e+02 1.277e+02 1.143e+01 7.468e+00 1.710e+01 4.686e+02 8.010e+00 7.169e+00 5.227e+00 5.453e+01 1.354e+01										
f_3	mean	6.001e+02 + 6.004e+02 + 6.000e+02 + 6.000e+02 + 6.007e+02 + 6.000e+02 + 6.000e+02 + 6.000e+02 + 6.000e+02 + 6.000e+02 +	6.000e+02									
	std	8.747e-02 4.371e-02 4.867e-03 1.542e-08 5.064e-04 2.844e-01 5.430e-07 4.115e-09 5.787e-09 3.496e-02 1.515e-12										
f_4	mean	8.037e+02 + 8.040e+02 + 8.040e+02 + 8.033e+02 + 8.019e+02 ≈ 8.032e+02 + 8.017e+02 ≈ 8.017e+02 ≈ 8.017e+02 ≈ 8.016e+02 ≈	8.016e+02	≈ 8.022e+02								
	std	3.996e-01 4.006e-01 4.162e-01 3.613e-01 2.872e-01 7.806e-01 2.754e-01 2.511e-01 2.161e-01 4.846e-01 7.902e-01										
f_5	mean	9.066e+02 + 9.143e+02 + 9.033e+02 + 9.000e+02 ≈ 9.022e+02 + 9.085e+02 + 9.005e+02 + 9.002e+02 ≈ 9.002e+02 ≈ 9.045e+02 +	9.002e+02	≈ 9.002e+02 ≈ 9.045e+02 + 9.002e+02 ≈ 9.002e+02 ≈ 9.002e+02								
	std	2.915e+00 1.709e+00 6.970e-01 1.330e-04 8.055e-01 3.914e+00 9.220e-02 1.334e-01 1.325e-01 2.363e+00 2.614e-01										
f_6	mean	3.238e+08 + 2.430e+08 + 4.729e+06 + 8.281e+06 + 8.552e+06 + 5.071e+08 + 2.822e+06 + 1.555e+06 + 1.307e+06 + 2.966e+05 +	3.030e+04									
	std	3.589e+08 9.634e+07 1.706e+06 3.867e+06 3.716e+06 4.458e+08 1.358e+06 6.212e+05 3.574e+05 4.020e+05 9.091e+03										
f_7	mean	3.040e+03 + 2.801e+03 + 2.319e+03 + 2.106e+03 + 2.227e+03 + 3.313e+03 + 2.095e+03 + 2.098e+03 + 2.080e+03 + 3.081e+03 +	2.051e+03									
	std	4.083e+02 2.627e+02 7.439e+01 1.983e+01 6.055e+01 6.917e+02 1.781e+01 1.599e+01 1.750e+01 5.580e+02 1.813e+01										
f_8	mean	3.254e+07 + 9.935e+04 + 2.393e+03 - 4.292e+03 + 3.361e+03 + 2.156e+07 + 3.029e+03 + 2.885e+03 + 2.733e+03 + 5.253e+03 +	2.545e+03									
	std	9.219e+07 2.161e+05 5.318e+01 8.681e+02 6.640e+02 7.962e+07 3.594e+02 2.609e+02 2.275e+02 1.972e+03 7.845e+02										
f_9	mean	3.150e+03 + 2.792e+03 + 2.650e+03 + 2.640e+03 + 2.721e+03 + 3.322e+03 + 2.650e+03 + 2.645e+03 + 2.646e+03 + 3.002e+03 +	2.638e+03									
	std	1.680e+02 3.941e+01 4.479e+00 1.765e+00 1.081e+01 3.664e+02 4.181e+00 3.635e+00 4.553e+00 5.176e+02 2.145e+00										
f_{10}	mean	2.855e+03 + 4.812e+03 + 3.518e+03 + 2.773e+03 ≈ 2.883e+03 + 3.094e+03 + 2.806e+03 + 2.794e+03 + 2.791e+03 + 5.102e+03 +	2.783e+03									
	std	8.157e+01 1.780e+03 1.441e+03 4.176e+01 1.383e+02 2.511e+02 1.612e+01 1.186e+01 8.762e+00 1.249e+03 4.896e+01										
f_{11}	mean	2.753e+03 + 2.745e+03 + 2.621e+03 + 2.600e+03 + 2.619e+03 + 2.948e+03 + 2.600e+03 + 2.600e+03 + 2.600e+03 + 2.725e+03 +	2.600e+03									
	std	1.534e+02 6.715e+01 2.936e+00 2.870e-01 2.775e+00 3.618e+02 4.058e-02 9.489e-03 9.309e-03 3.564e+02 7.622e-06										
f_{12}	mean	3.199e+03 + 2.956e+03 ≈ 2.955e+03 ≈ 2.942e+03 ≈ 2.989e+03 + 2.900e+03 - 2.943e+03 ≈ 2.943e+03 ≈ 2.944e+03 ≈ 3.082e+03 +	2.948e+03	≈ 2.948e+03 + 2.948e+03 ≈ 2.944e+03 ≈ 2.944e+03 ≈ 3.082e+03 + 2.948e+03								
	std	8.783e+01 5.295e+00 1.035e+01 7.204e+00 9.311e+00 7.089e-05 2.782e+00 2.440e+00 3.727e+00 1.059e+02 7.070e+00										
+/≈/-		12/0/0	11/1/0	10/1/1	9/3/0	11/1/0	11/0/1	10/2/0	9/3/0	9/3/0	11/1/0	-
Avg. ranks		9.3	9.4	6.6	4.0	6.7	9.3	4.5	3.3	3.3	7.4	2.0

Table 44

Experimental results and statistical analysis between ISHACDE and recently proposed optimizers on 10-D CEC2022.

Func.	MPA	FOX	POA	OOA	EVO	COA	FLA	RIME	DEA ² H ²	CDE	ISHACDE	
f_1	mean std	3.000e+02 – 5.057e-04	2.133e+03 + 2.664e+03	1.463e+03 + 1.105e+03	5.940e+02 + 2.474e+02	2.101e+03 + 1.428e+03	3.416e+03 + 1.055e+03	3.119e+02 + 5.596e+00	3.016e+02 + 2.194e+00	3.000e+02 – 7.031e-10	3.000e+02 ≈ 2.415e-02	3.001e+02 4.132e-01
f_2	mean std	4.125e+02 + 2.075e+01	5.242e+02 + 9.430e+01	4.318e+02 + 2.840e+01	4.547e+02 + 3.703e+01	4.750e+02 + 3.057e+01	5.041e+02 + 4.510e+01	4.085e+02 + 2.769e+00	4.087e+02 + 1.325e+01	4.128e+02 + 1.973e+01	4.022e+02 ≈ 2.573e+00	4.027e+02 2.893e+00
f_3	mean std	6.000e+02 + 1.870e-08	6.001e+02 + 6.692e-02	6.000e+02 + 2.270e-02	6.000e+02 + 9.574e-03	6.000e+02 + 5.603e-03	6.000e+02 + 4.022e-02	6.000e+02 + 1.421e-04	6.000e+02 + 1.487e-05	6.000e+02 – 9.166e-14	6.000e+02 – 1.331e-11	6.000e+02 – 7.661e-10
f_4	mean std	8.003e+02 – 2.226e-01	8.003e+02 – 2.186e-01	8.002e+02 – 5.323e-02	8.004e+02 – 2.096e-01	8.007e+02 ≈ 1.882e-01	8.004e+02 – 1.806e-01	8.002e+02 – 2.410e-01	8.002e+02 – 8.829e-02	8.007e+02 ≈ 7.417e-02	8.007e+02 ≈ 1.919e-01	8.007e+02 ≈ 1.524e-01
f_5	mean std	9.011e+02 + 1.653e+00	9.032e+02 + 1.532e+00	9.004e+02 + 4.967e-01	9.006e+02 + 5.239e-01	9.003e+02 + 5.271e-01	9.010e+02 + 4.133e-01	9.002e+02 + 2.762e-01	9.001e+02 + 3.241e-01	9.002e+02 + 2.728e-01	9.000e+02 + 2.610e-06	9.000e+02 + 8.101e-07
f_6	mean std	2.061e+04 + 1.247e+04	4.226e+04 + 2.146e+04	2.633e+04 + 1.153e+04	1.852e+04 + 1.256e+04	1.321e+06 + 3.256e+06	4.182e+05 + 6.932e+05	7.278e+04 + 3.427e+04	2.687e+04 + 1.094e+04	8.337e+03 + 9.708e+03	1.280e+04 + 7.132e+03	6.497e+03 4.687e+03
f_7	mean std	2.054e+03 + 4.774e+01	2.217e+03 + 1.630e+02	2.039e+03 ≈ 6.576e+00	2.043e+03 + 1.235e+01	2.070e+03 + 1.957e+01	2.033e+03 + 2.821e+01	2.028e+03 – 5.968e+00	2.028e+03 – 4.369e+00	2.026e+03 – 7.627e+00	2.034e+03 ≈ 3.256e+00	2.034e+03 ≈ 5.539e+00
f_8	mean std	2.264e+03 + 1.226e+02	2.963e+03 + 7.484e+02	2.249e+03 + 4.974e+01	2.272e+03 + 7.161e+01	1.051e+08 + 4.582e+08	2.447e+03 + 1.503e+02	2.353e+03 + 2.536e+02	2.225e+03 ≈ 4.613e+00	2.219e+03 – 5.870e+00	2.223e+03 ≈ 5.696e+00	2.224e+03 5.362e+00
f_9	mean std	2.574e+03 + 1.591e+02	2.748e+03 + 1.372e+02	2.482e+03 + 1.529e+02	2.598e+03 + 1.905e+02	2.614e+03 + 1.808e+02	2.679e+03 + 7.718e+01	2.594e+03 + 1.444e+02	2.575e+03 + 1.582e+02	2.551e+03 + 1.646e+02	2.300e+03 – 3.327e+02	2.301e+03 1.799e+00
f_{10}	mean std	2.665e+03 + 7.557e+01	2.806e+03 + 2.301e+02	2.614e+03 + 1.014e+01	2.632e+03 + 5.008e+01	2.631e+03 + 5.010e+01	2.635e+03 + 2.025e+01	2.616e+03 + 4.347e+01	2.637e+03 + 6.096e+01	2.603e+03 – 2.704e+00	2.599e+03 – 6.952e-01	2.611e+03 3.680e+01
f_{11}	mean std	2.648e+03 + 1.901e+02	2.864e+03 + 3.752e+02	2.613e+03 + 9.445e+00	2.618e+03 + 1.004e+01	2.632e+03 + 2.782e+01	2.647e+03 + 1.947e+01	2.689e+03 + 2.624e+02	2.602e+03 + 4.686e+00	2.603e+03 + 7.406e+00	2.600e+03 ≈ 2.727e-04	2.600e+03 ≈ 8.717e-04
f_{12}	mean std	2.867e+03 ≈ 1.481e+00	2.997e+03 + 5.178e+01	2.873e+03 + 5.947e+00	2.873e+03 + 8.666e+00	2.875e+03 + 7.535e+00	2.880e+03 + 8.044e+00	2.866e+03 ≈ 1.060e+00	2.866e+03 ≈ 1.031e+00	2.868e+03 + 1.824e+00	2.867e+03 ≈ 1.086e+00	2.866e+03 ≈ 1.053e+00
+/-	9/1/2	11/0/1	10/1/1	11/0/1	11/0/1	11/1/0	9/2/1	8/2/2	6/0/6	2/7/3	-	
Avg. ranks	6.2	10.0	5.7	7.2	8.2	9.5	5.9	4.3	3.0	2.9	3.0	

Table 45

Experimental results and statistical analysis between ISHACDE and recently proposed optimizers on 20-D CEC2022.

Func.	MPA	FOX	POA	OOA	EVO	COA	FLA	RIME	DEA ² H ²	CDE	ISHACDE	
f_1	mean std	3.001e+02 – 1.268e-01	1.835e+03 + 1.829e+03	7.120e+03 + 2.265e+03	1.044e+04 + 3.034e+03	1.150e+04 + 3.488e+03	2.068e+04 + 4.646e+03	3.556e+02 + 1.471e+01	3.038e+02 + 1.955e+00	3.000e+02 – 2.719e-07	3.000e+02 – 1.115e-03	3.002e+02 6.851e-01
f_2	mean std	4.575e+02 + 1.357e+01	4.980e+02 + 2.670e+01	6.477e+02 + 1.024e+02	8.657e+02 + 2.110e+02	6.858e+02 + 8.691e+01	1.093e+03 + 1.639e+02	4.631e+02 + 2.741e+01	4.554e+02 + 1.726e+01	4.538e+02 ≈ 1.027e+01	4.489e+02 ≈ 1.014e+01	4.502e+02 1.354e+01
f_3	mean std	6.000e+02 + 6.512e-07	6.000e+02 + 1.096e-03	6.004e+02 + 2.211e-01	6.005e+02 + 1.675e-01	6.001e+02 + 6.244e-02	6.006e+02 + 1.642e-01	6.000e+02 + 5.039e-04	6.000e+02 + 3.043e-05	6.000e+02 ≈ 4.292e-13	6.000e+02 ≈ 2.542e-14	6.000e+02 1.515e-12
f_4	mean std	8.009e+02 – 3.574e-01	8.009e+02 – 4.598e-01	8.007e+02 – 1.406e-01	8.018e+02 ≈ 5.300e-01	8.015e+02 – 7.832e-01	8.031e+02 + 3.663e-01	8.012e+02 – 5.243e-01	8.009e+02 – 3.508e-01	8.008e+02 – 5.478e-01	8.033e+02 + 5.958e-01	8.022e+02 7.902e-01
f_5	mean std	9.046e+02 + 2.567e+00	9.024e+02 + 1.433e+00	9.026e+02 + 9.029e-01	9.037e+02 + 1.456e+00	9.020e+02 + 8.990e-01	9.058e+02 + 1.974e+00	9.026e+02 + 1.708e+00	9.014e+02 + 1.230e+00	9.065e+02 + 2.418e+00	9.003e+02 + 4.283e-01	9.002e+02 + 2.614e-01
f_6	mean std	7.870e+04 + 2.199e+04	1.535e+05 + 3.914e+04	1.536e+05 + 1.320e+05	7.152e+06 + 1.417e+07	2.724e+07 + 3.757e+07	1.270e+08 + 1.003e+08	1.042e+06 + 5.549e+05	9.376e+04 + 2.621e+04	7.042e+04 + 1.942e+04	8.056e+05 + 5.641e+05	3.030e+04 9.091e+03
f_7	mean std	2.083e+03 + 1.327e+02	2.466e+03 + 2.026e+02	2.184e+03 + 1.335e+02	2.505e+03 + 1.993e+02	2.183e+03 + 9.174e+01	2.868e+03 + 3.534e+02	2.076e+03 + 3.393e+01	2.074e+03 + 3.294e+01	2.049e+03 ≈ 2.378e+01	2.056e+03 + 1.117e+01	2.051e+03 ≈ 1.813e+01
f_8	mean std	2.228e+03 ≈ 2.732e+00	2.693e+03 + 2.859e+02	3.487e+03 + 6.671e+02	3.933e+03 + 1.034e+03	9.264e+05 + 2.161e+06	1.236e+04 + 2.181e+04	3.867e+03 + 1.247e+03	3.425e+03 + 7.339e+02	2.249e+03 ≈ 1.958e+01	3.199e+03 + 4.211e+02	2.545e+03 7.845e+02
f_9	mean std	2.637e+03 ≈ 1.696e+00	2.842e+03 + 9.876e+01	2.826e+03 + 8.184e+01	2.981e+03 + 2.002e+02	2.881e+03 + 9.090e+01	3.113e+03 + 1.669e+02	2.647e+03 + 8.488e+00	2.648e+03 + 4.621e+00	2.644e+03 + 1.891e-02	2.638e+03 4.206e+00	2.638e+03 2.145e+00
f_{10}	mean std	3.996e+03 + 9.804e+02	5.343e+03 + 8.296e+02	3.026e+03 + 4.322e+02	3.809e+03 + 1.362e+03	3.256e+03 + 8.906e+02	3.006e+03 + 1.883e+02	3.788e+03 + 1.046e+03	3.225e+03 + 7.593e+02	4.181e+03 + 7.782e+02	2.780e+03 ≈ 4.241e+01	2.783e+03 4.896e+01
f_{11}	mean std	2.606e+03 + 8.539e+00	2.921e+03 + 5.162e+02	2.840e+03 + 3.843e+02	3.544e+03 + 1.213e+03	2.791e+03 + 2.405e+02	3.108e+03 + 3.089e+02	2.756e+03 + 4.594e+02	2.601e+03 + 3.031e-01	2.604e+03 + 7.981e+00	2.600e+03 + 8.830e-05	2.600e+03 7.622e-06
f_{12}	mean std	3.000e+03 + 6.057e+01	3.602e+03 + 1.958e+02	3.039e+03 + 3.694e+01	3.071e+03 + 7.036e+01	3.027e+03 + 3.452e+01	3.067e+03 + 4.792e+01	2.966e+03 + 2.216e+01	2.956e+03 + 1.218e+01	2.977e+03 + 2.168e+01	2.960e+03 + 9.614e+00	2.948e+03 7.070e+00
+/-	8/2/2	11/0/1	11/0/1	11/1/0	11/0/1	12/0/0	11/0/1	11/0/1	5/4/3	7/4/1	-	
Avg. ranks	4.7	7.2	6.7	9.3	7.9	9.8	6.3	4.3	3.7	3.5	2.6	

Table 46

Results of ablation experiments in 30-D CEC2017.

Func	SHACDE		ISHACDE	
	mean	std	mean	std
f_1	3.477e+03	3.509e+03	1.091e+02 –	1.371e+01
f_3	5.820e+04	2.752e+04	5.200e+04 ≈	2.980e+04
f_4	4.927e+02	2.257e+01	4.709e+02 –	3.320e+01
f_5	6.304e+02	1.977e+01	6.081e+02 –	2.124e+01
f_6	6.000e+02	1.897e+02	6.000e+02 ≈	1.053e+01
f_7	8.646e+02	1.906e+01	8.562e+02 ≈	2.282e+01
f_8	9.221e+02	1.813e+01	9.270e+02 ≈	1.904e+01
f_9	9.004e+02	5.958e+01	9.045e+02 +	5.228e+00
f_{10}	6.395e+03	3.269e+02	6.307e+03 ≈	6.485e+02
f_{11}	1.194e+03	4.653e+01	1.167e+03 –	1.022e+02
f_{12}	4.534e+05	1.801e+06	3.482e+04 ≈	2.320e+04
f_{13}	8.979e+04	3.676e+05	1.538e+04 ≈	3.371e+04
f_{14}	5.517e+04	1.080e+05	9.527e+03 –	2.180e+04
f_{15}	5.071e+04	1.515e+05	3.640e+03 –	7.982e+03
f_{16}	2.750e+03	2.116e+02	2.729e+03 ≈	3.318e+02
f_{17}	2.070e+03	1.128e+02	2.079e+03 ≈	9.101e+01
f_{18}	2.350e+05	3.842e+05	2.043e+05 ≈	3.481e+05
f_{19}	2.884e+03	4.039e+03	7.535e+04 ≈	3.199e+05
f_{20}	2.506e+03	9.714e+01	2.482e+03 ≈	1.391e+02
f_{21}	2.421e+03	1.792e+01	2.411e+03 –	2.955e+01
f_{22}	2.335e+03	1.423e+02	2.300e+03 –	1.012e+00
f_{23}	2.771e+03	1.909e+01	2.760e+03 –	2.663e+01
f_{24}	2.943e+03	2.238e+01	2.909e+03 –	5.042e+01
f_{25}	2.888e+03	7.112e-01	2.889e+03 ≈	8.112e+00
f_{26}	4.398e+03	6.541e+02	4.301e+03 ≈	5.494e+02
f_{27}	3.222e+03	1.114e+01	3.220e+03 ≈	9.614e+00
f_{28}	3.213e+03	1.462e+01	3.197e+03 –	3.291e+01
f_{29}	3.753e+03	1.463e+02	3.551e+03 –	8.170e+01
f_{30}	9.771e+03	3.079e+03	9.192e+03 ≈	2.828e+03
+/-	–	–	1/16/12	–
Avg. ranks	1.8	–	1.2	–

Table 47

Results of ablation experiments in 50-D CEC2017.

Func	SHACDE		ISHACDE	
	mean	std	mean	std
f_1	3.308e+03	4.165e+03	2.493e+03 ≈	2.654e+03
f_3	1.672e+05	3.612e+04	1.483e+05 ≈	6.234e+04
f_4	5.270e+02	5.704e+01	5.411e+02 ≈	5.692e+01
f_5	7.327e+02	2.056e+01	7.200e+02 –	6.052e+01
f_6	6.003e+02	1.204e+00	6.001e+02 –	2.403e+01
f_7	9.917e+02	2.156e+01	9.889e+02 ≈	3.230e+01
f_8	1.031e+03	2.123e+01	1.008e+03 ≈	4.744e+01
f_9	9.134e+02	1.422e+01	1.055e+03 –	1.299e+02
f_{10}	1.053e+04	3.624e+02	1.025e+04 –	7.786e+02
f_{11}	1.816e+03	1.196e+03	1.447e+03 –	4.691e+02
f_{12}	3.448e+05	2.571e+05	3.119e+05 ≈	3.168e+05
f_{13}	3.771e+03	1.916e+03	3.125e+03 ≈	2.130e+03
f_{14}	1.035e+05	4.435e+05	1.391e+05 ≈	2.975e+05
f_{15}	5.699e+03	2.257e+03	5.369e+03 ≈	2.466e+03
f_{16}	3.624e+03	2.178e+02	3.553e+03 ≈	4.484e+02
f_{17}	3.153e+03	1.921e+02	3.118e+03 ≈	2.763e+02
f_{18}	7.611e+05	1.890e+06	6.995e+05 ≈	1.950e+06
f_{19}	2.495e+04	9.893e+04	5.945e+03 –	4.632e+03
f_{20}	3.306e+03	1.947e+02	3.356e+03 ≈	1.405e+02
f_{21}	2.530e+03	2.638e+01	2.495e+03 –	6.831e+01
f_{22}	1.077e+04	3.355e+03	1.125e+04 ≈	3.406e+03
f_{23}	2.949e+03	2.254e+01	2.940e+03 ≈	5.263e+01
f_{24}	3.121e+03	2.177e+01	3.033e+03 –	5.422e+01
f_{25}	3.058e+03	2.884e+01	3.050e+03 ≈	4.196e+01
f_{26}	5.948e+03	2.610e+02	5.540e+03 –	7.310e+02
f_{27}	3.329e+03	4.025e+01	3.384e+03 ≈	5.523e+01
f_{28}	3.326e+03	3.267e+01	3.311e+03 ≈	2.266e+01
f_{29}	4.020e+03	1.822e+02	3.827e+03 –	2.368e+02
f_{30}	1.075e+06	1.740e+05	1.065e+06 ≈	3.454e+05
+/-	–	–	0/19/10	–
Avg. ranks	1.8	–	1.2	–

Table 48

Results of ablation experiments in 50-D CEC2020.

Func	SHACDE		ISHACDE	
	mean	std	mean	std
f_1	3.308e+03	4.165e+03	2.493e+03 ≈	2.654e+03
f_2	2.257e+05	2.552e+05	2.127e+05 ≈	2.685e+05
f_3	2.537e+04	4.437e+04	4.008e+03 –	1.321e+04
f_4	1.924e+03	2.475e+00	1.918e+03 –	9.852e+00
f_5	9.095e+04	4.489e+04	2.822e+05 ≈	8.107e+05
f_6	2.042e+03	2.051e+02	1.887e+03 –	1.701e+02
f_7	9.842e+04	4.627e+04	7.430e+04 –	4.542e+04
f_8	2.405e+03	8.562e+00	2.421e+03 ≈	9.753e+00
f_9	2.643e+03	1.285e+02	2.630e+03 –	9.247e+01
f_{10}	3.294e+03	2.446e+01	3.289e+03 ≈	3.150e+01
+/-	–	–	0/5/5	–
Avg. ranks	1.8	–	1.2	–

Table 49

Results of ablation experiments in 100-D CEC2020.

Func	SHACDE		ISHACDE	
	mean	std	mean	std
f_1	5.039e+03	7.851e+03	6.236e+03 ≈	6.388e+03
f_2	2.426e+05	2.399e+05	3.158e+05 ≈	2.524e+05
f_3	3.786e+04	3.255e+04	7.047e+04 ≈	1.099e+05
f_4	1.980e+03	1.093e+01	1.960e+03 –	1.259e+01
f_5	6.701e+05	2.346e+05	4.932e+05 –	2.436e+05
f_6	2.749e+03	4.193e+02	2.330e+03 –	3.894e+02
f_7	2.309e+05	1.706e+05	1.948e+05 ≈	1.314e+05
f_8	2.462e+03	1.629e+01	2.494e+03 ≈	2.309e+01
f_9	2.600e+03	3.645e-03	2.600e+03 –	1.139e-04
f_{10}	3.447e+03	3.312e+01	3.444e+03 ≈	2.769e+01
+/-	–	–	0/6/4	–
Avg. ranks	1.6	–	1.4	–

Appendix C. Experimental details on CEC2020

Tables 38 and **39** summarize the experimental results and statistical analysis between ISHACDE and state-of-the-art optimizers on CEC2020 benchmark functions. **Tables 40** and **41** summarize the experimental results and statistical analysis between ISHACDE and recently proposed optimizers on CEC2020 benchmark functions.

Appendix D. Experimental details on CEC2022

Tables 42 and **43** summarize the experimental results and statistical analysis between ISHACDE and state-of-the-art optimizers on CEC2022 benchmark functions. **Tables 44** and **45** summarize the experimental results and statistical analysis between ISHACDE and recently proposed optimizers on CEC2022 benchmark functions.

Appendix E. Ablation experiments on CEC benchmarks

Tables 46, **47**, **48**, **49**, **50**, and **51** summarize the experimental results and statistical analysis of ablation experiments on CEC benchmarks.

Data availability

The source code of this research can be downloaded from <https://github.com/RuiZhong961230/ISHACDE>.

Table 50

Results of ablation experiments in 10-D CEC2022.

Func	SHACDE		ISHACDE	
	mean	std	mean	std
f_1	3.697e+02	2.079e+02	3.001e+02 –	4.132e-01
f_2	4.024e+02	2.980e+00	4.027e+02 ≈	2.893e+00
f_3	6.000e+02	4.593e-08	6.000e+02 –	7.661e-10
f_4	8.007e+02	1.920e-01	8.007e+02 ≈	1.524e-01
f_5	9.000e+02	2.024e-03	9.000e+02 –	8.101e-07
f_6	2.316e+04	2.283e+04	6.497e+03 –	4.687e+03
f_7	2.037e+03	4.812e+00	2.034e+03 ≈	5.539e+00
f_8	2.229e+03	2.680e+00	2.224e+03 –	5.362e+00
f_9	2.300e+03	4.079e-01	2.301e+03 ≈	1.799e+00
f_{10}	2.606e+03	2.887e+01	2.611e+03 ≈	3.680e+01
f_{11}	2.600e+03	5.531e-02	2.600e+03 –	8.717e-04
f_{12}	2.867e+03	1.651e+00	2.866e+03 –	1.053e+00
+/-/-	–	–	0/5/7	–
Avg. ranks	1.8	–	1.2	–

Table 51

Results of ablation experiments in 20-D CEC2022.

Func	SHACDE		ISHACDE	
	mean	std	mean	std
f_1	3.441e+02	1.460e+02	3.002e+02 –	6.851e-01
f_2	4.510e+02	6.449e+00	4.502e+02 –	1.354e+01
f_3	6.000e+02	1.063e-08	6.000e+02 –	1.515e-12
f_4	8.021e+02	3.931e-01	8.022e+02 ≈	7.902e-01
f_5	9.000e+02	1.291e-04	9.002e+02 ≈	2.614e-01
f_6	1.111e+05	1.449e+05	3.030e+04 ≈	9.091e+03
f_7	2.065e+03	2.208e+01	2.051e+03 –	1.813e+01
f_8	2.625e+03	6.807e+02	2.545e+03 ≈	7.845e+02
f_9	2.644e+03	1.014e+01	2.638e+03 –	2.145e+00
f_{10}	2.771e+03	3.455e+01	2.783e+03 ≈	4.896e+01
f_{11}	2.600e+03	5.703e-03	2.600e+03 –	7.622e-06
f_{12}	2.956e+03	1.044e+01	2.948e+03 –	7.070e+00
+/-/-	–	–	0/5/7	–
Avg. ranks	1.8	–	1.2	–

References

- [1] M. Schlueter, M. Wahib, M. Munetomo, Numerical optimization of ESA's messenger space mission benchmark, in: Applications of Evolutionary Computation, Springer International Publishing, Cham, 2017, pp. 725–737.
- [2] F. De Grossi, P. Marzoli, M. Cho, F. Santoni, C. Circi, Trajectory optimization for the Horyu-VI international lunar mission, *Astrodynamicas* 5 (2021) 263–278.
- [3] N.P. Nurre, E. Taheri, Duty-cycle-aware low-thrust trajectory optimization using embedded homotopy, *Acta Astronaut.* 212 (2023) 630–642.
- [4] M. Schlueter, M. Munetomo, A mixed-integer extension for ESA's Cassini1 space mission benchmark, in: 2019 IEEE Congress on Evolutionary Computation, CEC, 2019, pp. 912–919.
- [5] A.C. Morelli, C. Hofmann, F. Topputo, Robust low-thrust trajectory optimization using convex programming and a homotopic approach, *IEEE Trans. Aerosp. Electron. Syst.* 58 (3) (2022) 2103–2116.
- [6] M. Bassetto, N. Perakis, A.A. Quarta, G. Mengali, Refined MagSail thrust model for preliminary mission design and trajectory optimization, *Aerosp. Sci. Technol.* 133 (2023) 108113.
- [7] J. Carrasco, S. García, M. Rueda, S. Das, F. Herrera, Recent trends in the use of statistical tests for comparing swarm and evolutionary computing algorithms: Practical guidelines and a critical review, *Swarm Evol. Comput.* 54 (2020) 100665.
- [8] Z. hui Zhan, L. Shi, K.C. Tan, J. Zhang, A survey on evolutionary computation for complex continuous optimization, *Artif. Intell. Rev.* 55 (2021) 59–110.
- [9] R. Zhong, F. Peng, J. Yu, M. Munetomo, Q-learning based vegetation evolution for numerical optimization and wireless sensor network coverage optimization, *Alex. Eng. J.* 87 (2024) 148–163.
- [10] Y. Zhang, S. Li, Y. Wang, Y. Yan, J. Zhao, Z. Gao, Self-adaptive enhanced learning differential evolution with surprisingly efficient decomposition approach for parameter identification of photovoltaic models, *Energy Convers. Manage.* 308 (2024) 118387.
- [11] R. Storn, K. Price, Differential evolution - A simple and efficient heuristic for global optimization over continuous spaces, *J. Global Optim.* 11 (1997) 341–359.
- [12] J. Brest, M.S. Maučec, B. Bošković, IL-SHADE: Improved L-SHADE algorithm for single objective real-parameter optimization, in: 2016 IEEE Congress on Evolutionary Computation, CEC, 2016, pp. 1188–1195.
- [13] P.P. Biswas, P.N. Suganthan, Large initial population and neighborhood search incorporated in LSHADE to solve CEC2020 benchmark problems, in: 2020 IEEE Congress on Evolutionary Computation, CEC, 2020, pp. 1–7.
- [14] R. Biedrzycki, J.a. Arabas, E. Warchulski, A version of NL-SHADE-RSP algorithm with midpoint for CEC 2022 single objective bound constrained problems, in: 2022 IEEE Congress on Evolutionary Computation, CEC, 2022, pp. 1–8.
- [15] H. Yan, L. Zhang, X. Wang, Q. Liu, M. Gu, W. Sheng, Differential evolution with clustering-based niching and adaptive mutation for global optimization, in: 2023 IEEE Congress on Evolutionary Computation, CEC, 2023, pp. 1–8.
- [16] X. Zhong, P. Cheng, Z. You, An improved differential evolution algorithm based on basis vector type and its application in fringe projection 3D imaging, *Knowl.-Based Syst.* 268 (2023) 110470.
- [17] Y. Song, X. Cai, X. Zhou, B. Zhang, H. Chen, Y. Li, W. Deng, W. Deng, Dynamic hybrid mechanism-based differential evolution algorithm and its application, *Expert Syst. Appl.* 213 (2023) 118834.
- [18] H. Zhao, L. Tang, J.R. Li, J. Liu, Strengthening evolution-based differential evolution with prediction strategy for multimodal optimization and its application in multi-robot task allocation, *Appl. Soft Comput.* 139 (2023) 110218.
- [19] X. Bu, Q. Zhang, H. Gao, H. Zhang, Multi-strategy differential evolution algorithm based on adaptive hash clustering and its application in wireless sensor networks, *Expert Syst. Appl.* 246 (2024) 123214.
- [20] M. Schlueter, M. Neshat, M. Wahib, M. Munetomo, M. Wagner, GTOPX space mission benchmarks, *SoftwareX* 14 (2021) 100666.
- [21] J. Zhang, A.C. Sanderson, JADE: Adaptive differential evolution with optional external archive, *IEEE Trans. Evol. Comput.* 13 (5) (2009) 945–958.
- [22] R. Zhong, Y. Cao, E. Zhang, M. Munetomo, Introducing competitive mechanism to differential evolution for numerical optimization, 2024, [arXiv:2406.05436](https://arxiv.org/abs/2406.05436).
- [23] R. Tanabe, A. Fukunaga, Success-history based parameter adaptation for Differential Evolution, in: 2013 IEEE Congress on Evolutionary Computation, 2013, pp. 71–78.
- [24] R. Tanabe, A.S. Fukunaga, Improving the search performance of SHADE using linear population size reduction, in: 2014 IEEE Congress on Evolutionary Computation, CEC, 2014, pp. 1658–1665.
- [25] X. Wang, C. Li, J. Zhu, Q. Meng, L-SHADE-E: Ensemble of two differential evolution algorithms originating from L-SHADE, *Inform. Sci.* 552 (2021) 201–219.
- [26] Y. Li, T. Han, H. Zhou, S. Tang, H. Zhao, A novel adaptive L-SHADE algorithm and its application in UAV swarm resource configuration problem, *Inform. Sci.* 606 (2022) 350–367.
- [27] Q. Gu, S. Li, W. Gong, B. Ning, C. Hu, Z. Liao, L-SHADE with parameter decomposition for photovoltaic modules parameter identification under different temperature and irradiance, *Appl. Soft Comput.* 143 (2023) 110386.
- [28] X. Ji, X. Lu, H. Li, P. Ma, S. Xu, Blade optimization design of savonius hydraulic turbine based on radial basis function surrogate model and L-SHADE algorithm, *Ocean Eng.* 286 (2023) 115620.
- [29] X. Yang, G. Zeng, Z. Cao, X. Huang, J. Zhao, Parameters estimation of complex solar photovoltaic models using bi-parameter coordinated updating L-SHADE with parameter decomposition method, *Case Stud. Therm. Eng.* 61 (2024) 104917.
- [30] R. Zhong, Y. Cao, J. Yu, M. Munetomo, Hierarchical adaptive differential evolution with local search for extreme learning machine, in: Y. Tan, Y. Shi (Eds.), Advances in Swarm Intelligence, Springer Nature Singapore, Singapore, 2024, pp. 235–246.
- [31] A. Kumar, G. Wu, M.Z. Ali, Q. Luo, R. Mallipeddi, P.N. Suganthan, S. Das, A benchmark-suite of real-world constrained multi-objective optimization problems and some baseline results, *Swarm Evol. Comput.* 67 (2021) 100961.
- [32] M. Schlueter, MIDACO software performance on interplanetary trajectory benchmarks, *Adv. Space Res.* 54 (4) (2014) 744–754.
- [33] M. Zuo, G. Dai, L. Peng, M. Wang, Z. Liu, C. Chen, A case learning-based differential evolution algorithm for global optimization of interplanetary trajectory design, *Appl. Soft Comput.* 94 (2020) 106451.
- [34] M. Zuo, G. Dai, L. Peng, Z. Tang, D. Gong, Q. Wang, A differential evolution algorithm with the guided movement for population and its application to interplanetary transfer trajectory design, *Eng. Appl. Artif. Intell.* 110 (2022) 104727.
- [35] J.H. Choi, J. Lee, C. Park, Deep-space trajectory optimizations using differential evolution with self-learning, *Acta Astronaut.* 191 (2022) 258–269.
- [36] Z. Tang, L. Peng, G. Dai, P. Wang, Y. Zhao, H. Yang, Z. Pu, M. Zuo, Enhancing the search ability of a hybrid LSHADE for global optimization of interplanetary trajectory design, *Eng. Optim.* 55 (4) (2023) 632–649.
- [37] L. Peng, Z. Yuan, G. Dai, M. Wang, Z. Tang, Reinforcement learning-based hybrid differential evolution for global optimization of interplanetary trajectory design, *Swarm Evol. Comput.* 81 (2023) 101351, <http://dx.doi.org/10.1016/j.swevo.2023.101351>.
- [38] Y. Song, W. Wu, H. Hu, M. Lin, H. Wang, J. Zhang, Gravity assist space pruning and global optimization of spacecraft trajectories for solar system boundary exploration, *Complex Intell. Syst.* 10 (1) (2024) 323–341, <http://dx.doi.org/10.1007/s40747-023-01123-2>.

- [39] Z. Yuan, L. Peng, G. Dai, M. Wang, J. Li, W. Zhang, Q. Yu, An improved multi-operator differential evolution with two-phase migration strategy for numerical optimization, *Inform. Sci.* 669 (2024) 120548.
- [40] J. Brest, M.S. Maučec, B. Bošković, Single objective real-parameter optimization: Algorithm jSO, in: 2017 IEEE Congress on Evolutionary Computation, CEC, 2017, pp. 1311–1318.
- [41] P. Biswas, P. Suganthan, G. Amaralunga, Optimal power flow solutions using algorithm success history based adaptive differential evolution with linear population reduction, in: 2018 IEEE International Conference on Systems, Man, and Cybernetics, SMC, 2018, pp. 249–254.
- [42] T. Kitamura, A. Fukunaga, Revisiting success-histories for adaptive differential evolution, in: 2020 IEEE Congress on Evolutionary Computation, CEC, 2020, pp. 1–8.
- [43] A. Ghosh, S. Das, A.K. Das, R. Senkerik, A. Viktorin, I. Zelinka, A.D. Masegosa, Using spatial neighborhoods for parameter adaptation: An improved success history based differential evolution, *Swarm Evol. Comput.* 71 (2022) 101057.
- [44] T. Nguyen, A framework of optimization functions using Numpy (OpFuNu) for optimization problems, 2020.
- [45] N. Van Thieu, S. Mirjalili, MEALPY: An open-source library for latest meta-heuristic algorithms in Python, *J. Syst. Archit.* 139 (2023) 102871.
- [46] J. Kennedy, R. Eberhart, Particle swarm optimization, in: Proceedings of ICNN'95 - International Conference on Neural Networks, Vol. 4, 1995, pp. 1942–1948, vol.4.
- [47] N. Hansen, A. Ostermeier, Completely derandomized self-adaptation in evolution strategies, *Evol. Comput.* 9 (2) (2001) 159–195.
- [48] A. Qin, P. Suganthan, Self-adaptive differential evolution algorithm for numerical optimization, in: 2005 IEEE Congress on Evolutionary Computation, Vol. 2, 2005, pp. 1785–1791.
- [49] J. Liang, A. Qin, P. Suganthan, S. Baskar, Comprehensive learning particle swarm optimizer for global optimization of multimodal functions, *IEEE Trans. Evol. Comput.* 10 (3) (2006) 281–295.
- [50] W.-C. Hong, Chaotic particle swarm optimization algorithm in a support vector regression electric load forecasting model, *Energy Convers. Manage.* 50 (1) (2009) 105–117.
- [51] M. Ghasemi, E. Akbari, A. Rahimnejad, E. Razavi, S. Ghavidel, L. Li, Phasor particle swarm optimization: a simple and efficient variant of PSO, *Soft Comput.* 23 (2019).
- [52] A. Faramarzi, M. Heidarinejad, S. Mirjalili, A.H. Gandomi, Marine predators algorithm: A nature-inspired metaheuristic, *Expert Syst. Appl.* 152 (2020) 113377.
- [53] H. Mohammed, T. Rashid, FOX: a FOX-inspired optimization algorithm, *Appl. Intell.* 53 (2022) 1–21.
- [54] P. Trojovský, M. Dehghani, Pelican optimization algorithm: A novel nature-inspired algorithm for engineering applications, *Sensors* 22 (3) (2022).
- [55] M. Dehghani, P. Trojovský, Osprey optimization algorithm: A new bio-inspired metaheuristic algorithm for solving engineering optimization problems, *Front. Mech. Eng.* 8 (2023) 1126450.
- [56] M. Azizi, U. Aickelin, H. Khorshidi, M. Baghalzadeh Shishehgarkhaneh, Energy valley optimizer: a novel metaheuristic algorithm for global and engineering optimization, *Sci. Rep.* 13 (2023) 226.
- [57] M. Dehghani, Z. Montazeri, E. Trojovská, P. Trojovský, Coati optimization algorithm: A new bio-inspired metaheuristic algorithm for solving optimization problems, *Knowl.-Based Syst.* 259 (2023) 110011.
- [58] F.A. Hashim, R.R. Mostafa, A.G. Hussien, S. Mirjalili, K.M. Sallam, Fick's Law Algorithm: A physical law-based algorithm for numerical optimization, *Knowl.-Based Syst.* 260 (2023) 110146.
- [59] H. Su, D. Zhao, A.A. Heidari, L. Liu, X. Zhang, M. Mafarja, H. Chen, RIME: A physics-based optimization, *Neurocomputing* 532 (2023) 183–214.
- [60] R. Zhong, J. Yu, DEA2H2: Differential evolution architecture based adaptive hyper-heuristic algorithm for continuous optimization, *Cluster Comput.* (2024) 1–28.
- [61] C.A. Coello Coello, Theoretical and numerical constraint-handling techniques used with evolutionary algorithms: a survey of the state of the art, *Comput. Methods Appl. Mech. Engrg.* 191 (11) (2002) 1245–1287.
- [62] R. Zhong, J. Yu, C. Zhang, M. Munetomo, SRIME: a strengthened RIME with latin hypercube sampling and embedded distance-based selection for engineering optimization problems, *Neural Comput. Appl.* (2024) 1–20.
- [63] K. Li, H. Huang, S. Fu, C. Ma, Q. Fan, Y. Zhu, A multi-strategy enhanced northern goshawk optimization algorithm for global optimization and engineering design problems, *Comput. Methods Appl. Mech. Engrg.* 415 (2023) 116199.
- [64] D. Wolpert, W. Macready, No free lunch theorems for optimization, *IEEE Trans. Evol. Comput.* 1 (1) (1997) 67–82.
- [65] J.H. Holland, Genetic algorithms, *Sci. Am.* 267 (1) (1992) 66–73.
- [66] S. Mirjalili, S.M. Mirjalili, A. Lewis, Grey Wolf optimizer, *Adv. Eng. Softw.* 69 (2014) 46–61.
- [67] S. Mirjalili, A. Lewis, The Whale optimization algorithm, *Adv. Eng. Softw.* 95 (2016) 51–67.
- [68] T. Li, Y. Meng, L. Tang, Scheduling of continuous annealing with a multi-objective differential evolution algorithm based on deep reinforcement learning, *IEEE Trans. Autom. Sci. Eng.* 21 (2) (2024) 1767–1780.
- [69] R. Zhong, E. Zhang, M. Munetomo, Cooperative coevolutionary surrogate ensemble-assisted differential evolution with efficient dual differential grouping for large-scale expensive optimization problems, *Complex Intell. Syst.* 10 (2023) 2129–2149.
- [70] Y. Zhang, H. Wu, T.A. Gulliver, J. Xian, L. Liang, Improved differential evolution for RSSD-based localization in Gaussian mixture noise, *Comput. Commun.* 206 (2023) 51–59.
- [71] Z. Cao, H. Jia, Z. Wang, C.H. Foh, F. Tian, A differential evolution with autonomous strategy selection and its application in remote sensing image denoising, *Expert Syst. Appl.* 238 (2024) 122108.
- [72] Y. Wang, Y. Pei, H. Shindo, Q. Liu, H.-P. Ren, An interactive differential evolution method with human auditory perception for sound composition, *IEEE Trans. Cogn. Dev. Syst.* (2023) 1–13.